COMPARATIVE *IN SILICO* ANALYSIS OF BIOACTIVE COMPOUNDS FROM *OCIMUM GRATISSIMUM, LAURUS NOBILIS, CYMBOGON CITRATUS PIPERER GUINEENSE,* AND *PSIDIUM GUAJAVA* FOR POTENTIAL ANTILIPIDEMIC ACTIVITY

BY

REGINA BAMIYO ANIEMEKE
PHA1908464

A DISSERTATION SUBMITTED TO THE DEPARTMENT OF PHARMACEUTICAL CHEMISTRY IN PARTIAL FULFILLMENT OF THE REQUIREMENT FOR THE AWARD OF THE DOCTOR OF PHARMACY (PHARM.D) DEGREE OF THE UNIVERSITY OF BENIN, BENIN CITY, EDO STATE.

SUPERVISED BY:
DR. AGHARAYE
CO-SUPERVISED BY:
DR UYI

NOVEMBER, 2025

CERTIFICATION

This is to certify that this project was carried out by REGINA BAMIYO ANIEMEKE in the Department of Pharmaceutical Chemistry, Faculty of Pharmacy, University of Benin, Benin City, Edo State, Nigeria.

_____ _____

DR.AGHARAYE DATE

PROJECT SUPERVISOR

_____ _____

DR UYI DATE

PROJECT CO-SUPERVISOR

_____ _____

DR. V.O. IMIEJE DATE

HEAD OF DEPARTMENT

DEDICATION

This project is dedicated to the Lord Almighty, whose boundless grace, wisdom, and strength have guided and sustained me through every challenge. His unfailing love and faithfulness have been my anchor, and to Him alone belong all glory and honor.

Acknowledgement

First and foremost, I give all glory, honor, and adoration to God Almighty, whose grace, wisdom, and strength have been my constant guide throughout this project and my entire academic journey. Without His divine favor, none of this would have been possible.

My deepest gratitude goes to my parents Mr Christopher Aniemeke and Mrs Catherine Aniemeke, and my siblings for their endless love, encouragement, and sacrifices that have carried me through every stage of my education.

I also sincerely appreciate my project supervisors Pharm. Dr Godfrey Agharaye and Pharm. Dr Uyi Ogbeide for their patience and guidance throughout the course of this work. And to my project mate; kluvet, Iwinosa, Isaac, Priscilla, Obinna, Ophurey, and Zoey I am grateful for the support I got from you all, which made this work both insightful and fulfilling.

Special thanks to Pharm. Dr Uyi Ogbeide, pharm. Dr Isioma Ogbeide, pharm. Tejiri Ometan, my Eltetmac Pharmacy family, Pharm Itohan, Pharm. Issac, and everyone who made Benin feel like home for their support, mentorship, and for creating an environment that has inspired both my academic and professional growth.

Finally, I extend heartfelt appreciation to my friends, Vanessa, Susan, Elaine, Ernest who stood by me at every single point sharing in my challenges, victories, and every step in between. Your constant encouragement, understanding, and faith in me made this journey worthwhile.

.

TABLE OF CONTENT

ABSTRACT

Abstract

Hyperlipidemia is a major risk factor for atherosclerotic cardiovascular disease (ASCVD), necessitating multi-target therapeutic strategies to counter excessive cholesterol synthesis, absorption, and poor triglyceride clearance (Ray *et al*., 2023). Given the side effects and limitations of synthetic lipid-lowering drugs, this *in silico* study evaluated phytochemicals from five Nigerian plants (*Ocimum gratissimum, Laurus nobilis, Cymbopogon citratus, Piper guineense,* and *Psidium guajava*) as natural antilipidemic agents. Molecular docking assessed the binding affinity (ΔG) of over 100 compounds against five key targets of lipid metabolism: 3-Hydroxy-3-methylglutaryl-coenzyme A Reductase (HMG-CoA Reductase, PDB ID 1HWK), Peroxisome Proliferator-Activated Receptor Gamma (PPAR-γ, PDB ID 6ENQ), PPAR-δ (PDB ID 7WGN), Hydroxycarboxylic Acid Receptor 2 (HM7A4, PDB ID 8K5B), and Niemann-Pick C1-Like 1 (NPC1L1, PDB ID 7DFZ). Promising hits demonstrating superior binding to established clinical standards were then subjected to ADMET (Absorption, Distribution, Metabolism, Excretion, and Toxicity) profiling to predict their pharmacokinetic and safety profiles. The screening identified several compounds displaying significantly stronger binding affinities than their respective clinical standards. Notably, the *Laurus nobilis* constituent, CID 91274708, showed unparalleled affinity for PPAR-δ (-8.57 kcal/mol), substantially surpassing the Pemafibrate standard (-7.16 kcal/mol). The potent HMG-CoA Reductase inhibitor, CID 165359504, also demonstrated robust binding (-7.86 kcal/mol) against the Atorvastatin standard (-5.40 kcal/mol), suggesting a novel poly-glycosidic scaffold for inhibition. Furthermore, the NPC1L1 inhibitor, CID 72

(Psidium guajava), showed enhanced binding (-5.18 kcal/mol) compared to Ezetimibe (-4.51 kcal/mol). ADMET analysis confirmed that the prioritized compounds, notably CID 91274708 and CID 72, possessed ideal pharmacokinetic profiles, while successfully filtering out candidates with high predicted toxicological risks, such as the genotoxic CID 6037 (Mohamed *et al*., 2024). The results validate the potential of compounds from Nigerian medicinal plants as structurally diverse, high-affinity leads for multi-target antilipidemic therapy, providing a computational basis for future in vitro and in vivo studies aimed at drug discovery (Yadav *et al.,* 2021).

CHAPTER ONE

1.1. INTRODUCTION

Hyperlipidemia is a disorder characterized by excessively high levels of lipids, also known as cholesterol and triglycerides, in the blood. It conditions people to atherosclerosis and atherosclerotic cardiovascular disease (ASCVD), which are leading causes of morbidity and death among the world population (American Heart Association, 2024; Hill, 2023). The deposition of excessive lipids in the walls of arteries triggers the formation of a plaque, leading to the constriction of arteries and poor blood circulation, which may eventually lead to a heart attack or stroke.

Due to the growing population health burden caused by lipid related diseases, the World Health Organization (WHO) has initiated a global campaign to remove the trans fats industrially produced in foodstuffs. Trans fats are a type of unsaturated fatty acid, which is abundant in processed and fried food, margarine, baked goods, and snacks and is associated with the elevation of low-density lipoprotein (LDL) cholesterol, the decreases of high-density lipoprotein (HDL) cholesterol, and the risk of hyperlipidemia and cardiovascular disease (WHO, 2023). It is in this realization that WHO aims to eliminate trans fats all round the world, so as to prevent millions of premature deaths.

With the poor side effects of synthetic fats and the shortcomings of traditional lipid-lowering therapeutics, there is an increasing enthusiasm with regard to applying medicinal plants and herbs as natural therapeutic substitutes. The botanicals used

contain bioactive compounds such as flavonoids, polyphenols, saponins, and alkaloids which have been reported to lower LDL cholesterol and triglycerides and increase in HDL cholesterol. Examples of representative species are Cymbopogon citratus (lemongrass), Allium sativum (garlic), Curcuma longa (turmeric) and Camellia sinensis (green tea). Such natural agents regulate lipid metabolism as well as offer antioxidant and anti-inflammatory effects which contribute to heart health.

Hyperlipidemia is a significant issue to the general population due to its correlation to critical complications. When the lipid levels (especially LDL -cholesterol and triglycerides) continue to be high, the fatty deposits are deposited on the walls of the arteries, which promotes the occurrence of atherosclerosis. These deposits gradually reduce the lumen of the arteries, weakening the blood flow and possibly triggering the rupture of the plaque, the thrombosis, and tissue injury (Cleveland Clinic, 2023).

The major consequences of hyperlipidemia include coronary artery disease, where the a*cymbopogon citratus*umulation of plaque in the coronary arteries hinders the blood flow to myocardial tissue, often leading to angina pectoris or myocardial infarction; cerebrovascular disease and stroke, when the plaque is deposited in the cerebral or carotid arteries, thus impairing the blood circulation to the brain tissue (NCBI, 2022); peripheral artery disease (PAD), the effect of lipid-induced arter

In addition to solitary vascular problems, hyperlipidemia is often co-morbid to metabolic ailments, such as obesity, insulin resistance, and diabetes mellitus, which only increases cardiovascular hazards. The continuous aspect of lipid dysregulation

damages its vessels, not only, but also promotes the development of multi-organ pathology, increasing the morbidity and mortality rates worldwide (Cleveland Clinic, 2023).

Hyperlipidemia and associated lipid abnormalities in Nigeria have been on the rise in the last three decades. A meta-analysis of the data acquired 1990 to 2018 systematically found that the prevalence of hypercholesterolemia was a pooled crude state of about 38 000 percent (95 percent CI: 26-51000 percent) among the people of Nigerian origin (Ogbera *et al*., 2020). High triglyceride rates were 21.4% prevalent (Ibrahim *et al*., 2022). Dyslipidemia can become up to 89 among people with diabetes and hypertension, which highlights the role of metabolic derangements in the formation of lipid disorders. In the same study, the prevalence of hypercholesterolemia in Nigerians was estimated at 8.2 million 20 years and older in 1995 and 21.9 million 20 years and older in 2015, which is an indication of increasing trends in the lipid-related disorders (Adedoyin *et al.,* 2020).

Urban developmental regions like Lagos were reported to have 38.9 % of adults with elevated total cholesterol which indicates high lifestyle and dietary factors that contribute to the disease burden (Onyemelikwe *et al.,* 2020). A different population-based study that involved 3,211 Nigerian adults found out that 7.5 per cent had high total cholesterol, 13.6 per cent had high LDL and a few of them had general lipid disorders (Erasmus *et al.*, 2012).

1.1.1. Key Lipid Profile Terms

Low-density lipoprotein (LDL): Low-density lipoprotein (LDL) is commonly referred to as bad cholesterol since larger levels of the lipoprotein allow the a*cymbopogon citratus*umulation of cholesterol in the arteries, the formation of atherosclerotic plaque, and an increased risk of cardiovascular diseases, including myocardial infarction and stroke (Grundy *et al*., 2023). LDL plays the primary role of carrying cholesterol between the liver and the peripheral tissues; LDL in the blood that is overly present is associated with endothelial damage and lipid deposition (Pappan, 24). It has been clinically advised to keep LDL levels under 100mg/dL to promote the health of the heart.

High-Density lipoprotein (HDL): Hdl is also known as good cholesterol because it helps to eliminate excess cholesterol in the blood and transports it back to the liver to be excreted through reverse cholesterol transport (Hill, 2023). HDL contains antioxidant and anti-inflammatory effects which provide resistance against atherosclerosis (Ruscica *et al.,* 2024). Men and women with HDL below 40mg and 50mg are considered to have an increased cardiovascular risk.

Triglycerides (TG): Triglycerides are the most common type of fat in the human body which is composed of three fatty acids and glycerol. They perform the roles of the main energy storage molecules (Kaminsky *et al.,* 2022). Some of the complications associated with hypertriglyceridemia include insulin resistance, metabolic syndrome, pancreatitis, and cardiovascular disease (Grundy *et al.,* 2023). Normal levels of triglycerides in the body become less than 150mg/dL in normal fasting.

Trans Fat: Trans fatty acids are unsaturated fatty acids which have been hydrogenated, and thus, they are hard at ambient temperature. They are typical of processed foods, margarine, and fried foods (Lichtenstein *et al*., 2021). Trans fats increase the LDL (bad) cholesterol and decrease the HDL (good) cholesterol, increasing the risk of cardiovascular problems (Ruscica et al., 2024). WHO advises the intake of trans-fats be a minimum of less than 1 percent of the daily energy consumption (WHO, 2023).

Total Cholesterol: Total cholesterol is a sum of LDL, HDL, and the very-low-density lipoprotein (VLDL) cholesterol in the bloodstream, which gives a comprehensive evaluation of the lipid status (Pappan, 2024). The concentrations of above 200 mg/dl are viewed as a significant risk factor of coronary artery disease and stroke (Grundy *et al*., 2023). Measures including decreasing the number of saturated fats in the diet and increasing physical activities are helpful in reducing total cholesterol (Hill, 2023).

1.1.2. Metabolism of lipids

Lipid metabolism refers to the complex biological processes that regulate the digestion, absorption, transport, and utilization of lipids within the human body. Dietary lipids, mainly triglycerides, cholesterol, and phospholipids, are first emulsified in the small intestine by bile salts, allowing pancreatic lipase to hydrolyze them into free fatty acids and monoglycerides. These smaller molecules are absorbed by intestinal mucosal cells and re-esterified to form triglycerides, which are subsequently packaged together with cholesterol and apolipoproteins to form lipoprotein particles known as chylomicrons. Chylomicrons are secreted into the

lymphatic system and eventually enter the bloodstream, where they are acted upon by the enzyme lipoprotein lipase (LPL). LPL breaks down the triglycerides within chylomicrons into free fatty acids that can be taken up by peripheral tissues, such as muscle and adipose tissue, for energy production or storage (Nelson & Cox, 2021; Feingold & Anawalt, 2023). The remnants of chylomicrons are cleared by the liver, which repackages lipids into very-low-density lipoproteins (VLDL). As VLDL circulates in the bloodstream, it loses triglycerides and becomes intermediate-density lipoprotein (IDL) and eventually low-density lipoprotein (LDL). LDL serves as the major carrier of cholesterol to peripheral tissues for membrane synthesis and steroid hormone production. In contrast, high-density lipoprotein (HDL) facilitates reverse cholesterol transport by carrying excess cholesterol from peripheral tissues back to the liver for excretion or recycling. This delicate balance between lipoprotein synthesis, transport, and clearance ensures lipid homeostasis and prevents the a*cymbopogon citratus*umulation of lipids in the bloodstream (Wang & Tall, 2020).

However, disturbances in any of these processes can result in abnormal lipid profiles, leading to hyperlipidemia. One of the major points where lipid metabolism can go wrong is during hepatic lipid synthesis. Excessive consumption of carbohydrates, alcohol, and trans fats stimulates triglyceride formation in the liver, leading to the overproduction of VLDL and elevated plasma triglyceride levels (Kumar *et al.*, 2023). Additionally, inherited or acquired deficiencies in lipoprotein lipase or its cofactor apolipoprotein C-II impair the clearance of triglyceride-rich lipoproteins, resulting in persistent hypertriglyceridemia (Zhao *et al.,* 2020). Another critical point of metabolic disturbance o*cymbopogon citratus*urs when LDL receptor function is defective.

Mutations in the LDL receptor gene or impaired receptor activity reduce LDL clearance, causing cholesterol a*cymbopogon citratus*umulation in the blood, as observed in familial hypercholesterolemia (Santos *et al.*, 2022). Abnormalities in HDL metabolism can also contribute to hyperlipidemia. When HDL synthesis or function is compromised, reverse cholesterol transport becomes inefficient, leading to increased total cholesterol levels and heightened cardiovascular risk. Dysregulation of the ATP-binding cassette transporter A1 (ABCA1) and lecithin-cholesterol acyltransferase (LCAT) further disrupts cholesterol efflux and HDL maturation (Wang & Tall, 2020). In addition, insulin resistance associated with metabolic syndrome alters hepatic lipid metabolism by promoting de novo lipogenesis and inhibiting LPL activity, producing a characteristic pattern of elevated triglycerides, low HDL cholesterol, and small dense LDL particles (Taskinen & Boren, 2021)

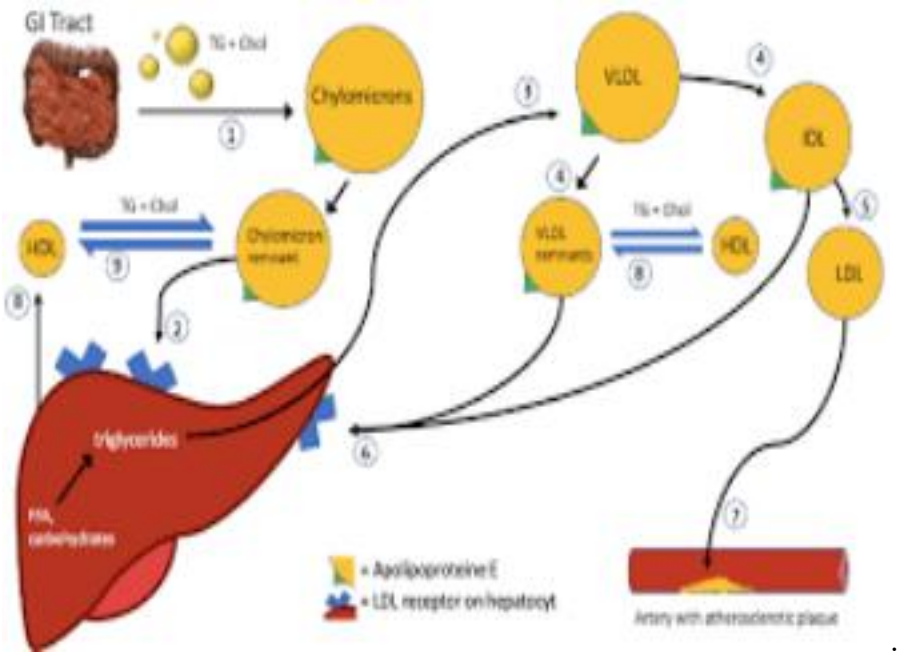

Figure 1. image of lipid metabolism.

1.1.3. Causes of hyperlipidemia

Hyperlipidemia can arise from both genetic (primary) and lifestyle or medical (secondary) causes. Primary hyperlipidemia results from inherited disorders that affect lipid metabolism, such as familial hypercholesterolemia, which leads to elevated low-density lipoprotein (LDL) cholesterol levels even in childhood (Hill, 2023). Secondary hyperlipidemia, on the other hand, develops due to modifiable factors including unhealthy diet, obesity, lack of physical activity, excessive alcohol intake, and smoking (Centers for Disease Control and Prevention [CDC], 2024). Certain medical conditions can also contribute to secondary hyperlipidemia. These include type 2 diabetes mellitus, hypothyroidism, chronic kidney disease, liver disease, and metabolic syndrome (Mayo Clinic, 2025; American Heart Association [AHA], 2024). Additionally, some medications such as corticosteroids, beta-blockers, thiazide diuretics, oral estrogen, and certain antiretroviral drugs can increase blood lipid levels (Hill, 2023; AHA, 2024). Environmental and behavioral factors—like high intake of saturated or trans fats and low consumption of fiber and omega-3 fatty acids—further worsen lipid imbalance (Cleveland Clinic, 2021). Therefore, prevention and management strategies for hyperlipidemia often focus on dietary modification, weight control, regular exercise, and medical treatment when necessary.

The diagnosis of hyperlipidemia is primarily based on blood lipid testing, also known as a lipid profile or lipid panel, which measures total cholesterol, low-density lipoprotein (LDL), high-density lipoprotein (HDL), and triglycerides (Centers for Disease Control and Prevention [CDC], 2024). This test is typically conducted after a 9–12-hour fast, although some newer guidelines permit non-fasting measurements

depending on clinical context (American Heart Association [AHA], 2024). A*cymbopogon citratus*ording to current recommendations, a fasting total cholesterol level above 200 mg/dL, LDL cholesterol above 130 mg/dL, HDL cholesterol below 40 mg/dL (for men) or below 50 mg/dL (for women), and triglyceride levels above 150 mg/dL indicate an increased risk of hyperlipidemia and cardiovascular disease (Mayo Clinic, 2025). The Atherogenic Index of Plasma (AIP) and non-HDL cholesterol are also used as additional markers to evaluate lipid-related risk (Hill, 2023). In some cases, genetic testing may be performed to identify inherited lipid disorders such as familial hypercholesterolemia, especially in patients with early-onset cardiovascular disease or strong family history (Cleveland Clinic, 2021; AHA, 2024). Regular screening is recommended for adults aged 20 years and older every 4–6 years, or more frequently in individuals with risk factors like diabetes, hypertension, or obesity (CDC, 2024).

1.2. Complications of Hyperlipidemia

Hyperlipidemia is one of the major predisposing factors of a range of cardiovascular and systemic problems. Atherosclerosis is the most significant expression and a long-term inflammatory disease of the arteries characterized by the presence of lipid-rich deposits in the internal layers of blood vessels. The process of low-density lipoprotein (LDL) cholesterol infiltrating the endothelium of the arteries and being oxidized triggers an inflammatory cascade and causes this pathology to develop (American

Heart Association [AHA], 2024). Immunocompetent cells, and in particular, macrophages migrate into the atherosclerotic niche, ingest the oxidized lipids and become foam cells, which forms the first of the histopathological hallmarks called fatty streaks (Hill, 2023). The further growth of vascular smooth muscle cells as well as deposition of extracellular matrix material over the fatty streaks result in the development of a fibrous cap, which wraps the lipid core. As such plaques grow progressively, luminal narrowing (stenosis) o*cymbopogon citratus*urs, and hinders haemodynamic flow (Mayo Clinic, 2025). As the plaques rupture, they release thrombogenic substances, which leads to the precipitation of thrombus that can result in myocardial infarction, stroke, or peripheral arterial disease (Centers for Disease Control and Prevention [CDC], 2024; Cleveland Clinic, 2021). Therefore, the resultant decrease in vascular perfusion is prone to coronary artery disease (CAD), angina pectoris, and myocardial infarction (Hill, 2023; Mayo Clinic, 2025).

Constant hypertriglyceridaemia can also promote pancreatitis, which is a possibly fulminant inflammatory disorder of the pancreas (Centers for Disease Control and Prevention [CDC], 2024). In addition, hyperlipidaemia causes cerebrovascular events, peripheral arterial disease (PAD), and carotid artery stenosis, which o*cymbopogon citratus*ur due to the atherosclerotic plaque formation in the dissimilar vascular beds (Cleveland Clinic, 2021).

Recurrent dyslipoproteinaemia may also impair renal functionality and can lead to the development of the chronic kidney disease, especially when it is a*cymbopogon*

*citratus*ompanied by hypertension and diabetes (AHA, 2024). In rare cases, high amounts of lipid can cause xanthamas fatty dermal deposits and lipemia retinalis, in which lipid concentration is deposited, and it breaks the integrity of vasculares in the retina (Hill, 2023).

1.3. RISK FACTORS OF HYPERLIPIDEMIA

1.3.1. Non-modifiable

Age: the concentration of cholesterol and triglycerides is likely to increase with age (Hill, 2023). Growth of the older age is strongly correlated with the developmental alterations in the lipid metabolism. The aging process is a*cymbopogon citratus*ompanied by a decrease in the hepatic LDL receptor activity, resulting in decreased blood low-density lipoprotein cholesterol (LDL) clearance. This process leads to the cholesterol and triglycerides a*cymbopogon citratus*umulation in the blood. As a result, older people are susceptible to hyperlipidemia and atherosclerosis than younger. Hormonal and metabolic alteration are also age related, which increases cholesterol production and reduces lipid oxidation, further worsening lipid imbalance.

Sex: men experience dyslipidemia sooner than women; the lipid profile in women who have passed menopause deteriorates (Pappan, 2024).The prevalence of hyperlipidemia, as well as its severity, is also affected by sex differences (Fularski *et al*., 2024; Cuchel *et al*., 2023). Women in premenopause tend to have *lower* total cholesterol and LDL-C levels than men, again in large measure because of the protective action of estrogen, which increases the activity of hepatic LDL receptors and facilitates HDL synthesis. Nonetheless, following menopause, the estrogen

concentration decreases, which raises the overall cholesterol and LDL-C, which makes older women as vulnerable to hyperlipidemia and cardiovascular diseases as before. Conversely, men are more likely to show elevated triglyceride and reduced HDL-C levels at an earlier age, which is in part related to the androgenic influence on lipid metabolism.

Genetics / familial hypercholesterolemia (FH): monogenic diseases (e.g., FH) result in significantly high levels of LDL -C and cardiovascular disease (Fularski *et al*., 2024; Cuchel *et al*., 2023). Genetics is a key factor in establishing the predisposition of a person to hyperlipidemia. As noted by Pappan (2024), inherited types of hyperlipidemia, including FH, are the products of mutations in lipid transport and metabolism genes, including LDLR, ApoB, and PCSK9. Such genetic defects lead to an impaired clearance of LDL cholesterol resulting in significantly increased levels of plasma cholesterol that start at early ages. Genetic predisposition does not just affect the baseline lipid levels but it is also used to determine how a person responds to lifestyle and lipid-lowering drugs. In the same way, it is also observed that genetic variations may influence the expression and activity of enzymes like lipoprotein lipase (LPL) and hepatic lipase and change the process of triglyceride metabolism, and HDL production. The genetic influences are the reasons why there are people who get severe hyperlipidemia even when they are living healthy lifestyles. What is more, family history of premature cardiovascular disease or hypercholesterolemia is

associated with a high probability of the development of lipid disorders, which proves the hereditary nature of the condition.

1.3.2. Modifiable / lifestyle & metabolic

Unhealthy diet: An unhealthy diet that contains large amounts of saturated fats, trans fats, and simple sugars can increase the levels of low-density lipoprotein cholesterol (LDL-C) and triglycerides in the blood. These types of fats and sugars promote fat buildup in the bloodstream, leading to a higher risk of cardiovascular diseases (Hill, 2023). Obesity, particularly when fat is concentrated around the abdomen (central adiposity), is closely linked with increased triglycerides (TG), reduced levels of high-density lipoprotein (HDL), and the presence of small, dense LDL particles — all of which contribute to a higher risk of heart disease (Obsa *et al*., 2022). Additionally, a lack of physical activity or a sedentary lifestyle reduces HDL cholesterol (the "good" cholesterol) and negatively affects the overall lipid profile, further increasing the likelihood of lipid disorders and related complications (Kaminsky *et al.,* 2022).

Tobacco smoking and excessive alcohol consumption: they both have harmful effects on blood lipid levels and overall cardiovascular health. Smoking reduces the level of high-density lipoprotein (HDL) cholesterol, which is known as the "good" cholesterol because it helps remove excess cholesterol from the bloodstream. Lower HDL levels make it easier for cholesterol to build up in the arteries, increasing the risk of atherosclerosis and heart disease. On the other hand, drinking alcohol in large amounts can lead to a rise in triglyceride levels, as alcohol is metabolized into

substances that promote fat production in the liver. Elevated triglycerides contribute to fatty buildup in blood vessels and can cause pancreatitis or worsen existing heart conditions. Therefore, smoking and heavy drinking together can significantly disturb lipid balance and heighten cardiovascular risk (Pappan, 2024)., 2024).

1.3.3. Clinical / secondary causes and medications

Hypothyroidism, a condition in which the thyroid gland produces insufficient thyroid hormones, can negatively affect lipid metabolism. Thyroid hormones help regulate the activity of LDL receptors in the liver, which are responsible for removing low-density lipoprotein cholesterol (LDL-C) from the bloodstream. When these hormones are low, LDL receptor activity decreases, leading to reduced clearance of LDL-C and, consequently, higher levels of LDL cholesterol in the blood (Hill, 2023).

Chronic kidney disease, particularly in cases of nephrotic syndrome, is often associated with significant disturbances in lipid metabolism. The condition increases triglyceride levels due to impaired lipid clearance and abnormal liver production of lipoproteins. It also alters the balance between HDL and LDL cholesterol, often resulting in lower HDL and higher LDL concentrations, both of which contribute to an increased risk of cardiovascular complications (Pappan, 2024).

Certain medications can also disrupt normal lipid metabolism and lead to elevated cholesterol or triglyceride levels. Examples include some antiretroviral agents used in HIV treatment, atypical antipsychotics, corticosteroids, thiazide diuretics, and older beta-blockers. These drugs may increase lipid levels by affecting liver function,

insulin sensitivity, or fat metabolism, thereby promoting higher levels of LDL and triglycerides (Hill, 2023; Giles, 2024).

Hormonal states such as pregnancy, polycystic ovary syndrome (PCOS), and estrogen deficiency can influence lipid levels as well. During pregnancy, hormonal changes can naturally increase cholesterol and triglyceride production to support fetal development. In PCOS, insulin resistance and elevated androgen levels can raise LDL and triglycerides while lowering HDL. Estrogen deficiency, as seen after menopause, often leads to reduced HDL and increased LDL levels, heightening the risk of atherosclerosis and cardiovascular disease (Giles, 2024).

1.3.4. Sociodemographic / environmental

Socioeconomic factors, urbanization, and dietary transition play major roles in the increasing rates of dyslipidemia across many regions, including Africa. As societies become more urbanized, people often shift from traditional diets that are high in fiber and low in fat to diets rich in processed foods, refined sugars, and saturated fats. This dietary transition leads to higher cholesterol and triglyceride levels. In addition, urban lifestyles tend to involve less physical activity due to sedentary jobs, increased use of motorized transport, and limited recreational exercise. These changes, combined with rising income levels and easier access to unhealthy foods, contribute to a growing prevalence of abnormal lipid levels particularly elevated LDL, reduced HDL, and increased triglycerides within urban populations (Obsa *et al*., 2022; Gu *et al*., 2024).

1.4. MANAGEMENT OF HYPERLIPIDEMIA.

1.4.1. Non-Pharmacological Management of Hyperlipidemia

Non-pharmacological management is the first-line approach to controlling hyperlipidemia and reducing cardiovascular disease (CVD) risk. It focuses on lifestyle and behavioral changes that improve lipid metabolism, reduce low-density lipoprotein cholesterol (LDL-C) and triglycerides (TG), and raise high-density lipoprotein cholesterol (HDL-C) (Grundy *et al.*, 2023). These interventions are essential both independently and as adjuncts to drug therapy (Pappan, 2024).

Dietary Modification: A heart-healthy diet is central to lipid control. Reduction of saturated and trans fats decreases LDL-C levels (Ruscica *et al*., 2024). Increased intake of polyunsaturated and monounsaturated fats (e.g., from olive oil, nuts, and fish) enhances HDL-C and lowers triglycerides (Lichtenstein *et al*., 2021). High consumption of fiber-rich foods, especially soluble fiber (e.g., oats, fruits, legumes), helps reduce cholesterol absorption (Mensink, 2022). Adoption of dietary patterns such as the Mediterranean or DASH (Dietary Approaches to Stop Hypertension)*)* diet has been associated with improved lipid profiles and cardiovascular outcomes (Schwingshackl *et al.*, 2022).

Weight Management: Excess body weight, particularly central obesity, is a major risk factor for dyslipidemia. Weight reduction through calorie restriction and increased activity can lower LDL-C and triglycerides while raising HDL-C (Obsa *et al*., 2022). Losing 5–10% of body weight significantly improves lipid levels and overall metabolic health (Amin *et al*., 2023).

Physical Activity: Regular physical activity increases HDL-C, decreases triglycerides, and improves insulin sensitivity. Aerobic exercises such as brisk walking, cycling, or swimming for at least 150 minutes per week are recommended (Kaminsky *et al.,* 2022). Resistance training also complements aerobic activity for better lipid control (Zaleski *et al*., 2023).

Smoking Cessation: Cigarette smoking lowers HDL-C and accelerates atherosclerosis. Smoking cessation improves HDL-C within weeks and reduces overall cardiovascular risk (Giles, 2024). Counseling and behavioral support are effective tools for long-term abstinence.

Limiting Alcohol Intake: Excessive alcohol consumption increases triglycerides and total cholesterol. Moderate alcohol use if any should not exceed one drink per day for women and two for men (Hill, 2023). Complete avoidance is recommended for individuals with hypertriglyceridemia (Banach *et al.,* 2022).

Stress Management: Stress management is an important non-pharmacological method for controlling hyperlipidemia because chronic stress can negatively affect lipid metabolism and overall cardiovascular health. When a person experiences ongoing stress, the body releases stress hormones such as cortisol and adrenaline, which can increase blood pressure, blood sugar, and fat levels in the blood. Elevated cortisol, in particular, stimulates the liver to produce more triglycerides and cholesterol, which can raise total cholesterol and LDL (“bad”) cholesterol while lowering HDL (“good”)

cholesterol. Stress-reduction strategies such as mindfu*Laurus nobilis*ess, yoga, or relaxation therapy contribute to healthier lipid levels (Mertens *et al.*, 2021).

Regular Monitoring and Health Education: Regular lipid screening and lifestyle counseling reinforce adherence to healthy habits. Patient education on reading food labels, cooking with low-fat methods, and maintaining consistent exercise routines improves long-term outcomes (Grundy *et al.*, 2023).

1.4.2. Pharmacological management

Pharmacologic therapy for hyperlipidemia aims to reduce low-density lipoprotein cholesterol (LDL-C), triglycerides (TG), and total cholesterol while raising high-density lipoprotein cholesterol (HDL-C) to prevent atherosclerotic cardiovascular disease (ASCVD) (Grundy *et al*., 2023). The selection of lipid-lowering agents depends on the lipid abnormality pattern, risk factors, and patient comorbidities (Mach *et al*., 2020). The main drug classes include statins, ezetimibe, PCSK9 inhibitors, bempedoic acid, fibrates, niacin, and omega-3 fatty acids (Ray *et al.,* 2023; Ruscica *et al*., 2024).

Statins (HMG-CoA Reductase Inhibitors)

Statins remain the cornerstone of therapy. They inhibit hepatic HMG-CoA reductase, reducing cholesterol synthesis and upregulating LDL receptors, leading to decreased LDL-C levels (Grundy *et al*., 2023). Common examples include atorvastatin,

rosuvastatin, simvastatin, and pravastatin. Statins can reduce LDL-C by 30–60% and lower ASCVD risk significantly (Mach *et al*., 2020).

Adverse effects may include myalgia, elevated liver enzymes, and rarely rhabdomyolysis (Ruscica *et al*., 2024).

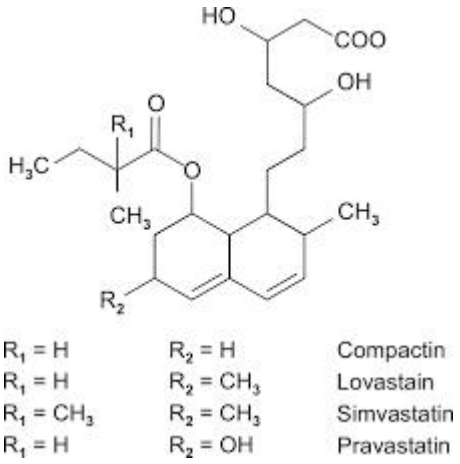

Figure 1 Structure of statin

Ezetimibe

Ezetimibe inhibits intestinal cholesterol absorption by blocking the Niemann–Pick C1-Like 1 (NPC1L1) transporter. It is often combined with statins to achieve further LDL-C reduction of 15–25% (Banach *et al*., 2022). By blocking this transporter, it decreases the intestinal uptake of dietary and biliary cholesterol. As a result, hepatic cholesterol stores are reduced, leading to upregulation of LDL receptors on hepatocytes and enhanced clearance of LDL from the blood (Ray *et al*., 2023).

Unlike statins, which inhibit cholesterol synthesis in the liver, ezetimibe targets the absorption pathway, making it a complementary therapy when used in combination

It is especially useful in patients intolerant to high-intensity statin therapy (Ray *et al*.,

2023). Ezetimibe is generally well tolerated. Reported side effects include mild gastrointestinal upset, fatigue, and elevated liver enzymes, particularly when used with statins (Ruscica *et al*., 2024). Rarely, myalgia and hypersensitivity reactions may o*cc*ur.

It is contraindicated in patients with active liver disease and should be used cautiously in pregnancy.

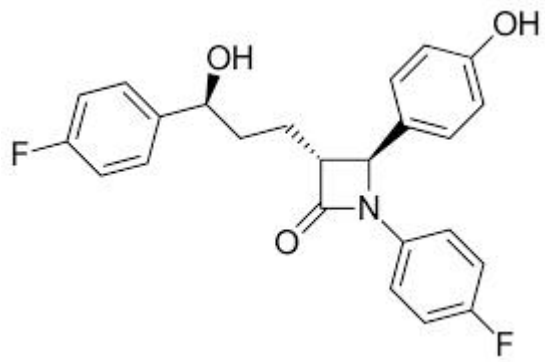

Figure 2 steucture of Ezetimibe

PCSK9 Inhibitors

Alirocumab and evolocumab are monoclonal antibodies that inhibit proprotein convertase subtilisin/kexin type 9 (PCSK9), preventing degradation of hepatic LDL receptors and promoting LDL clearance. They can reduce LDL-C by 50–60% beyond statin therapy (Sabatine *et al*., 2022).

These agents are indicated for familial hypercholesterolemia or patients with

atherosclerotic cardiovascular disease not achieving goals on statins and ezetimibe (Grundy *et al*., 2023)

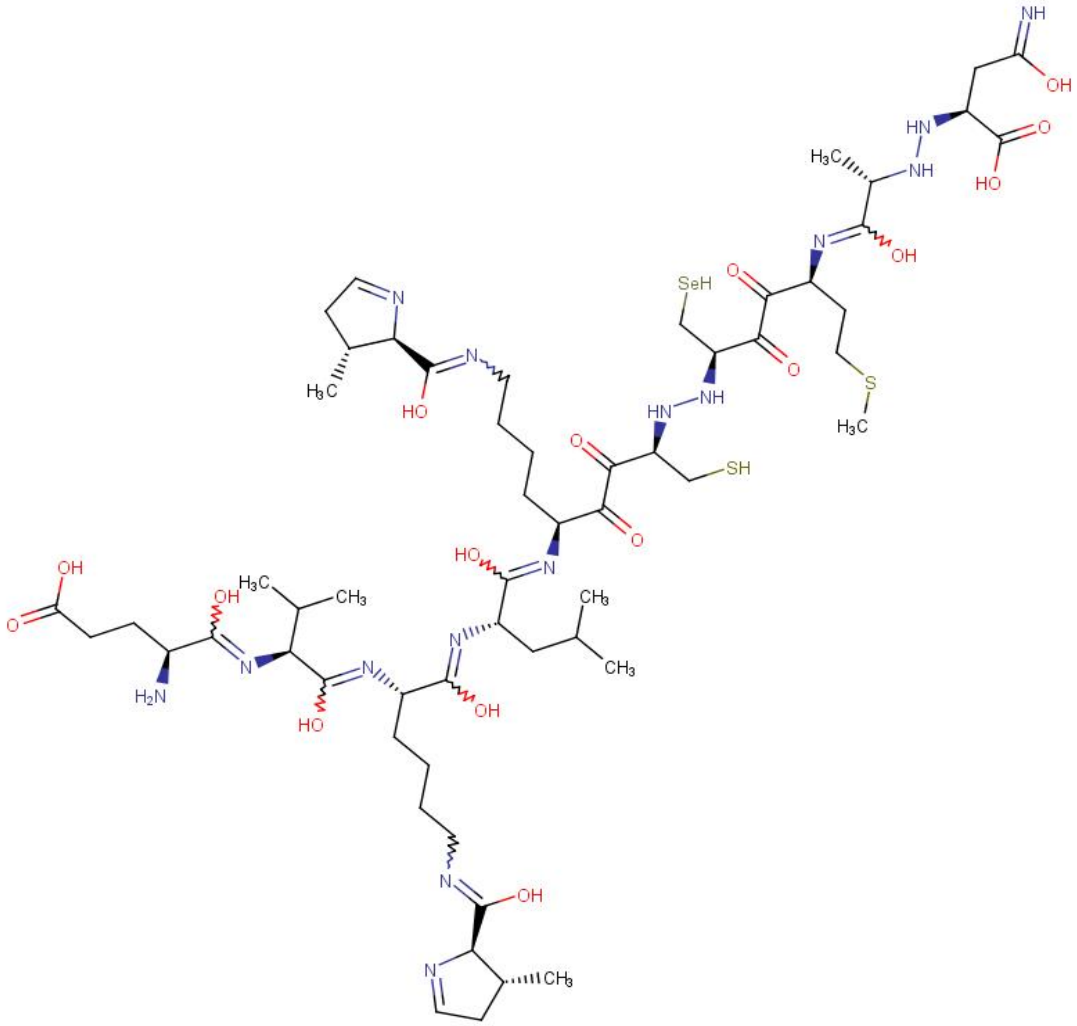

Figure 3 Strucure evolocumab

Bempedoic Acid

Bempedoic acid inhibits ATP-citrate lyase (ACL), an enzyme upstream of HMG-CoA reductase. It is approved for patients with statin intolerance or needing additional LDL reduction (Nissen *et al*., 2023).

It can lower LDL-C by about 18–25% and is often used in combination with ezetimibe (Ruscica *et al*., 2024).

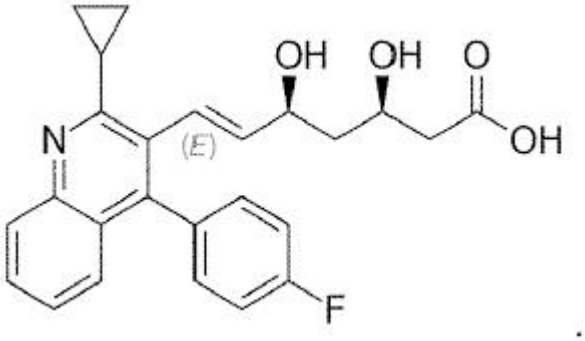

Figure 4 structure of Bempedoic Acid

Fibrates (PPAR-α Agonists)

Fenofibrate and gemfibrozil activate peroxisome proliferator-activated receptor-alpha (PPAR-α), increasing lipoprotein lipase activity, which enhances triglyceride clearance (Karr *et al*., 2021).

They reduce TG by 30–50% and are beneficial for patients with hypertriglyceridemia. However, they have limited effect on LDL-C and may increase the risk of myopathy when combined with statins (Banach *et al*., 2022).

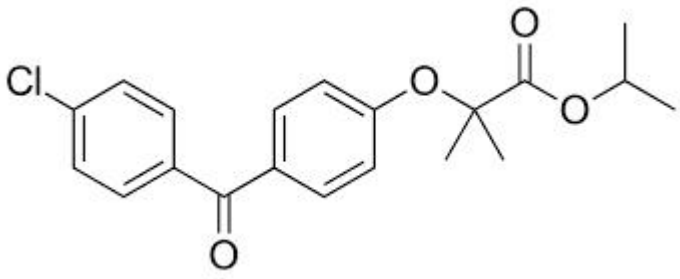

Figure 5 Structure of fenofibrate

Niacin (Nicotinic Acid)

Niacin reduces hepatic VLDL synthesis, lowering LDL-C and triglycerides while increasing HDL-C (Grundy *et al*., 2023).

However, its use has declined due to limited cardiovascular outcome benefits and adverse effects like flushing and hepatotoxicity (Ruscica *et al*., 2024).

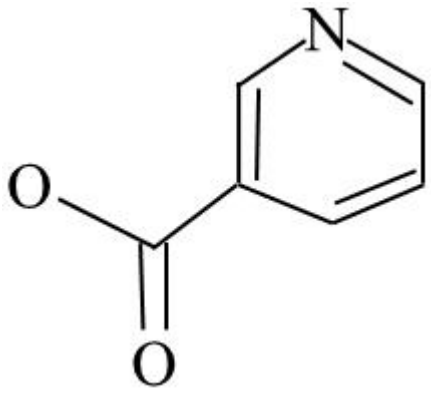

Figure 6 structure of niacin

Omega-3 Fatty Acids

Omega-3 ethyl esters (e.g., icosapent ethyl) reduce hepatic VLDL-triglyceride synthesis and are indicated for severe hypertriglyceridemia (>500 mg/dL) (Bhatt *et al*., 2019; Banach *et al*., 2022).

They can lower triglycerides by 20–50% and have been associated with reduced cardiovascular events in high-risk patients.

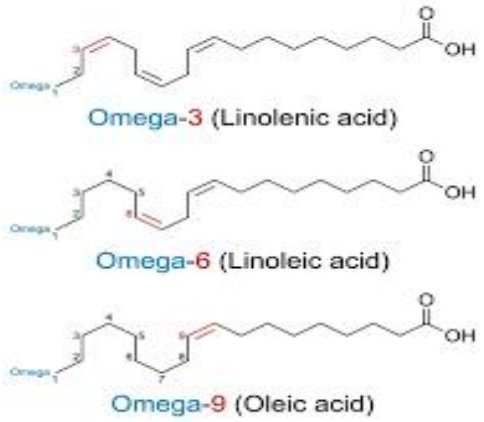

Figure 7 structures of omega 3 ethyl esters

Combination and Emerging Therapies

Combination therapy (e.g., statin + ezetimibe or statin + PCSK9 inhibitor) enhances lipid control in patients who do not reach LDL-C targets on monotherapy (Ray *et al*., 2023).

Emerging agents include inclisiran, a small interfering RNA (siRNA) that inhibits hepatic PCSK9 synthesis, offering long-term LDL reduction with twice-yearly dosing (Ray *et al*., 2023).

1.5. Traditional and Herbal Approaches to Hyperlipidemia

Herbal and traditional medicines remain widely used worldwide to prevent and manage metabolic disorders including hyperlipidemia. Many plants used in ethnomedicine contain bioactive phytochemicals (flavonoids, phenolics, terpenes, sterols) that improve lipid metabolism through antioxidant activity, inhibition of

intestinal cholesterol absorption, modulation of hepatic lipid synthesis, and enhancement of lipolysis. Integrating evidence from preclinical and recent human studies supports the role of selected herbs as adjuncts in hyperlipidemia care. PMC+1.

Ocimum gratissimum (Scent Leaf)

Figure 8 image of Ocimum gratissimum

Taxonomy and Common Name

Family: Lamiaceae

Genus & species: *Ocimum gratissimum* L.

Common names: Scent leaf, African basil, “Efirin gbami” in Yoruba (Nigeria) (Patil *et al*., 2023).

Plant and Geographical Distribution

Ocimum gratissimum is indigenous to tropical Africa and has been introduced widely into tropical Asia. It grows as a perennial shrub in warm climates and is common in Nigeria, Ghana, and India (Obsa *et al*., 2022).

Phytochemical Profile

Phytochemical screening of *O. gratissimum* has shown the presence of flavonoids, tannins, saponins, terpenoids, cardiac glycosides, and steroids (Akinmoladun *et al*., 2025). A comparative GC-MS study found numerous phytochemicals including volatile compounds, phenolics, vitamins, and minerals in *O. gratissimum* leaf extracts (Umoh & Effiong, 2024).

Evidence for Lipid-Lowering Activity and Mechanism

In diabetic rat models, *O. gratissimum* leaf extract produced significant reductions in serum triglycerides, total cholesterol, and LDL while increasing HDL, indicating hypolipidemic activity (Sani *et al*., 2021). These effects are attributed to antioxidant flavonoids and modulation of hepatic lipid enzymes.

Limitations

Most evidence is preclinical, with few human studies and limited data on standardized dosage and long-term safety (Ruscica *et al*., 2024).

Laurus nobilis (Bay Laurel)

Figure 9 image ofLaurus nobilis

Taxonomy and Common Name

Family: Lauraceae

Genus & species: *Laurus nobilis* L.

Common names: Bay laurel, Sweet bay (Khdhir *et al*., 2024).

Plant and Geographical Distribution

An aromatic evergreen shrub native to the Mediterranean region; cultivated in Europe, North Africa, and Western Asia (Anonymous, 2024).

Phytochemical Profile

Essential oil components include 1,8-cineole, linalool, and α-terpineol; leaves also contain rutin, quercetin, and other polyphenols (Anonymous, 2024).

Evidence for Lipid-Lowering Activity and Mechanism

In Triton WR-1339-induced dyslipidemic rats, *L. nobilis* essential oil (80 mg/kg) lowered total cholesterol and triglycerides and improved atherogenic indices (Anonymous, 2024). Mechanisms include antioxidant and anti-inflammatory effects of its monoterpenes (Duru *et al*., 2023).

Limitations

Human data remain limited; essential oils may cause mucosal irritation or mild hepatotoxicity at high doses (Khdhir *et al*., 2024).

1Cymbopogon citratus (Lemongrass)

Figure 10 image of Cymbopogon citratus

Taxonomy and Common Name

Family: Poaceae

Genus & species: *Cymbopogon citratus* (DC.) Stapf

Common names: Lemongrass, Citronella grass (Naz *et al*., 2024).

Plant and Geographical Distribution

Native to tropical Asia (India, Sri Lanka) and widely cultivated in tropical/subtropical regions across Africa and Latin America (Assis Júnior *et al*., 2024).

Phytochemical Profile

Contains polyphenols (luteolin, luteolin-7-O-glucoside), flavonoids, tannins, and essential oils rich in citral (Naz *et al*., 2024).

Evidence for Lipid-Lowering Activity and Mechanism

Phenolic compounds from *C. citratus* disrupt micellar cholesterol solubility, reducing intestinal absorption (Mdpi, 2023). In animal studies, lemongrass extract improved lipid profiles and showed antioxidant effects (Assis Júnior *et al*., 2024).

Limitations

Evidence is mostly from in vitro and animal models; high doses of essential oil can irritate gastric mucosa (Ruscica *et al*., 2024).

Psidium guajava (Guava)

Figure 11 image of Psidium guajava

Taxonomy and Common Name

Family: Myrtaceae

Genus & species: *Psidium guajava* L.

Common names: Guava (Huynh *et al*., 2025).

Plant and Geographical Distribution

Native to tropical America but widely cultivated in Africa and Asia (Huynh *et al*., 2025).

Phytochemical Profile

Contains flavonoids (quercetin, guaijaverin, avicularin), tannins, phenolic acids, and phytosterols (β-sitosterol) (Mdpi, 2021).

Evidence for Lipid-Lowering Activity and Mechanism

Guava leaf extract reduces total cholesterol, LDL, and triglycerides while raising HDL through antioxidant and enzyme modulatory effects (Huynh *et al*., 2025). Phytosterols in the leaves inhibit cholesterol absorption and enhance bile acid excretion (Mdpi, 2020).

Limitations

Few human trials exist; high concentrations of leaf extract may cause mild gastrointestinal discomfort (Ruscica *et al*., 2024).

Piper guineense (African Black Pepper / Uziza)

Taxonomy and Common Name

Family: Piperaceae

Genus & species: *Piper guineense* Schumach. & Thonn.

Common names: West African Black Pepper, Ashanti Pepper, Uziza (Olajide *et al*., 2024).

Plant and Geographical Distribution

Native to West and Central Africa; widely used as a spice and medicinal plant in Nigeria, Ghana, and Cameroon (Olajide *et al*., 2024).

Phytochemical Profile

Contains alkaloids (piperine), flavonoids, phenolics, essential oils, and sterols (Medical Laboratory Journal, 2023).

Evidence for Lipid-Lowering Activity and Mechanism

P. guineense extract significantly reduces total cholesterol and triglycerides and improves HDL in hypercholesterolemic animal models (Olajide *et al*., 2024). Piperine enhances antioxidant defense and modulates lipid metabolic enzymes.

Limitations

Scarcity of human studies and standardized dosages; piperine can interact with cytochrome P450 enzymes, affecting drug metabolism (Nwanna *et al*., 2023).

LIMITATION OF HERBAL APPROACH

The five plants (*Ocimum gratissimum, Laurus nobilis, Cymbopogon citratus, Psidium guajava,* and *Piper guineense*) share bioactive compounds such as flavonoids, phenolics, terpenes, and phytosterols with documented antioxidant and lipid-modulating properties. They reduce LDL and triglycerides and increase HDL by inhibiting cholesterol absorption, suppressing lipid synthesis, and enhancing antioxidant defense systems (Huynh *et al*., 2025; Naz *et al*., 2024). However, major limitations include a paucity of human clinical trials, non-standardized extracts, and limited toxicological data (Ruscica *et al*., 2024). Future research should focus on dose standardization and clinical validation to support their integration with conventional therapy (Grundy *et al*., 2023

1.6. Justification of the Study

Diets rich in trans fats have been identified as major contributors to hyperlipidemia and cardiovascular diseases due to their ability to elevate low-density lipoprotein (LDL) cholesterol and lower high-density lipoprotein (HDL) cholesterol levels. In Nigeria, food insecurity and the high cost of healthy cooking oils have forced many households and food vendors to rely heavily on cheap, processed oils and fats that often contain trans fats. This dietary pattern significantly increases the risk of lipid disorders and related metabolic complications. Although the World Health Organization (WHO) set a global target to eliminate industrially produced trans fats by 2023, studies have shown that many fast foods and baked products in Nigeria still

contain considerable levels of these harmful fats (Agharaye *et al*., 2022; Huang *et al*., 2023).

Given the persistent presence of trans fats in commonly consumed foods and the economic realities of food insecurity, complete elimination of trans fats from the Nigerian diet may not be immediately feasible. Therefore, a more practical and culturally relevant approach is to identify and utilize locally available vegetables and herbs with proven lipid-lowering potentials as adjuncts in food preparation. These herbs could help reduce the negative impact of trans fat consumption while improving lipid profiles and overall cardiovascular health. This study is thus justified as it aims to evaluate the lipid-lowering potentials of selected herbs, providing scientific evidence that could inform dietary recommendations and public health strategies in Nigeria (WHO, 2018; Marklund *et al*., 2024)

1.7. Statement of the Problem

Despite global efforts to eliminate industrially produced trans fats, including the World Health Organization's REPLACE initiative, these fats remain present in many fast and processed foods consumed in Nigeria. Food insecurity and economic hardship have led many households and food vendors to depend on cheap cooking fats and oils that often contain trans fats. Consequently, complete elimination of trans-fat-containing foods may be unrealistic for vulnerable populations, as affordability and accessibility remain key concerns in achieving dietary balance.

This situation necessitates the exploration of alternative strategies—such as the incorporation of locally available vegetables and herbs with lipid-lowering potentials—into trans-fat-containing meals. These plant-based ingredients may help mitigate the negative lipid effects of trans-fat consumption while supporting food security and sustainable nutrition. Therefore, this study seeks to determine the lipid-lowering potential of selected herbs commonly used in Nigerian diets as a practical approach to managing hyperlipidemia within the context of persistent trans-fat exposure and food insecurity (WHO, 2018; Agharaye *et al*., 2022; Huang *et al*., 2023; Marklund *et al*., 2024).

1.8. Drug discovery

Drug discovery is the scientific process through which new therapeutic substances are identified, designed, and developed to prevent or treat diseases. It involves understanding the biological basis of a disease, identifying potential molecular targets such as enzymes or receptors, and screening chemical or natural compounds that can modulate those targets to produce a desired therapeutic effect. The process integrates disciplines such as biochemistry, pharmacology, medicinal chemistry, and computational biology. Modern drug discovery often begins with target identification and validation, followed by hit identification, lead optimization, and preclinical testing before a candidate drug progresses to clinical trials (Sliwoski *et al*., 2023; Hughes *et al*., 2022).

Over the past decade, drug discovery has evolved from traditional trial-and-error methods to more precise, mechanism-based approaches supported by advances in

genomics, bioinformatics, and artificial intelligence. Computer-aided drug design, in particular, has enhanced the ability to predict molecular interactions and optimize drug candidates efficiently, thereby reducing development time and cost. In addition, natural products, including plant-derived compounds, continue to play a vital role in discovering bioactive molecules with novel mechanisms of action. Overall, drug discovery serves as the foundation of pharmaceutical innovation and global health improvement by translating basic scientific knowledge into effective and safe therapeutic agents (Paul *et al*., 2021; Wang *et al*., 2020).

1.8.Key steps in drug identification

Target Identification and Validation

This is the foundational step in drug discovery, where researchers identify a specific biological molecule (such as an enzyme, receptor, or gene product) that plays a critical role in disease development. Once identified, the target is validated to confirm that modulating its activity can influence the disease process. Advanced technologies such as genomics, proteomics, and bioinformatics are commonly used at this stage to understand disease pathways and ensure that the selected target is both relevant and druggable (Hughes *et al*., 2022).

Hit Identification (Screening and Selection)

After a target is validated, potential compounds, known as “hits,” are identified that can bind to and modulate the target’s function. This is achieved using techniques such

as high-throughput screening, virtual screening, and fragment-based drug design. Computational methods and artificial intelligence now play a crucial role in predicting molecular interactions and acclerating hit discovery (Sliwoski *et al*., 2023).

Lead Optimization

In this stage, the identified hits are chemically modified to improve their pharmacological properties. Lead optimization focuses on enhancing potency, selectivity, absorption, distribution, metabolism, and excretion (ADME) profiles while reducing toxicity. The goal is to produce a compound with the best balance of safety and efficacy that can be taken forward into preclinical studies (Wang *et al*., 2020).

Preclinical Testing

Preclinical studies involve evaluating the optimized drug candidates in laboratory (in vitro) and animal (in vivo) models. These studies assess pharmacodynamics (how the drug affects the body), pharmacokinetics (how the body affects the drug), and toxicology to predict safety and efficacy in humans. Only compounds that demonstrate a*cymbopogon citratus*eptable safety margins and desirable biological activity proceed to human clinical trials (Paul *et al*., 2021).

Clinical Trials

Clinical development occurs in three major phases—Phase I, II, and III.

Phase I focuses on assessing the safety, tolerability, and pharmacokinetics of the drug in a small group of healthy volunteers.

Phase II evaluates the efficacy and optimal dosing in a larger group of patients with the target disease.

Phase III confirms the drug's effectiveness and monitors adverse reactions in diverse populations.

Clinical trials are essential for providing the data required by regulatory authorities to determine whether the drug can be approved for public use (Hughes *et al*., 2022; Stokes *et al*., 2020).

Regulatory Approval and Post-Market Surveillance

After successful clinical trials, a comprehensive dossier containing all preclinical and clinical data is submitted to regulatory agencies such as the U.S. Food and Drug Administration (FDA) or Nigeria's National Agency for Food and Drug Administration and Control (NAFDAC). Once approved, the drug is marketed and continues to be monitored for long-term safety and effectiveness in the general population. This stage ensures that any rare or delayed adverse effects are detected and managed appropriately (Paul *et al*., 2021).

1.9. Computer-Aided Drug Design (CADD)

Computer-Aided Drug Design (CADD) refers to the application of computational techniques in the discovery, design, and optimization of therapeutic molecules. It uses structural and chemical data to predict how potential drugs interact with biological targets, estimate their binding affinities, and optimize their pharmacological properties before laboratory testing. CADD helps streamline the drug development process by reducing time, cost, and experimental workload while increasing the likelihood of success (Agu *et al*., 2023; Wang *et al*., 2024).

There are two main approaches in CADD: structure-based drug design (SBDD) and ligand-based drug design (LBDD). Structure-based methods use the three-dimensional structure of a biological target, such as a protein obtained from X-ray crystallography or cryo-electron microscopy, to design molecules that can bind to its active site. Ligand-based methods, on the other hand, rely on knowledge of known active compounds to develop pharmacophore models or quantitative structure–activity relationships (QSAR) that predict biological activity (Alshehri *et al*., 2023). Common computational tools used in CADD include molecular docking, which predicts how a small molecule fits into a target protein's active site, and virtual screening, which evaluates large compound libraries to identify molecules with the highest predicted affinity. Other techniques include molecular dynamics (MD) simulations, used to study the stability and conformational flexibility of protein–ligand complexes over time, and in silico ADMET (Absorption, Distribution, Metabolism, Excretion, and Toxicity) prediction, which helps assess pharmacokinetic and safety profiles before in vitro testing (Sliwoski *et al*., 2023; Agu *et al*., 2023).

Recent advances in artificial intelligence (AI) and machine learning (ML) have revolutionized CADD. Deep learning algorithms can now predict biological activity, desired physicochemical properties (Paul *et al*., 2020; Dhudum *et al*., 2024). Furthermore, AI-based protein structure prediction tools such as AlphaFold have significantly enhanced the ability of researchers to model drug–target interactions accurately (Wang *et al*., 2024).

Despite its advantages, CADD has limitations. The accuracy of computational predictions depends heavily on the quality of input data, including protein structures and ligand conformations. Moreover, computational models may not fully capture biological complexity such as allosteric modulation or in vivo metabolism. Therefore, computational predictions must be complemented with experimental validation to ensure reliability. When effectively integrated, however, CADD remains one of the most powerful and cost-effective tools in modern drug discovery (Alshehri *et al*., 2023; Wang *et al*., 2024).

1.10. AIM OF THE STUDY

The aim of the study is to assess the probable lipid lowering activity of the phytochemical constituents of C*ymbopogon citratus*, *Laurus nobilis, , Piper guineense,* and *Psidium guajava* using *in silico* methods.

1.11. SPECIFIC OBJECTIVES

1. To identify and compile the comprehensive phytochemical constituents of the five selected vegetables from peer-reviewed literature and publicly accessible chemical databases.

2. To retrieve the two-dimensional (2D) or three-dimensional (3D) structured data files (SDF) of the identified phytochemical ligands from chemical databases such as PubChem.

3. To obtain the crystal structures of established therapeutic target proteins from the Protein Data Bank (PDB) to serve as receptors for docking.

4. To perform site-specific molecular docking of the phytoconstituents against the selected ligands.

5. To predict the Absorption, Distribution, Metabolism, Excretion, and Toxicity (ADMET) properties of the promising ligands using ADMETLAB.

6. To conduct post-docking analysis of the resulting ligand-protein complexes of the ligands using better binding affinities and relative safety

.

CHAPTER TWO: MATERIALS AND METHODS

2.1. MATERIALS

The materials for the in silico investigation of treatment and management of hyperlipidemia include:

2.1.1. Computer System

Image of a laptop

A computer system with the following specifications was used:

Operating system: Windows 10 Pro

Processor: Core i5, 2.40GHz

RAM: 16GB

System type: 64-bit

Mouse: External pointing device

2.1.2 **Databases**

2.1.2.1. PubChem

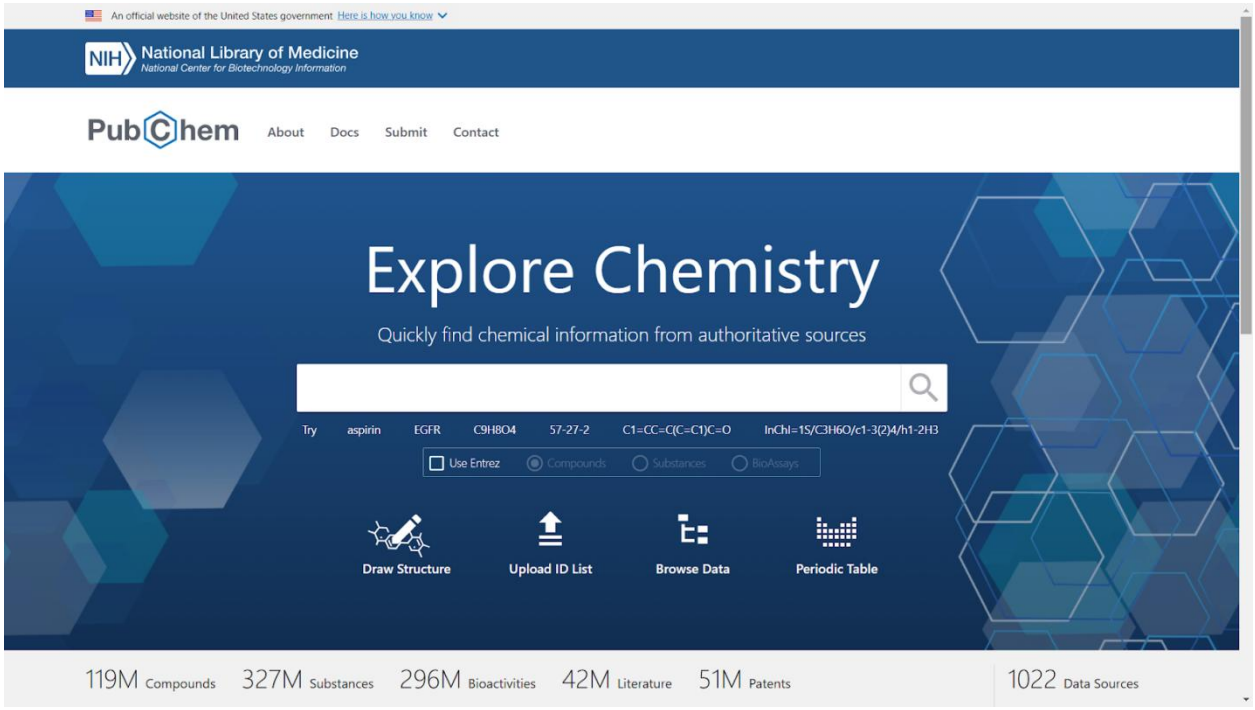

Image of pubchem

Website:https://pubchem.ncbi.nlm.nih.gov/

PubChem is a publicly a*cymbopogon citratus*essible chemical information database designed to support drug discovery and research *(*Wang *et al.,* 2009). It provides comprehensive data on small molecules, including their chemical structures, properties, and bioactivities, making it an essential resource for researchers exploring drug design and molecular interaction s (Li *et al., 2*010*).* In this study, PubChem was utilized to retrieve structural data files (SDF) for phytochemicals derived from the investigated plants and reference hypolipidemic activity. These SDF files were integral to molecular docking analyses, enabling the evaluation of interactions between the compounds and their target receptors. By offering detailed molecular

information, PubChem facilitates the assessment of bioactivity and the identification of potential therapeutic agents, including hypolipidemic activity.

2.1.2.2. Protein Data Bank (PDB)

Image of PDB

Website:https://www.rcsb.org/

The Protein Data Bank (PDB) is an essential global repository that provides a*cymbopogon citratus*ess to 3D structural data of biological macromolecules such as proteins, nucleic acids, and their complexes (Berman *et al., 2000)*. This repository supports a wide range of research in molecular modeling, drug discovery, structural bioinformatics, and related fields by delivering experimentally determined structures alongside computed structure models *(*Burley *et al.,* 2020; Burley *et al.,* 2022*)*. The structural data in PDB facilitates the study of macromolecular architecture, function, and interactions, enabling advancements in biomedicine and bioengineering *(*Burley *et al.,* 2020; Ballante *et al.,* 2021*)*.

In this study, the PDB was utilized to retrieve the 3D crystal structures of hydroxyl methyl glutaryl CoA (HMG-CoA), proliferator activated receptor (PPAR), negatively

charged bile acid, hydroxylcarboxylic acid (HM7A4), niemann- pick C1 protein (NCP1L1), proprotein convertase subtilisin/kexin type 9 (PCSK9) proteins. These receptor structures are crucial for molecular docking simulations, which aim to analyze the interactions between plant-derived compounds and target proteins. This approach supports the identification of potential hypolipidemic agents by providing insights into the binding affinities and mechanisms of the compounds under investigation.

2.1.2.3. SwissADME

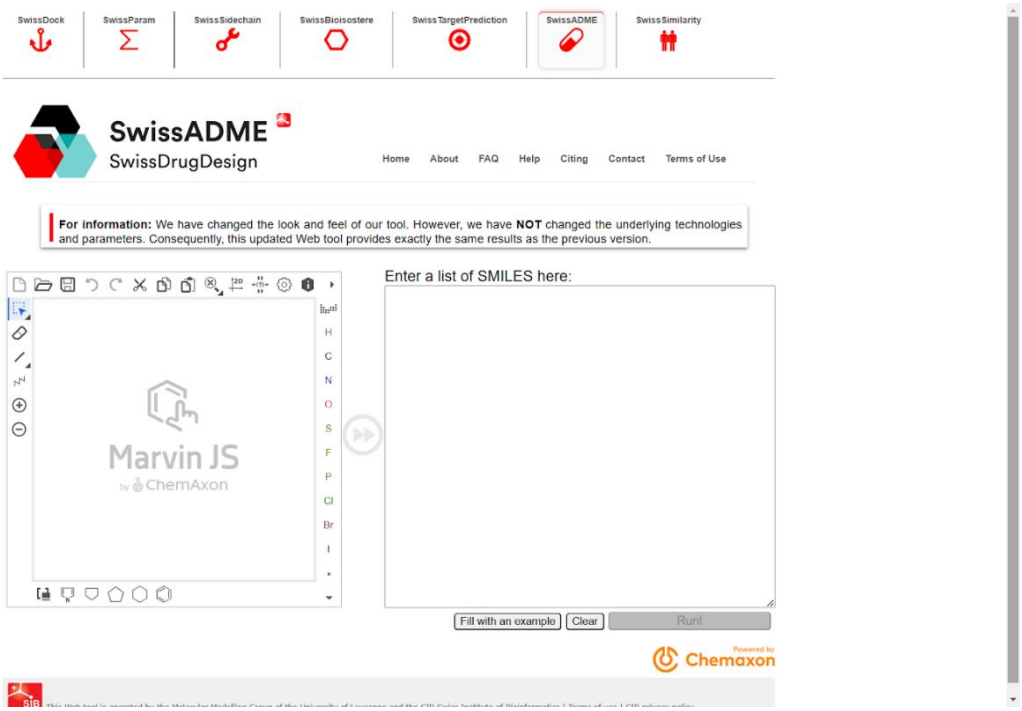

Image of swiss adme

Website: http://www.swissadme.ch/

SwissADME is a freely available web-based tool designed to evaluate the absorption, distribution, metabolism, excretion, and toxicity (ADMET) properties of chemical compounds. It also assesses drug-likeness and medicinal chemistry friendliness using parameters such as molecular weight, lipophilicity, solubility, and bioavailability (Daina *et al.,* 2017). SwissADME plays a critical role in predicting the pharmacokinetic and physicochemical profiles of compounds, offering researchers insights into their potential as therapeutic agents.

In this study, SwissADME was utilized to predict the ADMET properties and drug-likeness of plant ligands under investigation. This evaluation is crucial for identifying compounds with favorable pharmacological characteristics, such as optimal bioavailability and reduced toxicity. By combining these assessments with other tools,

such as SWISS-MODEL for homology modeling of protein structures (Waterhouse *et al., 2018;* Bienert *et al.,* 2016*)*, SwissADME helps streamline the selection of plant-derived molecules with the highest likelihood of exhibiting desirable hypolipidemic activity.

2.1.2.4. ProTox-II

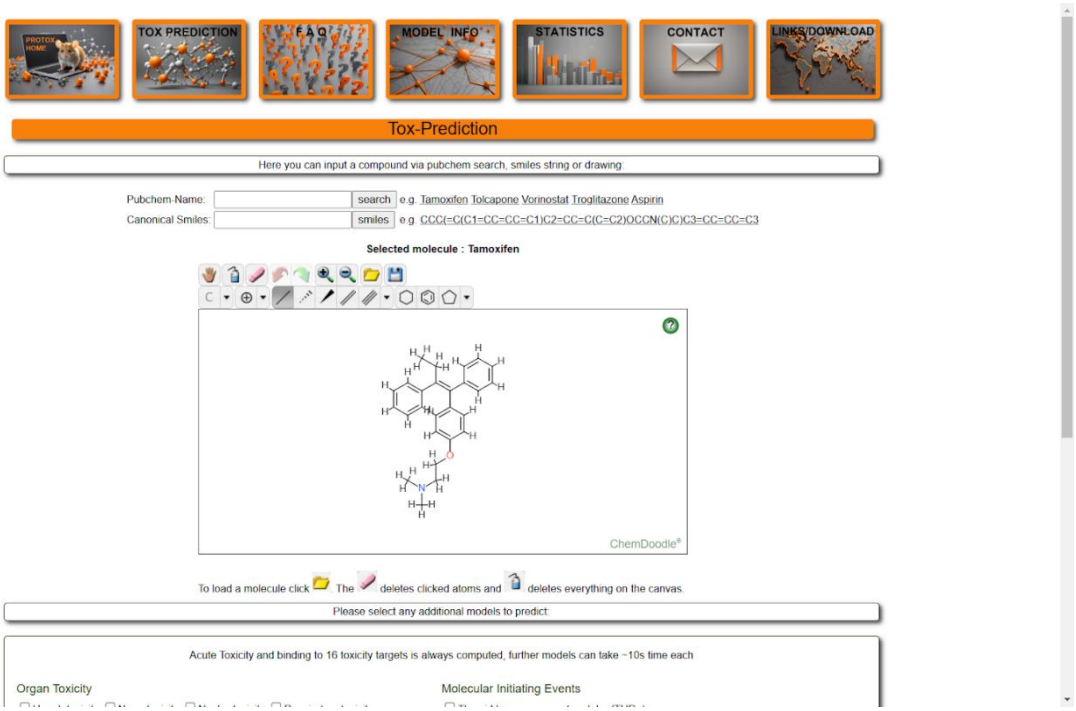

Image of protox-ii

Website:https://tox-new.charite.de/protox_II/

ProTox-II is a state-of-the-art web-based platform designed for in silico prediction of the toxicity profiles of chemical compounds. Leveraging advanced computational algorithms and machine learning models, it predicts a wide range of toxicity endpoints, including acute toxicity, hepatotoxicity, immunotoxicity, mutagenicity, and cytotoxicity (Banerjee *et al.,* 2018). Additionally, it classifies compounds into toxicity classes and provides estimates for LD50 values, enhancing the understanding of toxicological pathways and risk profiles *(*Drwal *et al.,* 2014).

This tool is an invaluable resource in drug discovery and development, allowing researchers to evaluate the safety of candidate molecules early in the research process. By offering detailed insights into the potential toxic effects of compounds, ProTox-II facilitates the identification of safer and more promising therapeutic agents.

In this study, ProTox-II was employed to predict the toxicity profiles of the plant ligands under investigation. The tool provided critical data on acute toxicity, hepatotoxicity, and other toxicological properties, enabling a comprehensive assessment of the safety of these compounds. By integrating ProTox-II's toxicity predictions, the study identified plant-derived ligands with a*cymbopogon citratus*eptable safety profiles, supporting their potential as viable candidates for further development as hypolipidemic agents.

2.1.3. Software

2.1.3.1. Maestro (Schrödinger Suite)

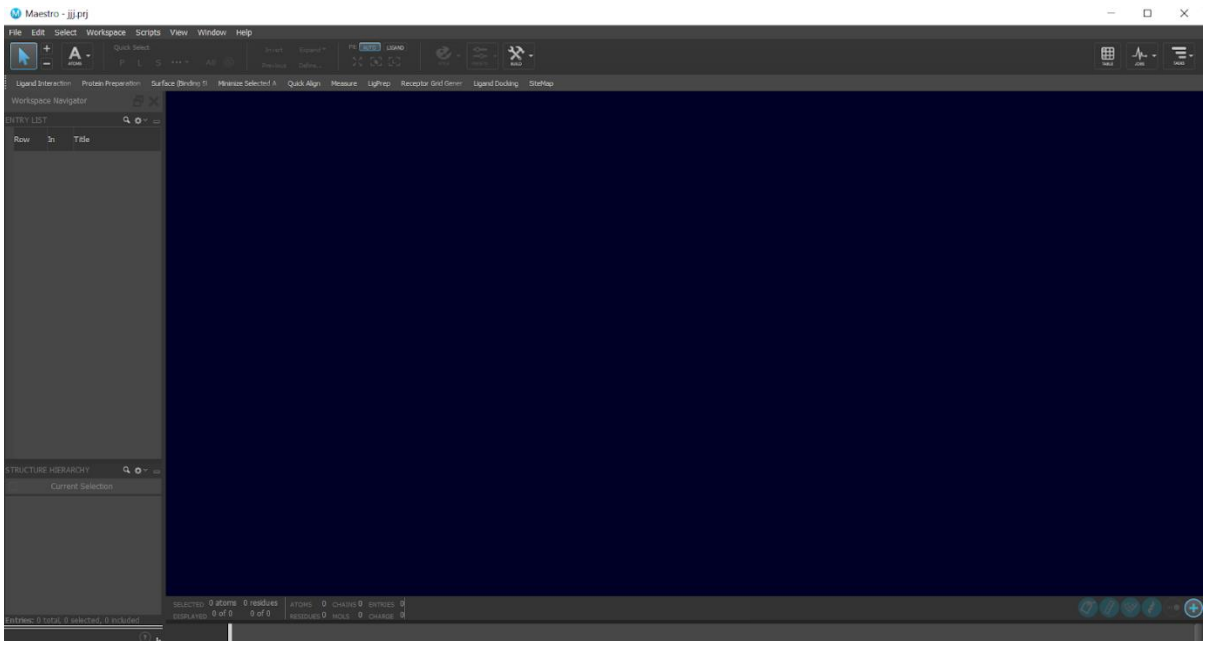

Image of maestro software

Maestro, part of the Schrödinger Suite, is a comprehensive software platform designed for computational drug discovery and molecular modeling. It provides an integrated environment with advanced tools for ligand and protein preparation, virtual screening, docking simulations, and post-docking analysis. Its modules allow users to optimize molecular structures, predict ligand-receptor interactions, and analyze binding affinities with precision (Kwon *et al.,* 2020; Laimer *et al*., 2015).

In this study, Maestro was utilized for the preparation and optimization of both ligands and receptor proteins to ensure the a*cymbopogon citratus*uracy of docking simulations. The software's robust capabilities for post-docking analysis were instrumental in refining molecular interactions and evaluating binding affinities between plant-derived ligands and dopaminergic or serotonergic receptors. This approach was pivotal in identifying bioactive compounds with potential antipsychotic properties *(*Kwon *et al.,* 2020*)*. The docking study employed a sequential use of

HTVS, SP, and XP docking protocols. HTVS served as a broad screening tool, while SP and XP docking provided more precise simulations to identify optimal candidates based on their binding energy and interactions *(*James *et al.,* 2021; Kumar *et al.,* 2022; Yadav *et al.,* 2021*)*

Maestro's versatility and high computational efficiency make it a valuable tool in the field of molecular docking and structure-based drug design, contributing significantly to the discovery and analysis of therapeutic agents (Laimer *et al.,* 2015).

2.1.3.2 Graph pad prism

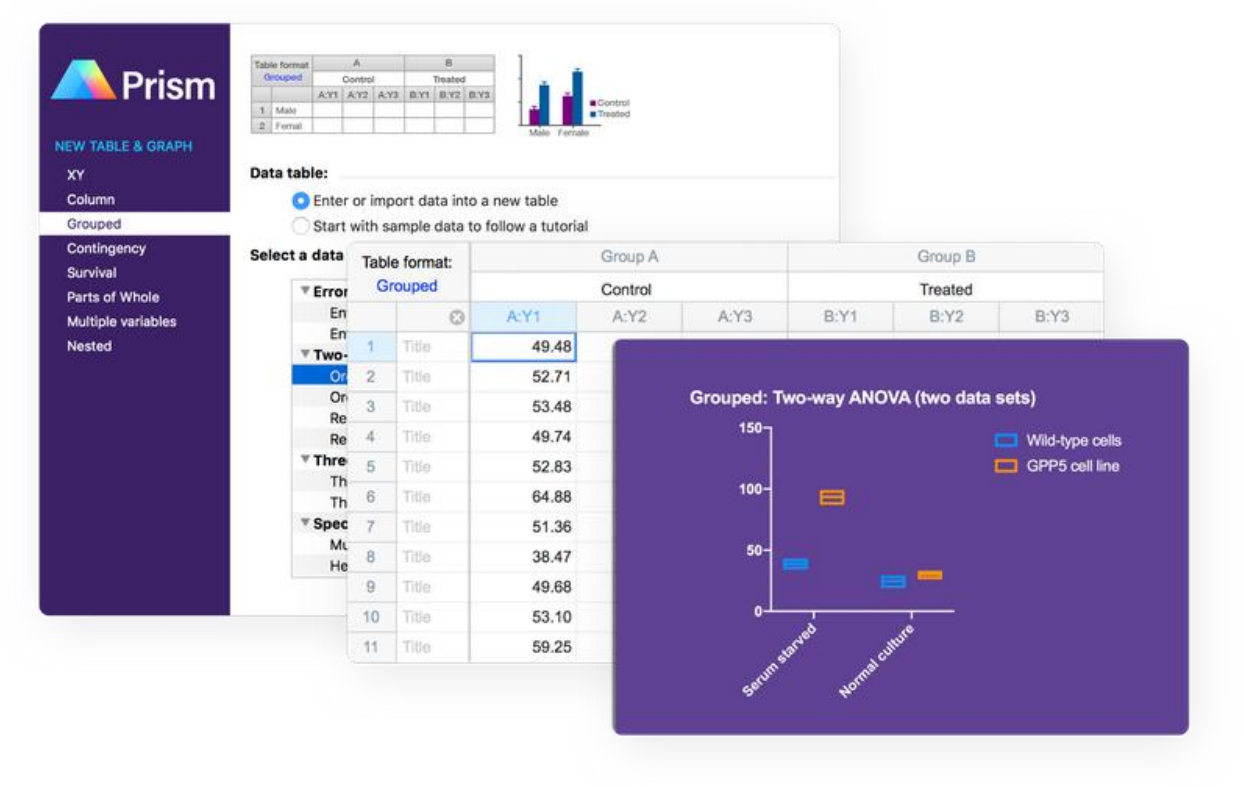

Image of graph pad prism

GraphPad Prism is a widely used scientific software designed for statistical analysis, data visualization, and graphing, particularly in biological and pharmaceutical research. It combines powerful statistical tools with an intuitive interface, making it a*cymbopogon citratus*essible for both beginners and advanced researchers. Unlike traditional spreadsheet software, GraphPad Prism simplifies complex statistical analyses, offering built-in templates, guided analysis, and automated graphing options. In molecular docking and in-silico studies, GraphPad Prism is particularly useful for comparing docking scores, visualizing trends, and identifying lead compounds. The heatmap feature, for example, allows researchers to assess binding affinities through color-coded representations, making data interpretation more intuitive. Furthermore,

its ability to export high-quality graphs in multiple formats ensures seamless integration into research papers, presentations, and reports.

2.2. METHOD

2.2.1. Ligand Selection and Preparation

Phytochemical ligands were selected from five Nigerian medicinal plants traditionally used for hyperlipidemia. These plants include *Ocimum gratissimum, Laurus nobilis, Cymbopogon citratus, Psidum guajava and Piper guineense*, based on their reported therapeutic applications. The chemical structures of these ligands were retrieved in SDF format from the PubChem database.

Reference compounds representing hypolipidemic agents were sourced from PubChem and used as standards for comparative docking analysis. These reference compounds include simvastatin, lanifibranor, pemafibrate, PCSK9 inhibitor, niacin, ezetimibe with their corresponding PubChem IDs as follows; simvastatin (54454), lanifibranor(68677842), pemafibrate (11526038), PCSK9 inhibitor, niacin (71558), ezetimibe (150311).

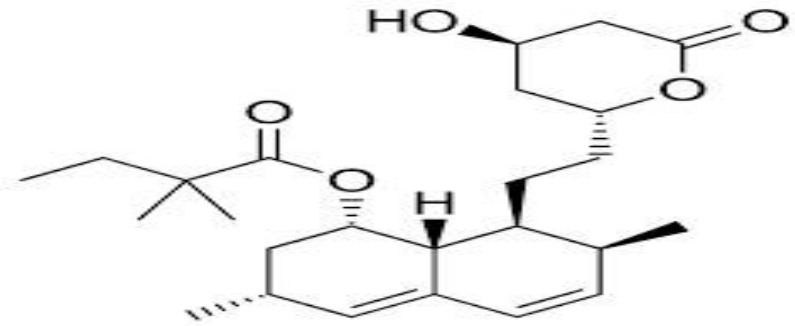

Image of simuvastatin.

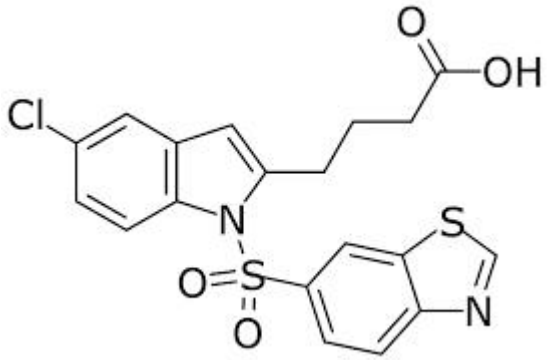

Image of lanifibranor.

Image of pemafibrate.

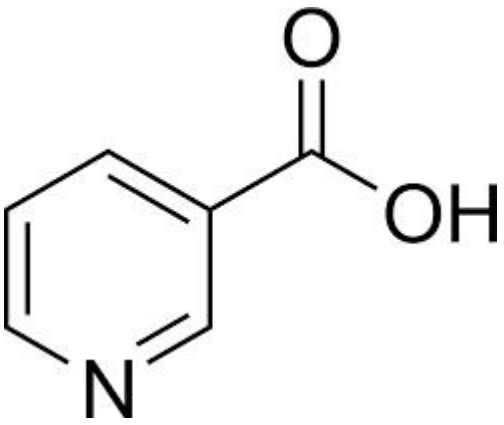

Image of niacin

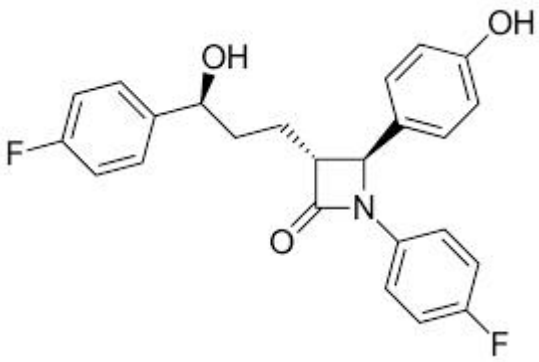

Image of ezetimibe.

These reference compounds serve as controls to assess the docking scores and interactions with key receptors involved in hyperlipidemia, allowing for a comparative evaluation of the plant ligands' potential hypolipidemicactivity.

Ligand Preparation Process

1. Ligand Structure Generation

The initial step involved generating the chemical structures of the selected phytochemicals. The structures were retrieved from PubChem and saved in SDF format for computational analysis.

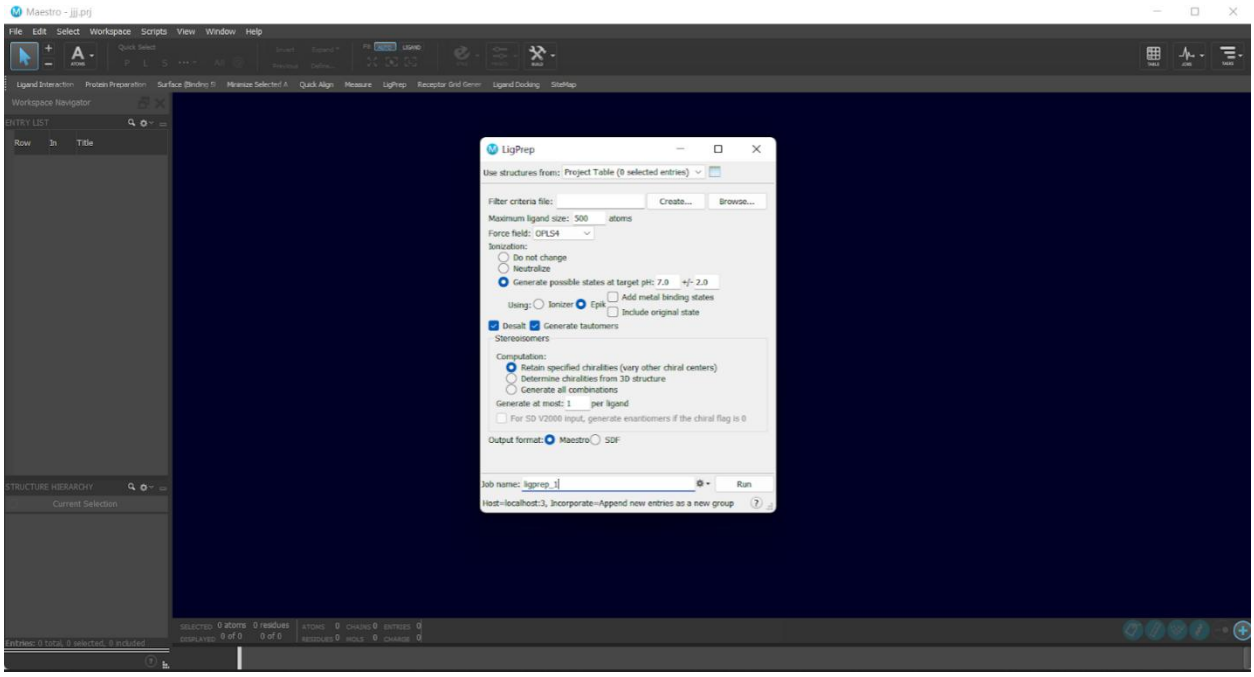

Image of ligprep on maestro

2. Ligand Optimization Using LigPrep

To ensure a*cymbopogon citratus*urate molecular docking, ligands were prepared using the LigPrep module in Maestro (Schrödinger Suite). This module was employed to:

Generate 3D structures of the ligands

Optimize ligand geometry

Assign correct ionization states at physiological pH

Generate relevant tautomeric and stereoisomeric forms

This step ensured that all ligands were correctly represented for docking studies (Shri, Nayak, & Pai, 2024*)*.

2.2.2. Protein Selection and Preparation

The hydroxyl methyl glutaryl CoA (HMG-CoA), proliferator activated receptor (PPAR), negatively charged bile acid, hydroxylcarboxylic acid (HM7A4), niemann-pick C1 protein (NCP1L1), proprotein convertase subtilisin/kexin type 9 (PCSK9) proteins were selected as targets due to their pivotal roles in the pathophysiology of hyperlipidemia and their frequent targeting by hypolipidemic drugs. The crystal structures of these receptors were obtained from the Protein Data Bank (PDB), with the following PDB IDs: HMG-CoA (54454), PPAR(7WGN), HM7A4 (8IJA), NCP1L1 (150311), PCSK9 () proteins

\

Protein Selection Using PDB

Selecting the appropriate protein structure is a critical step in in silico drug discovery. Multiple crystal structures may exist for the same protein, and selecting the most relevant structure involves evaluating factors such as resolution, completeness, and biological relevance (Murumkar *et al.,* 2022). A systematic approach is necessary to ensure that the selected structure is suitable for molecular docking and other computational studies.

Protein Preparation Using Maestro

The receptor structures were prepared for molecular docking using the Protein Preparation Wizard in Maestro, a widely used tool for refining PDB structures in computational drug discovery *(*Shri, Nayak, and Pai, 2024*)*. The preparation steps included:

1. Assigning bond orders and optimizing hydrogen-bonding networks
2. Adding hydrogen atoms and ensuring proper titration states
3. Removing water molecules beyond 5 Å from the binding site
4. Minimizing the receptor structures to enhance energy stability (Martínez-Rosell, Giorgino, and Fabritiis, 2017).

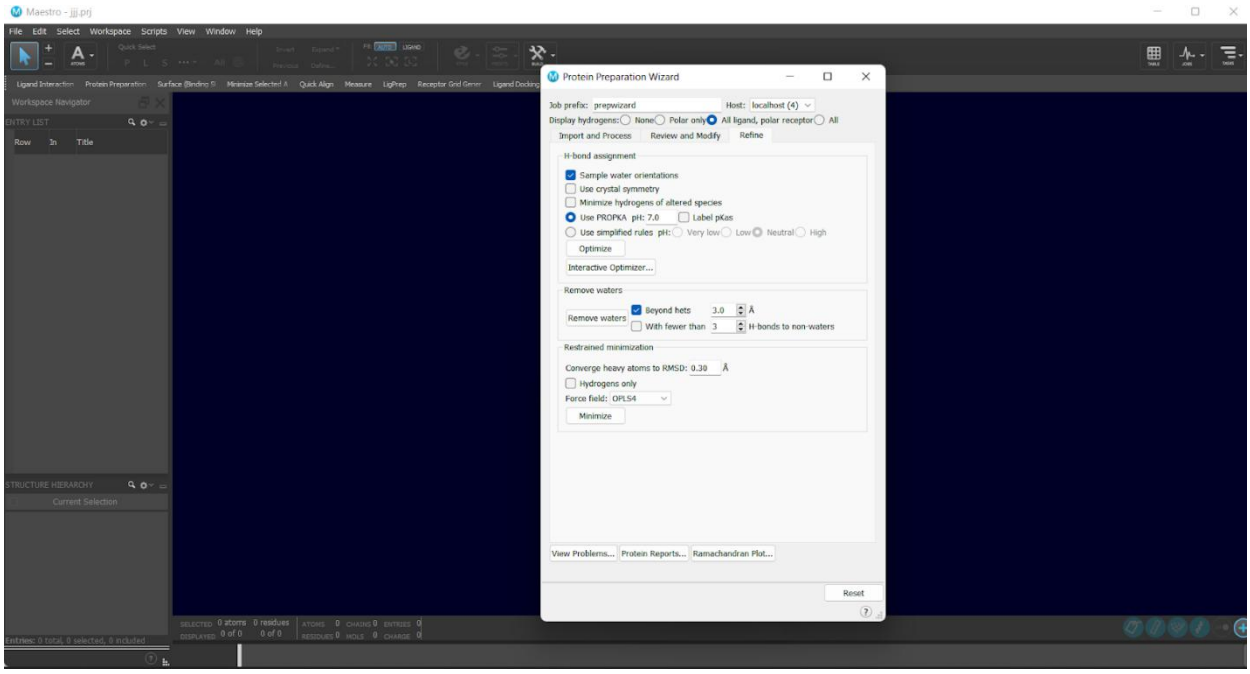

Image of protein preparation on maestro

This preparation ensures that the protein is in a suitable state for molecular docking and molecular dynamics simulations, which are essential for predicting interactions between proteins and potential drug compounds (*Mehta and Pathak, 2017).* After preparation, the receptors were saved and ready for docking studies in the Maestro software.

2.2.3. Receptor Grid Preparation and Screening

Before docking, the receptor grid was carefully prepared to ensure a*cymbopogon citratus*urate ligand docking within the active sites of hydroxyl methyl glutaryl CoA (HMG-CoA), proliferator activated receptor (PPAR), negatively charged bile acid, hydroxylcarboxylic acid (HM7A4), niemann- pick C1 protein (NCP1L1), proprotein convertase subtilisin/kexin type 9 (PCSK9) proteins . A grid box was defined around the active site residues of each receptor with dimensions of X: 20.0 Å, Y: 20.0 Å, and Z: 20.0 Å. These dimensions were chosen to ensure comprehensive coverage of the receptor binding sites, allowing for effective docking of ligands.

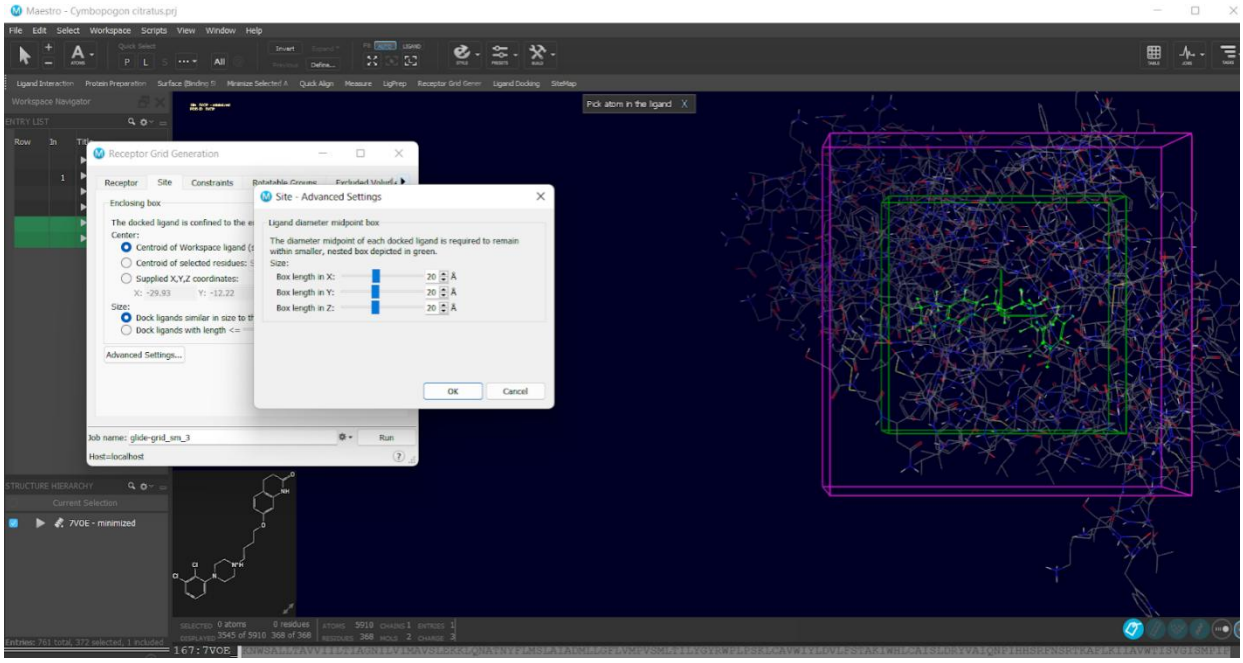

Image of receptor grid generation on Maestro

Once the receptor grid was set, HTVS was conducted using the Glide module in Maestro. This initial screening was employed to efficiently sift through a large set of compounds, identifying promising hits.

T

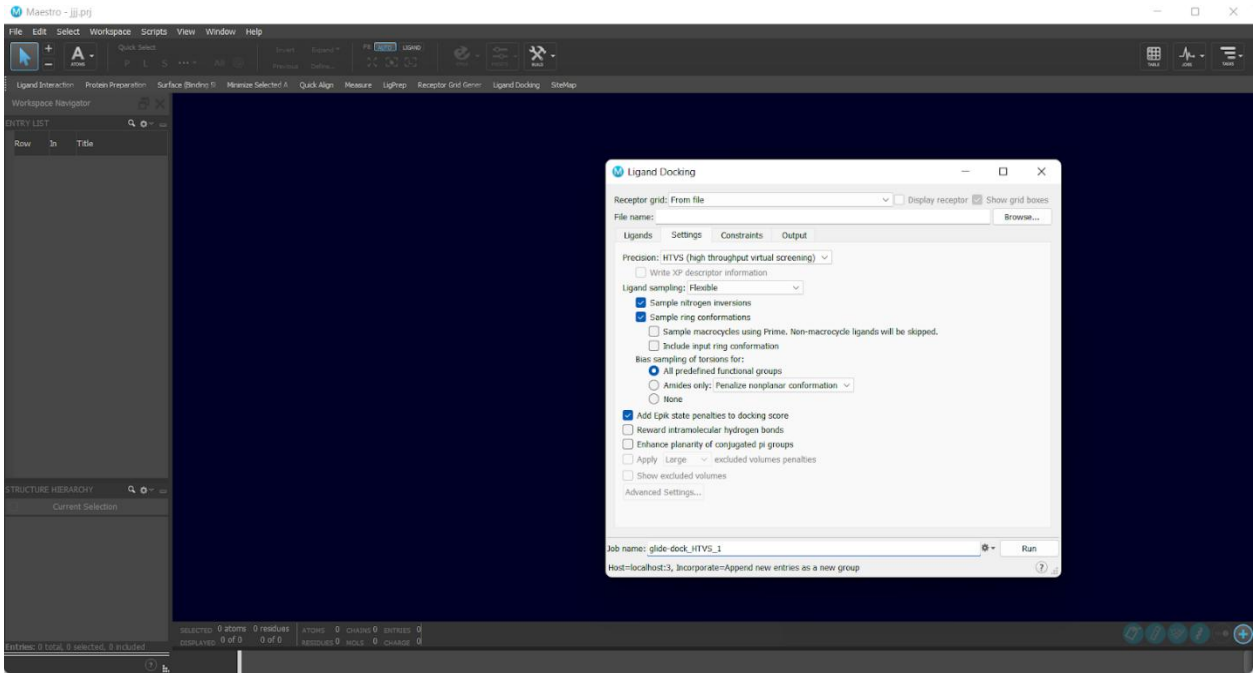

Image of ligand docking on maestro

The docking outcomes were analyzed by recording the binding affinities (in kcal/mol) and generating detailed interaction profiles between the ligands and receptors. These interaction profiles provided insights into the specific interactions, such as hydrogen bonding, hydrophobic interactions, and electrostatic forces, between the ligands and receptor binding sites.

2.2.4. ADMET Analysis of Selected Ligands

Following molecular docking, the binding affinities of the docked ligands were compared to those of standard hypolipidemic reference compounds, including simvastatin, lanifibranor, pemafibrate, PCSK9 inhibitors, niacin and ezetimibe. Ligands demonstrating binding affinities comparable to or better than these reference

compounds were selected as promising candidates for further evaluation. To assess their drug-likeness and pharmacokinetic properties, the selected ligands underwent

ADMET (Absorption, Distribution, Metabolism, Excretion, and Toxicity) analysis using SwissADME and ProTox-II. These tools provided insights into key pharmacokinetic parameters, ensuring that the compounds met essential drug discovery criteria.

1. Drug-Likeness and Lipinski's Rule of Five

The selected ligands were evaluated for oral bioavailability based on Lipinski's Rule of Five (RO5), which predicts drug-likeness using the following criteria (Leeson *et al.,* 2021)*:*

1. Molecular weight ≤ 500 Da
2. LogP (lipophilicity) ≤ 5
3. Hydrogen bond donors ≤ 5
4. Hydrogen bond a*cymbopogon citratus*eptors ≤ 10

Ligands that comply with RO5 were considered to have favourable oral bioavailability and were prioritized for further analysis.

CHAPTER THREE: RESULTS

3.1 Molecular Docking Results

The phytochemical constituents of *ocimum gratissimum, laurus nobilis, cymbogon citratus piperer guineense,* and *psidium guajava* were evaluated for their potential in managing and treating hyperlipidemia by docking them against HMG-CoA (1HWK), PPAR(6ENQ), HM7A4 (8K5B), NCP1L1 (7DF2), PCSK9 (8FPO) receptors using the Maestro docking suite. The molecular docking results were compared with those of reference antilipidemic agents to serve as standards for evaluating the binding affinity of the plant-derived compounds

Docking Results for Standard

The docking scores of the reference antilipidemic agent atorvastatin, lanifibranor, pemafibrate, niacin—serve as benchmark values for evaluating the binding affinity of plant-derived ligands to the targeted receptors. These reference compounds are well-established antilipidemic agents known for their action on HMG-CoA, PPAR, HM7A4 , NCP1L1, PCSK9.

Table 3.1 Docking scores of standard reference antilipidemics

S/N	COMPOUND CID	IUPAC NAME	1HWK (kcal/mol)	6ENQ docking scores	8k5b Docking scores	7wgn docking scores	7dfz docking scores
1	68677842	4-[1-(1,3-benzothiazol-6-ylsulfonyl)-5-chloroindol-2-yl]butanoic acid		-6.98			
2	21829311	2-deuteriopyridine-3-carboxylic acid			-8.76		
3	11526038	(2R)-2-[3-[[1,3-benzoxazol-2-yl-[3-(4-methoxyphenoxy)propyl]amino]methyl]phenoxy]butanoic acid				-7.16	
4	150311	(3R,4S)-1-(4-fluorophenyl)-3-[(3S)-3-(4-fluorophenyl)-3-hydroxypropyl]-4-(4-hydroxyphenyl)azetidin-2-one					-4.51
5	60823	(3R,5R)-7-[2-(4-fluorophenyl)-3-phenyl-4-(phenylcarbamoyl)-5-propan-2-ylpyrrol-1-yl]-3,5-dihydroxyheptanoic acid	-5.40				

Docking scores by plants

HTVS screening was used for docking and from the results the ligands with docking scores equal to or more than that of the standards were selected . the selected ligands and their respective score are presented below.

DOCKING RESULT OF *Cymbopogon citratus*

A total of 152 natural products of *Cymbopogon citratus* were downloaded from pubchem for docking studies. The docking score for those compounds were analysed for their interaction with HMG-CoA (1HWK), PPAR(6ENQ), HM7A4 (8K5B), NCP1L1 (7DF2), PCSK9 (8FPO) receptors. The results below highlight compounds that meet the established criteria for potential antilipidemic activity, focusing on their docking scores relative to the reference standard.

Table 3.2 Docking scores for *Cymbopogon citratus*

COMPOUND CID	IUPAC NAME	1HWK docking scores	6ENQ docking scores	8K5B Docking scores	7WGN docking scores	7DFZ docking scores
938	pyridine-3-carboxylic acid	-6.59		-8.76		
445858	3,7-dimethylocta-2,6-dien-1-ol					-4.65
6037	(2S)-2-[[4-[(2-amino-4-oxo-1H-pteridin-6-yl)methylamino]benzoyl]amino]pentanedioic acid	-7.43	-6.98			
6654	2,6,6-trimethylbicyclo[3.1.1]hept-2-ene					-4.58
6987	3-methyl-6-propan-2-ylcyclohex-2-en-1-one					-4.77
7410	1-phenylethanone					-4.54

7462	1-methyl-4-propan-2-ylcyclohexa-1,3-diene			-4.62
9989	3,7-dimethylocta-2,6-dienoic acid			-4.53
689043	(E)-3-(3,4-dihydroxyphenyl)prop-2-enoic acid	-6.22		
1549106	(Z)-3-(4-hydroxyphenyl)prop-2-enoic acid	-5.49		
1794427	(1S,3R,4R,5R)-3-[(E)-3-(3,4-dihydroxyphenyl)prop-2-enoyl]oxy-1,4,5-trihydroxycyclohexane-1-carboxylic acid	-7.58	-7.45	
5280373	5,7-dihydroxy-3-(4-methoxyphenyl)chromen-4-one		-7.40	
5280633	(1R,3R,4S,5R)-3-[(E)-3-(3,4-dihydroxyphenyl)prop-2-enoyl]oxy-1,4,5-trihydroxycyclohexane-1-carboxylic acid	-6.02		
5281675	2-(3,4-dihydroxyphenyl)-5,7-dihydroxy-8-[(2S,3R,4R,5S,6R)-3,4,5-trihydroxy-6-	-5.65		

	(hydroxymethyl)oxan-2-yl]chromen-4-one		
5281804	5-hydroxy-3-(4-hydroxyphenyl)-7-methoxychromen-4-one		-7.28
11592917	3-[(2S,3R,4S,5S,6R)-4,5-dihydroxy-3-[(2R,3R,4R,5R,6S)-3,4,5-trihydroxy-6-methyloxan-2-yl]oxy-6-[[(2R,3R,4R,5R,6S)-3,4,5-trihydroxy-6-methyloxan-2-yl]oxymethyl]oxan-2-yl]oxy-5,7-dihydroxy-2-(4-hydroxyphenyl)chromen-4-one	-6.98	
15901362	(1R,3S,4S,5S)-1,3,4-trihydroxy-5-[(E)-3-(4-hydroxy-3-methoxyphenyl)prop-2-enoyl]oxycyclohexane-1-carboxylic acid	-7.38	
24862012	2-(3,4-dihydroxyphenyl)-5,7-dihydroxy-6-[(2S,3R,4S,5S)-4-hydroxy-5-(hydroxymethyl)-3-	-6.50	

	[(2S,3R,4R,5R,6S)-3,4,5-trihydroxy-6-methyloxan-2-yl]oxyoxolan-2-yl]chromen-4-one		
50993776	6-[(2S,3R,4S,5S,6R)-4,5-dihydroxy-6-(hydroxymethyl)-3-[(2S,3R,4R,5R,6S)-3,4,5-trihydroxy-6-methyloxan-2-yl]oxyoxan-2-yl]-2-(3,4-dihydroxyphenyl)-5,7-dihydroxychromen-4-one	-5.71	
51402809	5,7-dihydroxy-2-(4-hydroxy-3-methoxyphenyl)-3-[(2S,3R,4R,5S,6R)-3,4,5-trihydroxy-6-(hydroxymethyl)oxan-2-yl]oxychromen-4-one	-5.56	
91825557	2-(3,4-dihydroxyphenyl)-5-hydroxy-7-methoxy-6-[(2S,3R,4R,5S,6R)-3,4,5-trihydroxy-6-(hydroxymethyl)oxan-2-yl]-4a,8a-dihydrochromen-4-one		-7.40

101105499	(2S)-4-[(E)-2-[(2R)-2-carboxy-5-hydroxy-6-[(2S,3R,4S,5S,6R)-3,4,5-trihydroxy-6-[[(E)-3-(4-hydroxy-3-methoxyphenyl)prop-2-enoyl]oxymethyl]oxan-2-yl]oxy-2,3-dihydroindol-1-yl]ethenyl]-2,3-dihydropyridine-2,6-dicarboxylic acid	-7.22
125528541	2-(3,4-dihydroxyphenyl)-5,7-dihydroxy-3-[(2S,3R,4S,5S,6R)-3,4,5-trihydroxy-6-[[(2R,3S,4S,5R,6S)-3,4,5-trihydroxy-6-methyloxan-2-yl]oxymethyl]oxan-2-yl]oxychromen-4-one	-5.58
154496793	5,7-dihydroxy-2-(4-hydroxy-3-methoxyphenyl)-3-[(2S,3S,4R,5R,6R)-3,4,5-trihydroxy-6-[[(2R,3R,4S,5R,6S)-3,4,5-trihydroxy-6-	-5.65

	methyloxan-2-yl]oxymethyl]oxan-2-yl]oxychromen-4-one	
157009723	3-[(2R,3S,4S,5R)-3,4-dihydroxy-5-(hydroxymethyl)oxolan-2-yl]oxy-2-(4-hydroxyphenyl)chromenylium-5,7-diol	-6.15
162992009	[(3S,4R,5S)-5-[(2S,3R,4S,5S,6R)-4,5-dihydroxy-2-(4-hydroxy-2-methoxyphenoxy)-6-(hydroxymethyl)oxan-3-yl]oxy-3,4-dihydroxyoxolan-3-yl]methyl 4-hydroxy-3,5-dimethoxybenzoate	-5.50
163186337	3-[(2S,3R,4S,5R,6R)-3-[(2S,3R,4R)-3,4-dihydroxy-4-(hydroxymethyl)oxolan-2-yl]oxy-4,5-dihydroxy-6-[[(2R,3R,4R,5R,6S)-3,4,5-trihydroxy-6-methyloxan-2-yl]oxymethyl]oxan-	-5.64

	2-yl]oxy-5,7-dihydroxy-2-(3-hydroxy-4-methoxyphenyl)chromen-4-one	
165359504	4-[2-[2-carboxy-5-hydroxy-6-[3,4,5-trihydroxy-6-[3-(4-hydroxyphenyl)prop-2-enoyloxymethyl]oxan-2-yl]oxy-2,3-dihydroindol-1-yl]ethenyl]-2,3-dihydropyridine-2,6-dicarboxylic acid	-7.86

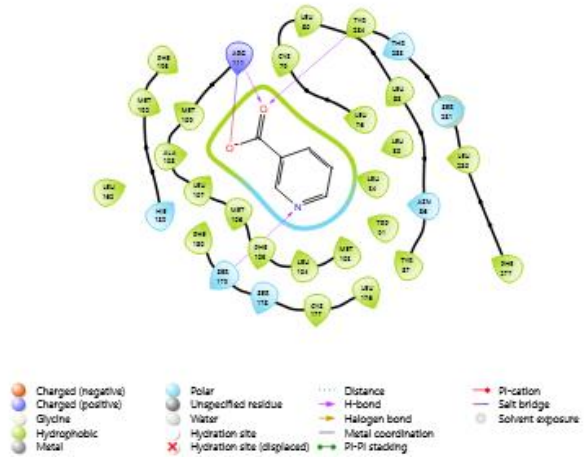

Figure 3.1.1 2D interactions of 938 from *Cymbopogon citratus* with 8K5B

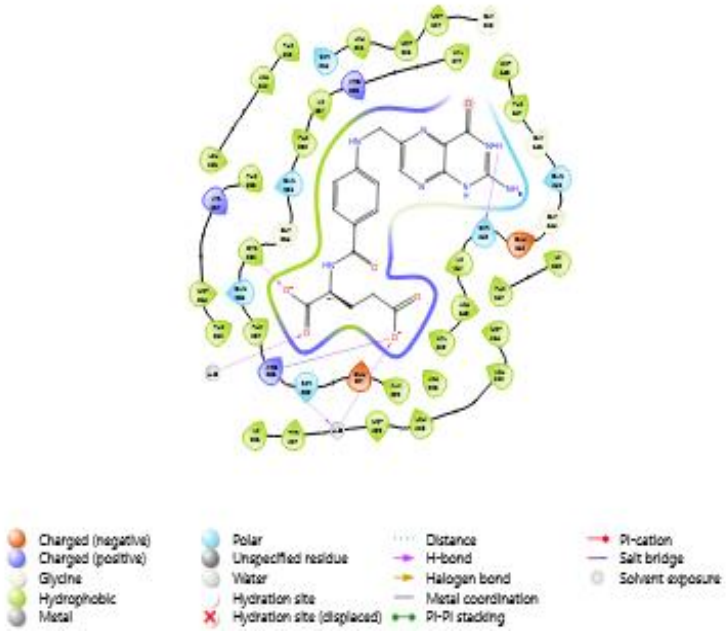

2D interaction of 6037 *Cymbopogon citratus* with 6ENQ

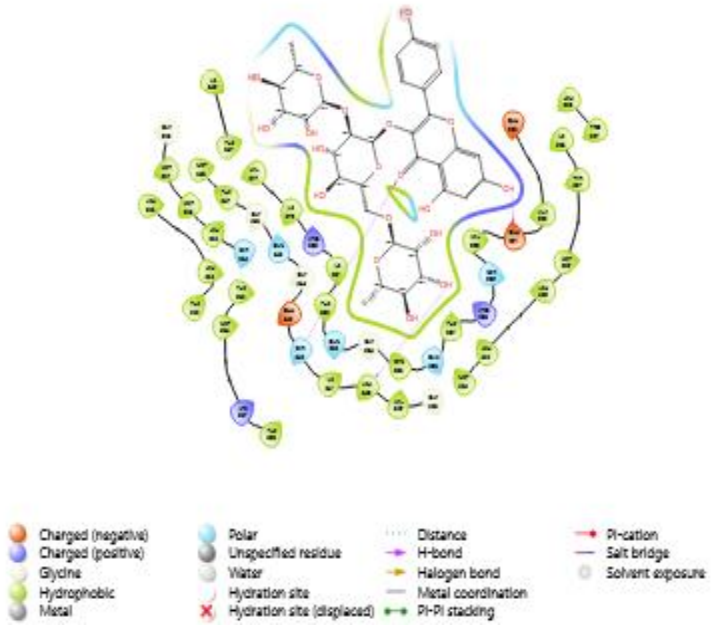

2D interaction of 11592917 *Cymbopogon citratus* with 6ENQ

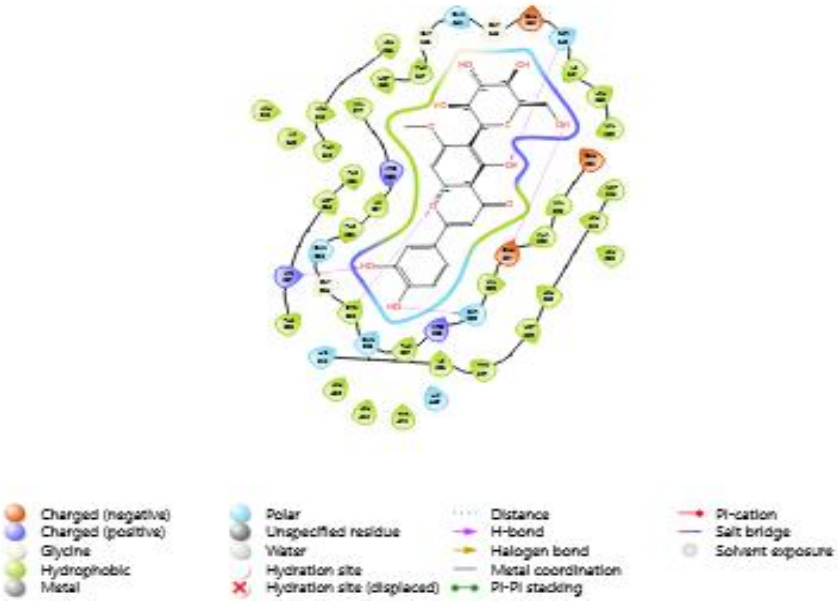

2D interaction of 162822832 *Cymbopogon citratus* with 6ENQ

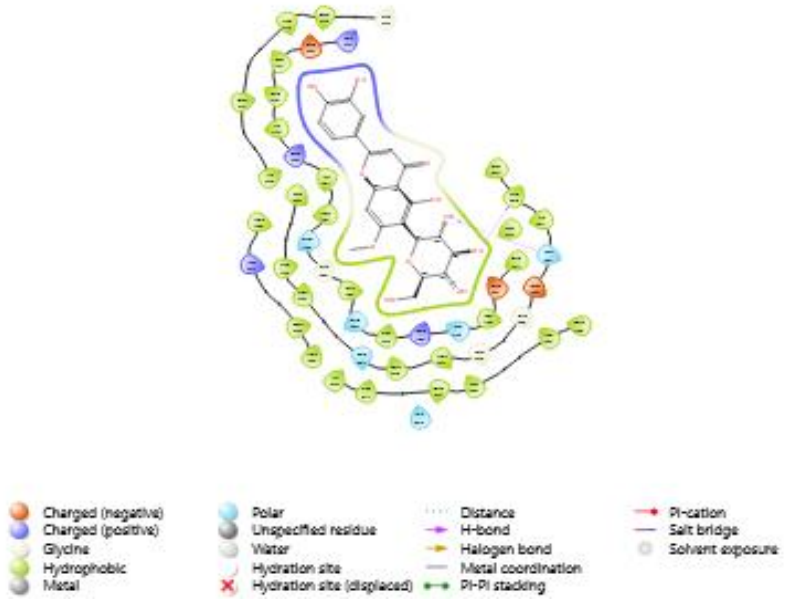

2D interaction of 91825557 *Cymbopogon citratus* with 6ENQ

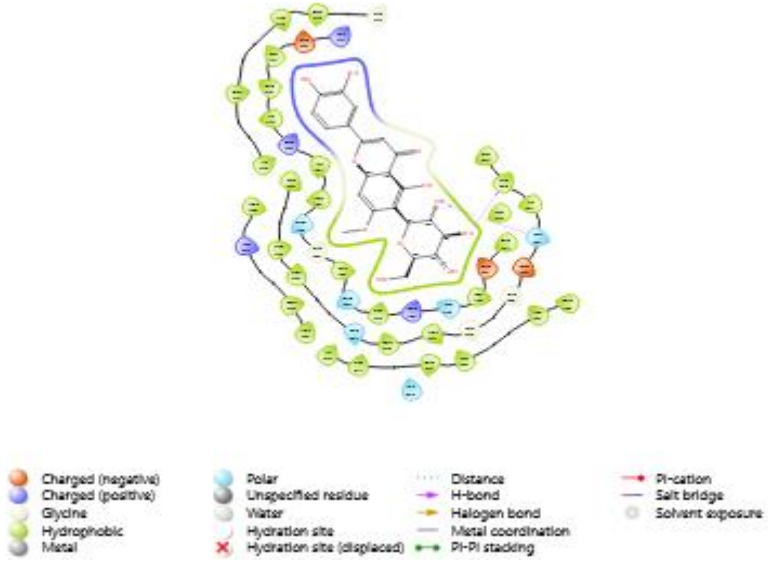

2D interaction of 603715961362 *Cymbopogon citratus* with 6ENQ

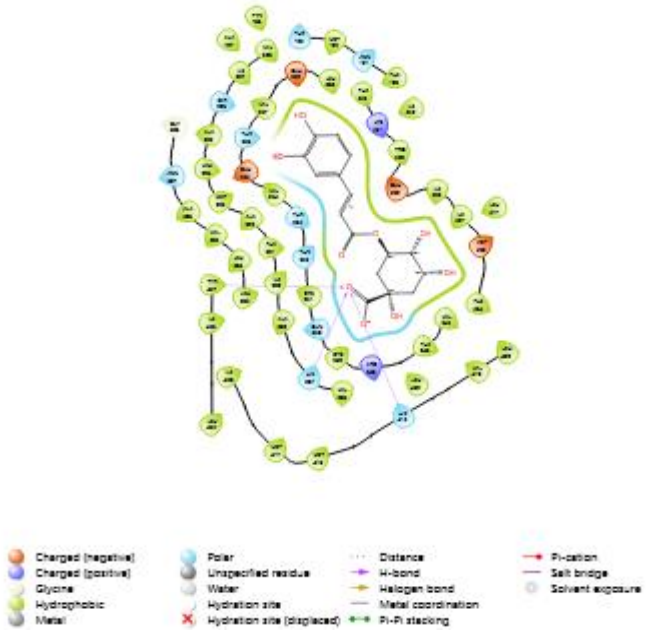

2D interaction of 174427 *Cymbopogon citratus* with 7WGN

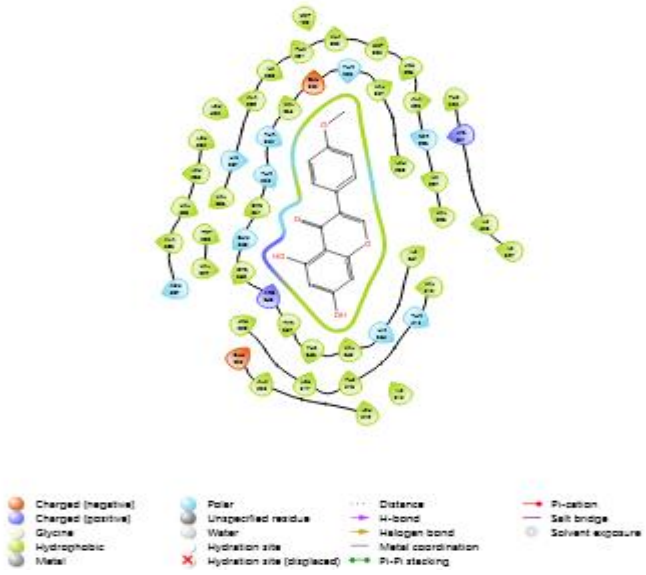

2D interaction of 5280373 *Cymbopogon citratus* with 7WGN

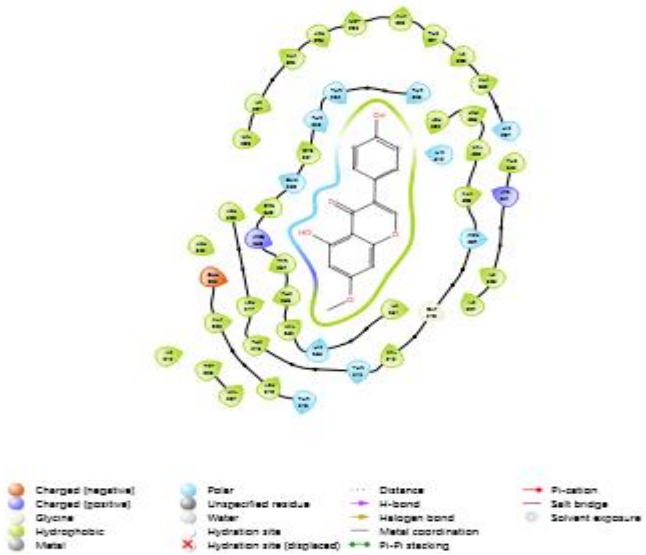

2D interaction of 528104 *Cymbopogon citratus* with 7WGN

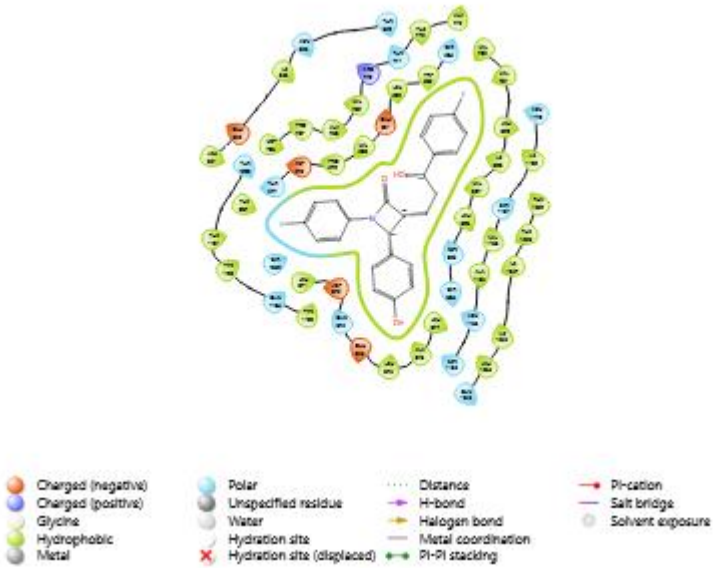

2D interaction of 445858 *Cymbopogon citratus* with 7DFZ

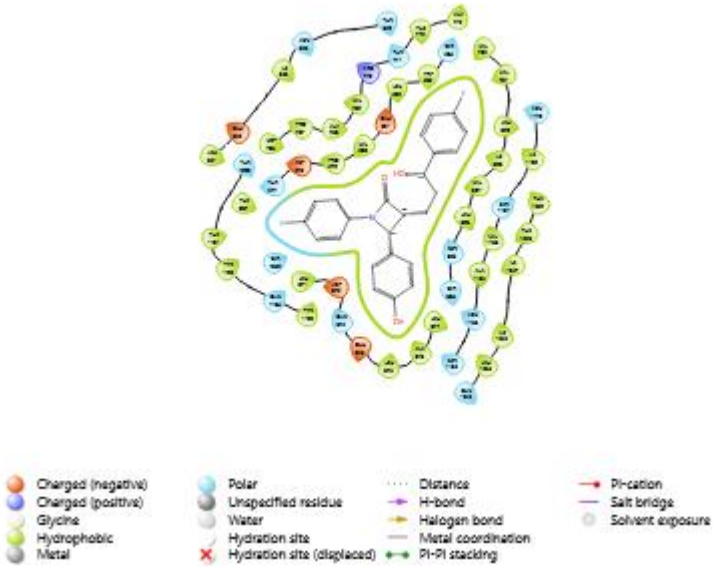

2D interaction of 6987 *Cymbopogon citratus* with 7DFZ

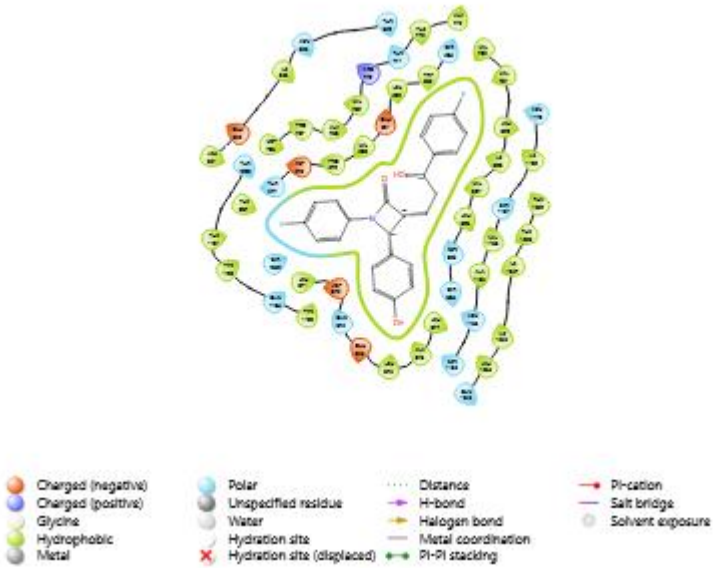

2D interaction of 7462 *Cymbopogon citratus* with 7DFZ

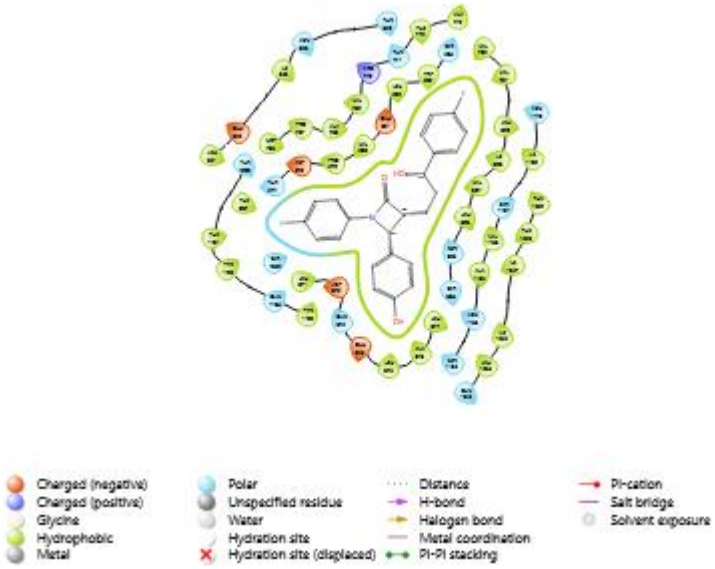

2D interaction of 6654 *Cymbopogon citratus* with 7DFZ

DOCKING RESULTS OF P*sidium guajava*

A total of 145 natural products of *psidium guajava* were retrieved from PubChem for docking studies. The docking scores for these compounds were analyzed for their interactions with HMG-CoA (1HWK), PPAR(6ENQ), HM7A4 (8K5B), NCP1L1 (7DF2), receptors. The results below highlight compounds that meet the established criteria for potential antilipidemic activity, focusing on their docking scores relative to the reference standards.

Table 3.3 Docking scores for P*sidium guajava*

COMPOUND CID	IUPAC NAME	1HWK BINDING AFFINITY	6ENQ BINDING AFFINITY	8K5B BINDING AFFINITY	7WGN BINDING AFFINITY	7DFZ BINDING AFFINITY
72	3,4-dihydroxybenzoic acid	-5.89				-5.18
370	3,4,5-trihydroxybenzoic acid	-5.54				
674	N-methylmethanamine					-4.95
6902	(3S,4R,5R)-oxane-2,3,4,5-tetrol	-5.72				
7462	1-methyl-4-propan-2-ylcyclohexa-1,3-diene					-4.54
7463	1-methyl-4-propan-2-ylbenzene					-4.62
8468	4-hydroxy-3-methoxybenzoic acid					-5.05
10225	1,6-dimethyl-4-propan-2-y*Laurus nobilis*aphthalene		-7.11			-4.55

11463	1-methyl-4-propan-2-ylidenecyclohexene			-4.53
220001	2,3,4,5-tetrahydroxyhexanal	-5.77		
445858	E)-3-(4-hydroxy-3-methoxyphenyl)prop-2-enoic acid			-4.83
689043	(E)-3-(3,4-dihydroxyphenyl)prop-2-enoic acid	-6.22		
3707243	2-phenyl-3,4-dihydro-2H-chromen-3-ol		-7.45	-4.65
5280343	2-(3,4-dihydroxyphenyl)-3,5,7-trihydroxychromen-4-one	-5.85		
5281670	2-(2,4-dihydroxyphenyl)-3,5,7-trihydroxychromen-4-one	-6.10		
5281672	3,5,7-trihydroxy-2-(3,4,5-trihydroxyphenyl)chromen-4-one	-6.36		
5281855	6,7,13,14-tetrahydroxy-2,9-			-4.66

	dioxatetracyclo[6.6.2.04,16.011,15]hexadeca-1(15),4,6,8(16),11,13-hexaene-3,10-dione			
5318135	6,7,14-trihydroxy-13-[(2S,3R,4S,5S,6R)-3,4,5-trihydroxy-6-[[(2R,3R,4S,5S,6R)-3,4,5-trihydroxy-6-(hydroxymethyl)oxan-2-yl]oxymethyl]oxan-2-yl]oxy-2,9-dioxatetracyclo[6.6.2.04,16.011,15]hexadeca-1(15),4,6,8(16),11,13-hexaene-3,10-dione	-5.61		
5352543	[(Z)-hex-3-enyl] hexanoate	5.78		
6429077	(1S,4S)-1,6-dimethyl-4-propan-2-yl-1,2,3,4-tetrahydronaphthalene		-7.26	
9828626	1,3,3-trimethyl-2-[(1E,3E,5E,7E,9E,11E,13E,15Z,17E)-3,7,12,16-tetramethyl-18-(2,6,6-			-4.71

	trimethylcyclohexen-1-yl)octadeca-1,3,5,7,9,11,13,15,17-nonaenyl]cyclohexene	
10119810	[(2R,3S,4S,5R,6S)-6-(4-benzoyl-3,5-dihydroxyphenoxy)-3,4,5-trihydroxyoxan-2-yl]methyl 3,4,5-trihydroxybenzoate	-5.70
10166868	(2R,3S,4S,5R,6S)-6-(4-benzoyl-3,5-dihydroxy-2,6-dimethylphenoxy)-3,4,5-trihydroxyoxan-2-yl]methyl 3,4,5-trihydroxybenzoate	-5.68
10455578	2-(2,4-dihydroxyphenyl)-5,7-dihydroxy-3-[(2S,3R,4R,5S)-3,4,5-trihydroxyoxan-2-yl]oxychromen-4-one	-6.20
11410680	[(2S,3R,4R,5S)-5-[2-(3,4-dihydroxyphenyl)-5,7-dihydroxy-4-oxochromen-3-yl]oxy-3,4-	-6.40

	dihydroxyoxolan-2-yl]methyl 3,4,5-trihydroxybenzoate		
11966988	[(2S,3R,4S,5S,6R)-2-[5,7-dihydroxy-2-[3-hydroxy-4-[(E)-2-propanoyloxyethenoxy]phenyl]-4-oxochromen-3-yl]oxy-4,5-dihydroxy-6-(hydroxymethyl)oxan-3-yl] 3,4,5-trihydroxybenzoate	-5.43	
69573531	2-(2,4-dihydroxyphenyl)-5,7-dihydroxy-3-[(2S,3R,4S,5S)-3,4,5-trihydroxyoxan-2-yl]oxychromen-4-one	-6.27	
102469980	[(2R,3S,4S,5R,6S)-3,4-dihydroxy-5-(3,4,5-trihydroxybenzoyl)oxy-6-(3,4,5-trimethoxyphenoxy)oxan-2-yl]methyl 3,4,5-	-5.73	-7.90

trihydroxybenzoate

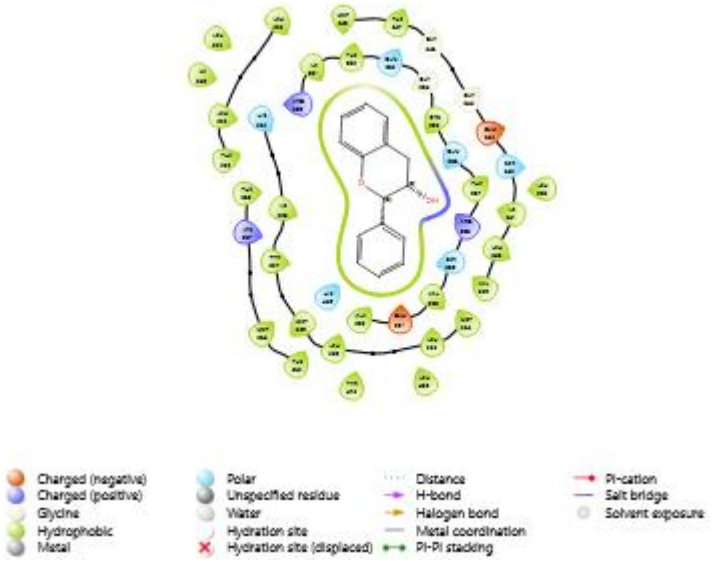

2D interaction 10225 of P*sidium guajava* with 6ENQ

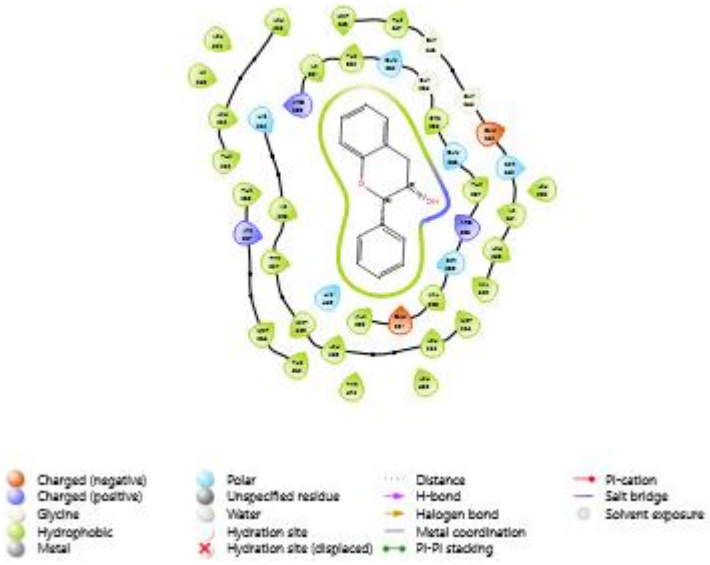

2D interaction of 3707243 P*sidium guajava* with 6ENQ

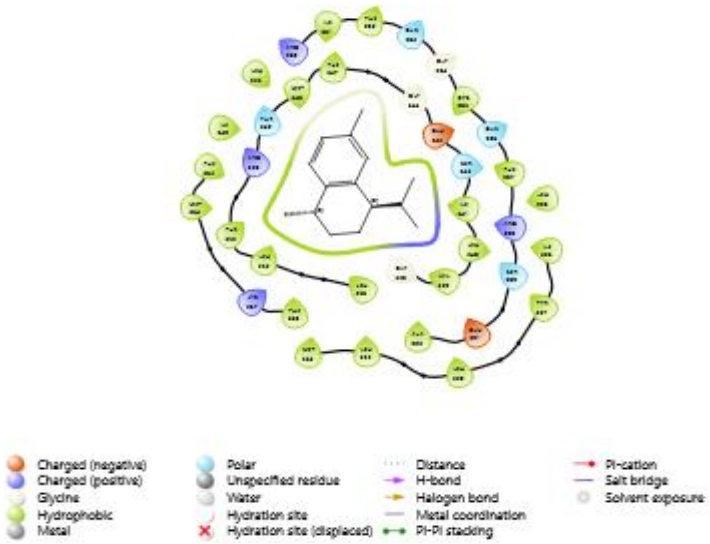

2D interaction of 6429077P*sidium guajava* with 6ENQ

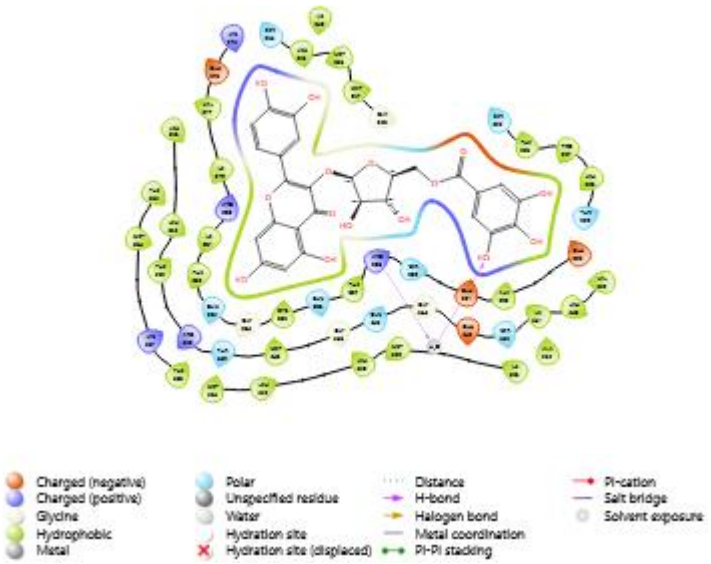

2D interaction of 11410680 P*sidium guajava* with 6ENQ

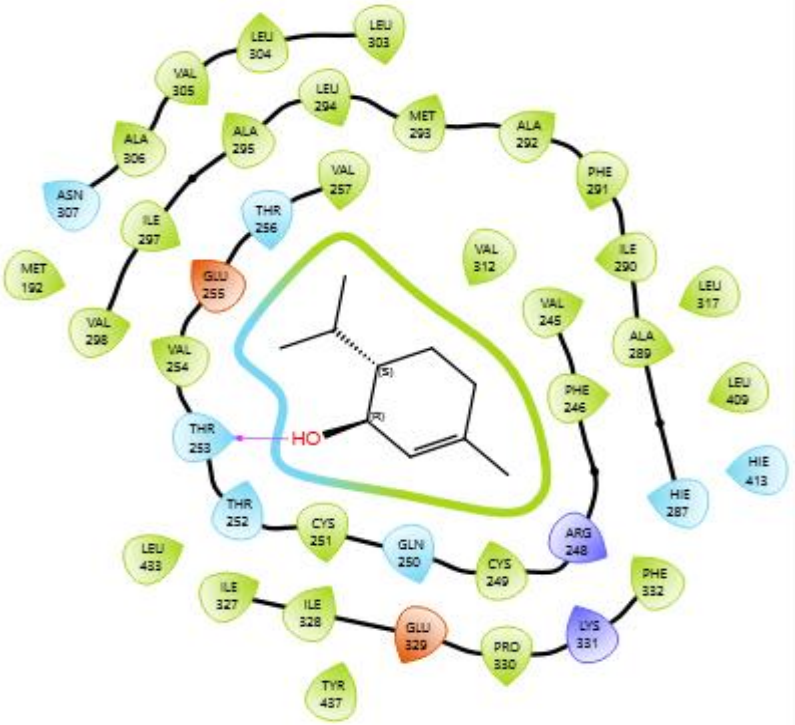

2D interaction of 10282 P*sidium guajava* with 7WGN

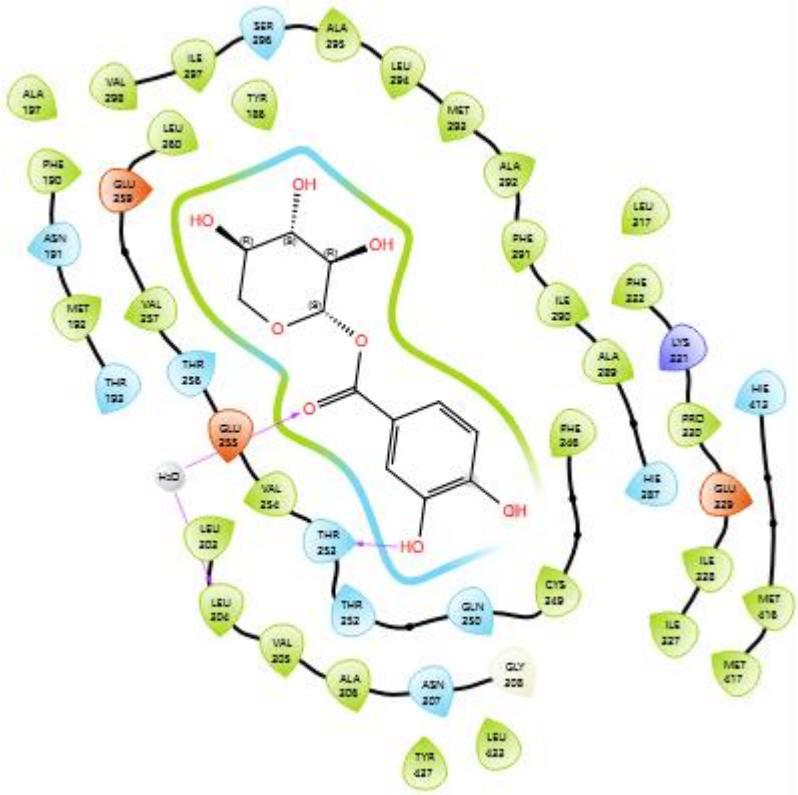

2D interaction of 132594 P*sidium guajava* with 7WGN

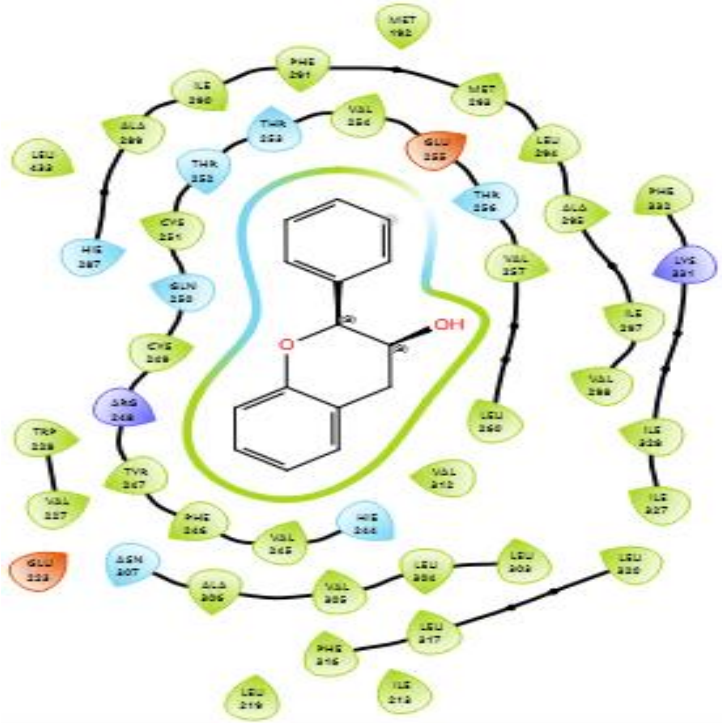

2D interaction of 3707243 P*sidium guajava* with 7WGN

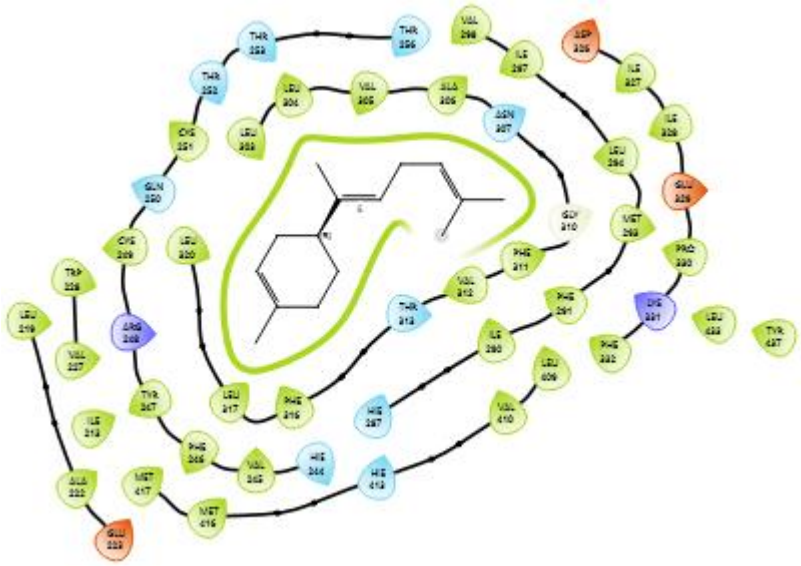

2D interaction of 5315468 P*sidium guajava* with 7WGN

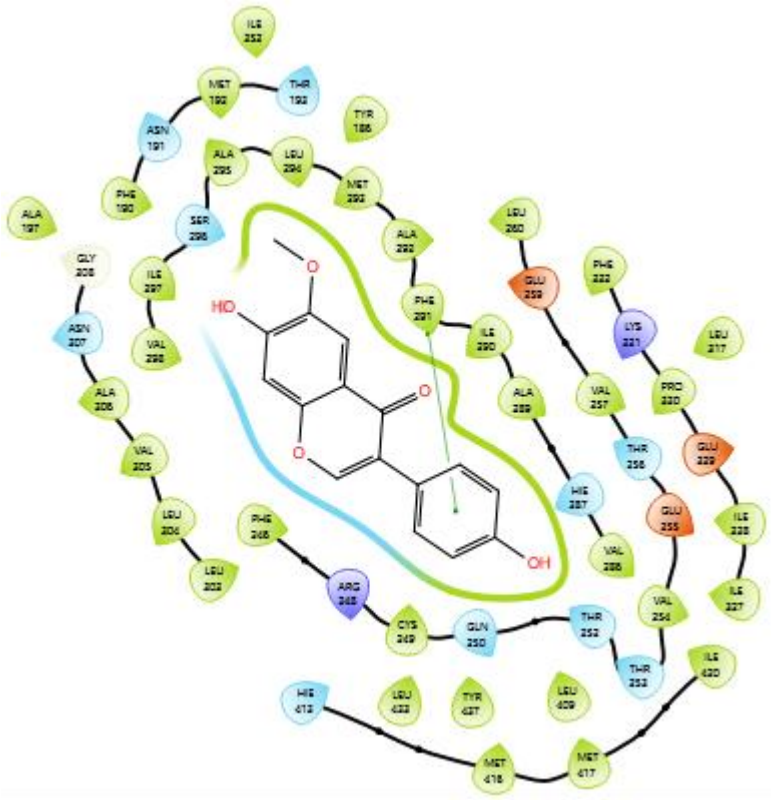

2D interaction of 5317750 P*sidium guajava* with 7WGN

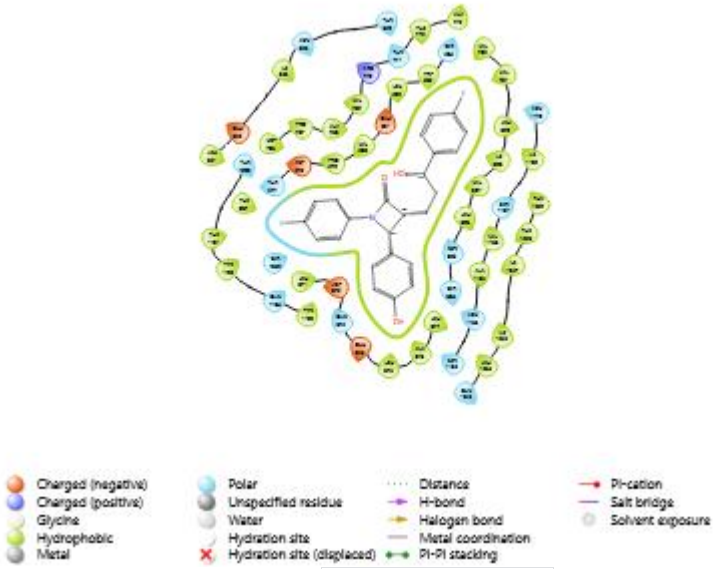

2D interaction of 5315468 P*sidium guajava* with 7WGN

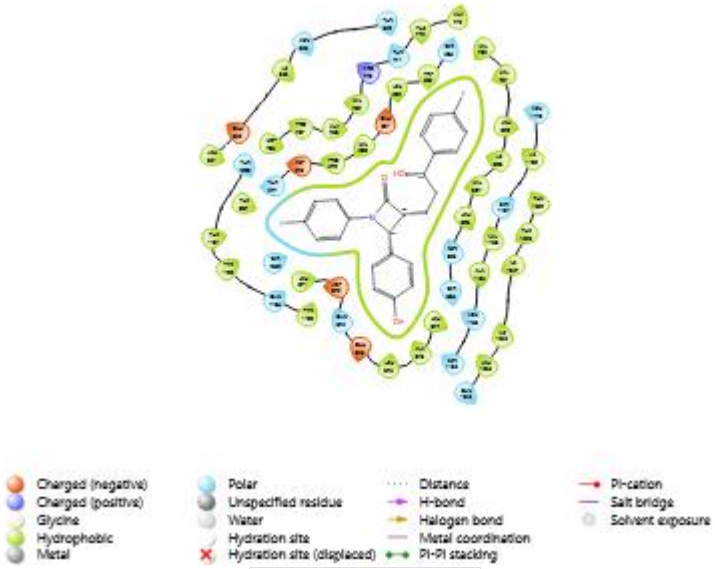

2D interaction Of 72 P*sidium guajava* with 7DFZ

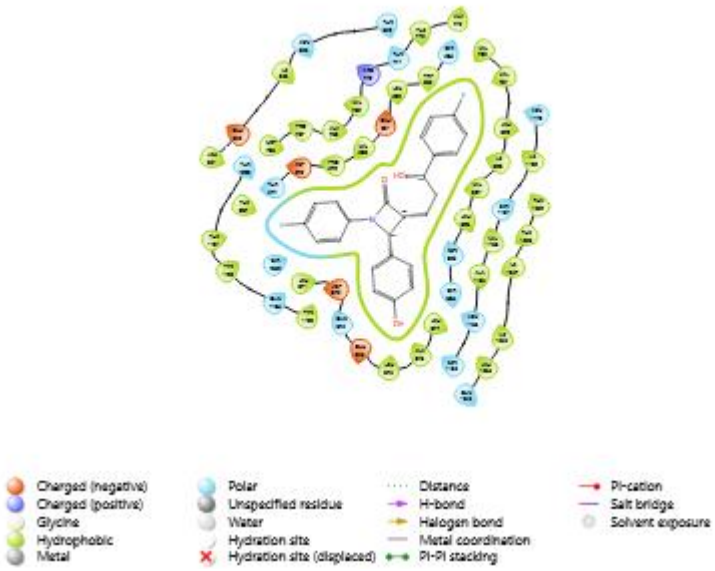

2D interaction Of 674 P*sidium guajava* with 7DFZ

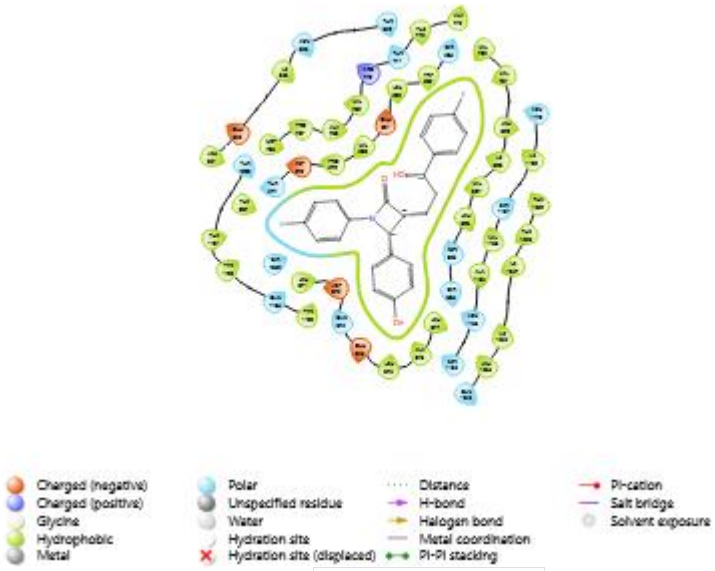

2D interaction Of 445858 P*sidium guajava* with 7DFZ

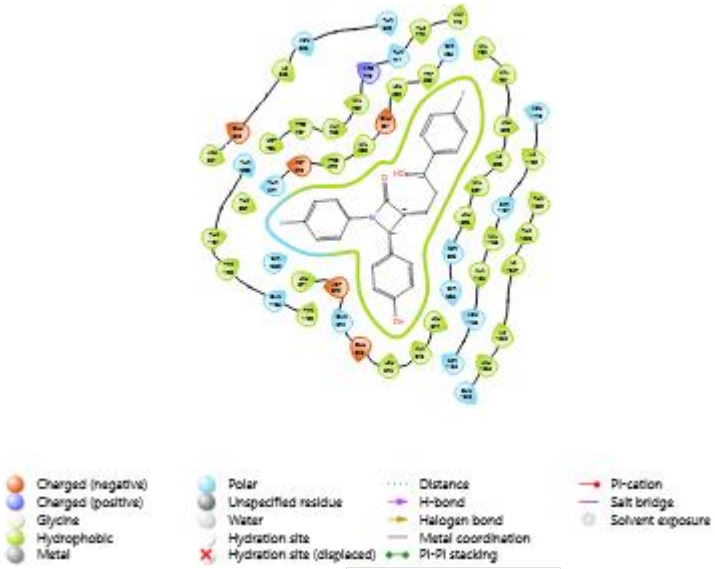

2D interaction Of 9828626 P*sidium guajava* with 7DFZ

DOCKING RESULT OF *Laurus nobilis*

Total of 114 natural products of *Laurus nobilis* were retrieved from PubChem for docking studies. The docking scores for these compounds were evaluated based on their interactions with HMG-CoA (1HWK), PPAR(6ENQ), HM7A4 (8K5B), NCP1L1 (7DF2), PCSK9 (8FPO) receptors. The results below highlight compounds that meet the established criteria for potential antilipidemic activity, focusing on their docking scores relative to the reference standard.

Table 3.4 Docking scores of *Laurus nobilis*

COMPOUND CID	IUPAC NAME	1HWK Docking score	6ENQ Docking score	7DFZ Docking score	8K5B Docking score	7WGN DOCKING SCORE
91274708	7-(1,3-benzodioxol-5-yl)-1-piperidin-1-ylhepta-2,4,6-trien-1-one		-7.52			
287685	3,4-bis(1,3-benzodioxol-5-ylmethyl)oxolan-2-ol					-8.21
117669	5-(1,3-benzodioxol-5-yl)-1-pyrrolidin-1-ylpenta-2,4-		-7.45			-8.02

	dien-1-one			
276753	5-(1,3-benzodioxol-5-yl)-1-piperidin-1-ylpent-2-en-1-one			-7.50
5320618	(E)-5-(1,3-benzodioxol-5-yl)-1-piperidin-1-ylpent-2-en-1-one			-7.50
54930	3-(1,3-benzodioxol-5-yl)-1-piperidin-1-ylprop-2-en-1-one	-7.15		
6429077	1S,4S)-1,6-dimethyl-4-propan-2-yl-1,2,3,4-tetrahydronaphthalene	-7.26		
101716	1,1,4,7-tetramethyl-2,3,4a,5,6,7,7a,7b-octahydro-1aH-cyclopropa[e]azulen-4-ol		-4.87	
117669	5-(1,3-benzodioxol-5-yl)-1-pyrrolidin-1-ylpenta-2,4-dien-1-one			-7.59
91274708	7-(1,3-benzodioxol-5-yl)-1-piperidin-1-ylhepta-2,4,6-			-8.57

	trien-1-one		
441005	(1S,8aR)-4,7-dimethyl-1-propan-2-yl-1,2,3,5,6,8a-hexahydronaphthalene	-7.28	
4840	5-(1,3-benzodioxol-5-yl)-1-piperidin-1-ylpenta-2,4-dien-1-one	-7.88	-7.21
287685	3,4-bis(1,3-benzodioxol-5-ylmethyl)oxolan-2-ol	-7.00	
54930	3-(1,3-benzodioxol-5-yl)-1-piperidin-1-ylprop-2-en-1-one		-8.42
641115	(E)-3-(1,3-benzodioxol-5-yl)-1-piperidin-1-ylprop-2-en-1-one		-8.42
90785	2-(3,8-dimethyl-1,2,3,3a,4,5,6,7-octahydroazulen-5-yl)propan-2-ol	-7.08	
276753	5-(1,3-benzodioxol-5-yl)-1-piperidin-1-ylpent-2-en-1-one		-8.13

117669	5-(1,3-benzodioxol-5-yl)-1-pyrrolidin-1-ylpenta-2,4-dien-1-one	-7.16	-7.79
155328	5-(6-methoxy-1,3-benzodioxol-5-yl)-1-piperidin-1-ylpenta-2,4-dien-1-one		-7.46
91274708	7-(1,3-benzodioxol-5-yl)-1-piperidin-1-ylhepta-2,4,6-trien-1-one		-8.15
4840	5-(1,3-benzodioxol-5-yl)-1-piperidin-1-ylpenta-2,4-dien-1-one		-7.72
1548913	(2Z,4E)-5-(1,3-benzodioxol-5-yl)-1-piperidin-1-ylpenta-2,4-dien-1-one		-7.72
162986	5-(6-methoxy-1,3-benzodioxol-5-yl)-1-piperidin-1-ylpent-2-en-1-one		-7.77
6441090	(E)-5-(6-methoxy-1,3-benzodioxol-5-yl)-1-piperidin-1-ylpent-2-en-1-one		-7.77

6987	3-methyl-6-propan-2-ylcyclohex-2-en-1-one	-4.58	
162986	5-(6-methoxy-1,3-benzodioxol-5-yl)-1-piperidin-1-ylpent-2-en-1-one		-7.44
92231	(1aR,4aR,7S,7aR,7bR)-1,1,7-trimethyl-4-methylidene-1a,2,3,4a,5,6,7a,7b-octahydrocyclopropa[h]azulen-7-ol	-4.97	
5320621	(2E,4E)-5-(1,3-benzodioxol-5-yl)-N-(2-methylpropyl)penta-2,4-dienamide		-7.57
6987	3-methyl-6-propan-2-ylcyclohex-2-en-1-one	-4.77	
7460	2-methyl-5-propan-2-ylcyclohexa-1,3-diene	-4.59	
11142	3-methylidene-6-propan-2-ylcyclohexene	-4.53	
7460	2-methyl-5-propan-2-ylcyclohexa-1,3-diene	-4.59	
11463	1-methyl-4-propan-2-ylidenecyclohexene	-4.53	
92037727	5-(1,3-benzodioxol-5-yl)-N-(10-methylundec-5-enyl)penta-2,4-dienamide		-7.77

5281772	(E)-3-(1,3-benzodioxol-5-yl)-N-(2-methylpropyl)prop-2-enamide					-7.32
101716	1,1,4,7-tetramethyl-2,3,4a,5,6,7,7a,7b-octahydro-1aH-cyclopropa[e]azulen-4-ol			-4.96		
92037727	5-(1,3-benzodioxol-5-yl)-N-(10-methylundec-5-enyl)penta-2,4-dienamide				-8.76	
68677842	4-[1-(1,3-benzothiazol-6-ylsulfonyl)-5-chloroindol-2-yl]butanoic acid	-5.87	-6.98			
938	pyridine-3-carboxylic acid	-6.59		-4.51		
5991	(8R,9S,13S,14S,17R)-17-ethynyl-13-methyl-7,8,9,11,12,14,15,16-octahydro-6H-			-4.65		
6037	(2S)-2-[[4-[(2-amino-4-oxo-1H-pteridin-6-yl)methylamino]benzoyl]amino]pentanedioic acid	-7.43				
7463	1-methyl-4-propan-2-ylbenzene			-4.62		

11463	1-methyl-4-propan-2-ylidenecyclohexene			-4.53
98958	6-hydroxy-5a-methyl-3,9-dimethylidene-		-7.11	-4.59
444212	(E)-prop-1-ene-1,2,3-tricarboxylic acid	-5.40		
497804	(12S)-18-methoxy-3,5-dioxa-11-azapentacyclo[10.7.1.02,6.08,20.014,19]icosa-1(20),2(6),7,14(19),15,17-hexaen-17-ol			-4.57
556919	6,10-dimethyl-3-methylidene-3a,4,5,8,9,11a-hexahydrocyclodeca[b]furan-2-one			-4.58
4426320	3,6,9-trimethylidene-3a,4,5,6a,7,8,9a,9b-octahydroazuleno[4,5-b]furan-2-one		-7.05	-5.08
5280343	2-(3,4-dihydroxyphenyl)-3,5,7-trihydroxychromen-4-one	-5.85		
5280863	3,5,7-trihydroxy-2-(4-hydroxyphenyl)chromen-4-one	-5.99		
5318956	17-methoxy-3,5-dioxa-11-	-5.61	-7.42	

5367559	azapentacyclo[10.7.1.02,6.08,20.014,19]icosa-1(20),2(6),7,14(19),15,17-hexaen-18-ol			-4.58
10064778	(6Z,10Z)-6,10-dimethyl-3-methylidene-3a,4,5,8,9,11a-hexahydrocyclodeca[b]furan-2-one		-7.55	
44234540	(12S)-13-methyl-5,7,19,21-tetraoxa-13-azahexacyclo[10.10.1.02,10.04,8.016,23.018,22]tricosa-1(23),2,4(8),9,16,18(22)-hexaene			-4.53
131752050	methyl 2-[(1S,2S,4aR,5R,8aS)-1,5-dihydroxy-4a-methyl-8-methylidene-1,2,3,4,5,6,7,8a-octahydronaphthalen-2-yl]prop-2-enoate		-7.31	-4.77
137918199	(5Z,9Z)-4-hydroxy-6,10-dimethyl-3-methylidene-3a,4,7,8,11,11a-hexahydrocyclodeca[b]furan-2-one			
	3-[(2S,3R,4S,5R,6R)-3,5-dihydroxy-6-(hydroxymethyl)-4-[(2S,3R,4S,5S,6R)-3,4,5-	-5.94		

	trihydroxy-6-(hydroxymethyl)oxan-2-yl]oxyoxan-2-yl]oxy-5,7-dihydroxy-2-(4-hydroxyphenyl)chromen-4-one		
139595854	(13S,17S)-17-[(1S)-1-hydroxypropyl]-11-oxo-1,5,10-triazabicyclo[11.4.0]heptadec-14-ene-5-carbaldehyde		-4.51
162849740	7-[(2S,3R,4S,5S,6R)-4,5-dihydroxy-6-(hydroxymethyl)-3-[(2S,3R,4S,5S,6R)-3,4,5-trihydroxy-6-(hydroxymethyl)oxan-2-yl]oxyoxan-2-yl]oxy-5-hydroxy-2-(4-hydroxyphenyl)-3-[(2S,3R,4S,5S,6R)-3,4,5-trihydroxy-6-[[(2R,3R,4R,5R,6S)-3,4,5-trihydroxy-6-methyloxan-2-yl]oxymethyl]oxan-2-yl]oxychromen-4-one	-7.57	-4.76
162871101	(13R,17S)-17-[(1S)-1-hydroxypropyl]-1,5,10-triazabicyclo[11.4.0]heptadec-15-en-11-one	-5.42	

162905976	2-(3,4-dihydroxyphenyl)-5-hydroxy-7-[(2R,3S,4R,5R,6S)-3,4,5-trihydroxy-6-(hydroxymethyl)oxan-2-yl]oxy-3-[(2R,3S,4R,5R,6S)-3,4,5-trihydroxy-6-[[(2S,3S,4R,5R,6S)-3,4,5-trihydroxy-6-methyloxan-2-yl]oxymethyl]oxan-2-yl]oxychromen-4-one	-5.61	-5.12
163033371	5-hydroxy-2-(4-hydroxyphenyl)-7-[(2R,3S,4R,5R,6S)-3,4,5-trihydroxy-6-(hydroxymethyl)oxan-2-yl]oxy-3-[(2R,3S,4R,5R,6S)-3,4,5-trihydroxy-6-[[(2S,3S,4R,5R,6S)-3,4,5-trihydroxy-6-methyloxan-2-yl]oxymethyl]oxan-2-yl]oxychromen-4-one	-5.73	

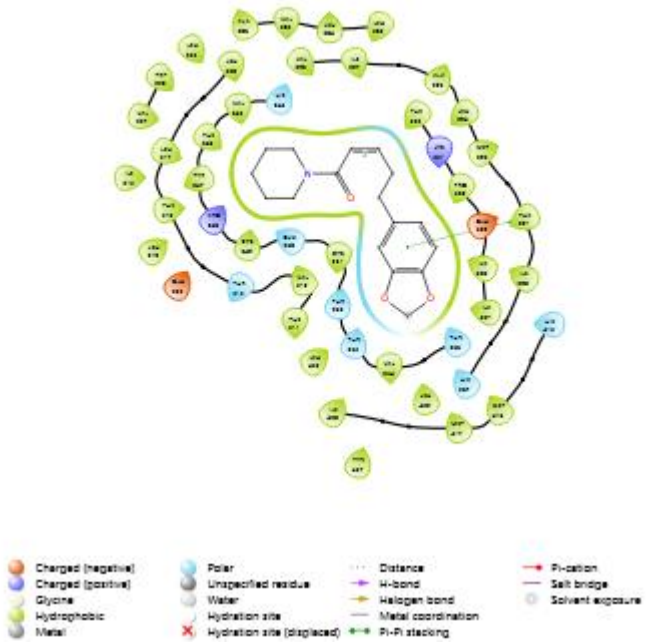

2D interaction of 276753 *Laurus nobilis* with 7WGN

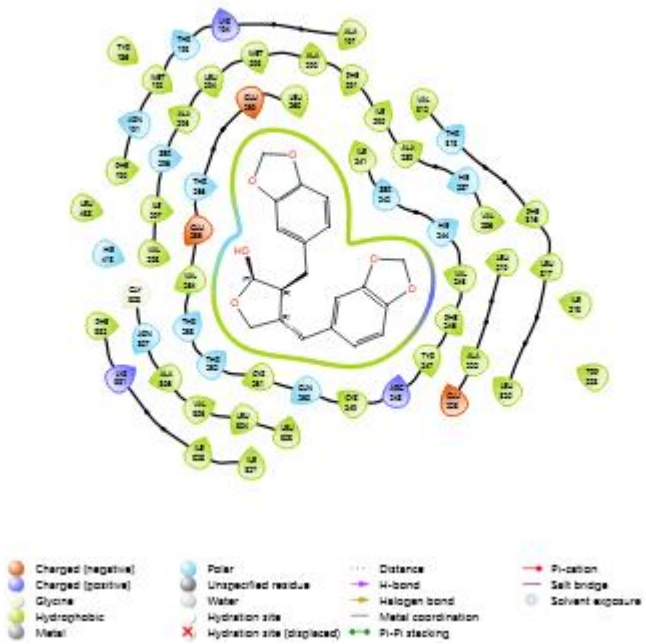

2D interaction of 287685 *Laurus nobilis* with 7WGN

2D interaction of 641115 *Laurus nobilis* with 7WGN

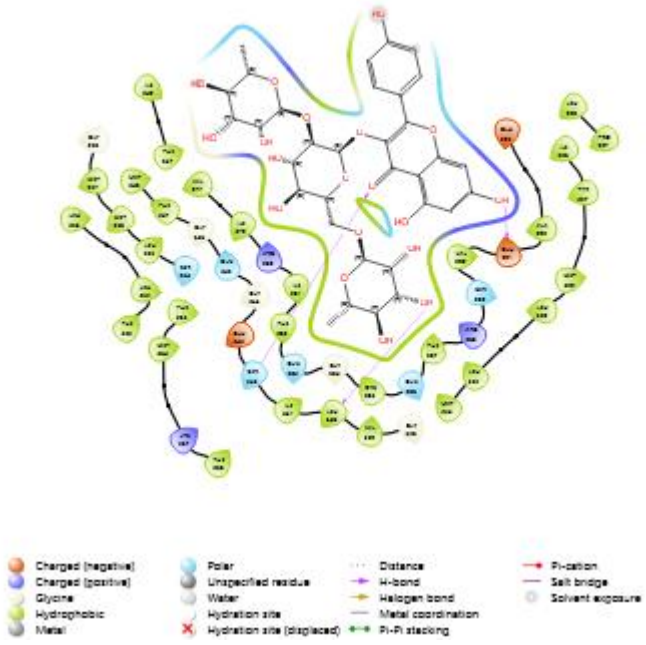

2D interaction of 91274708 *Laurus nobilis* with 7WGN

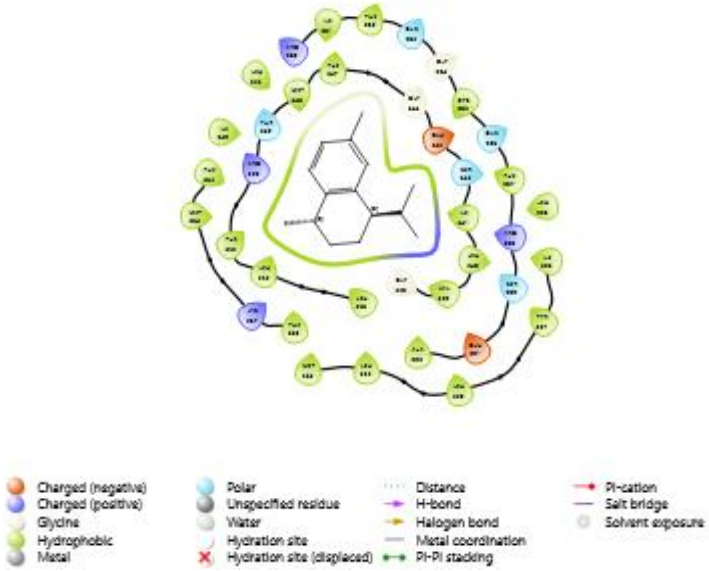

2D interaction of 4840 *Laurus nobilis* with 6ENQ

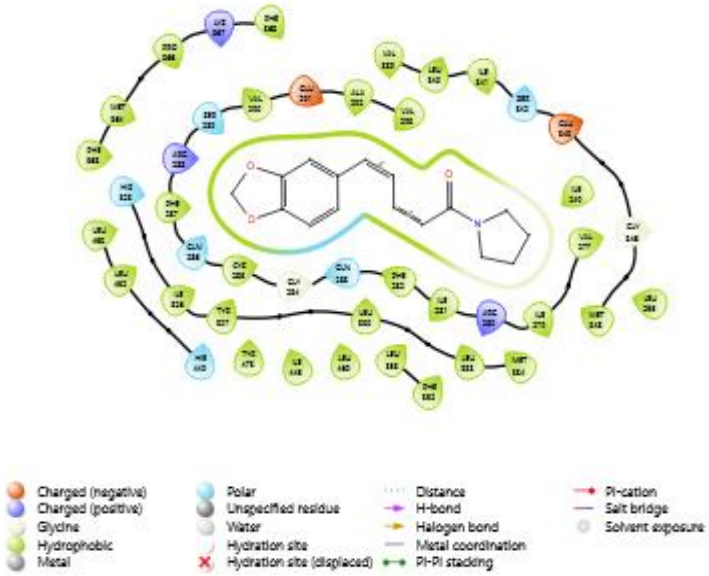

2D interaction of 117669 *Laurus nobilis* with 6ENQ

2D interaction of 5318956 *Laurus nobilis* with 6ENQ

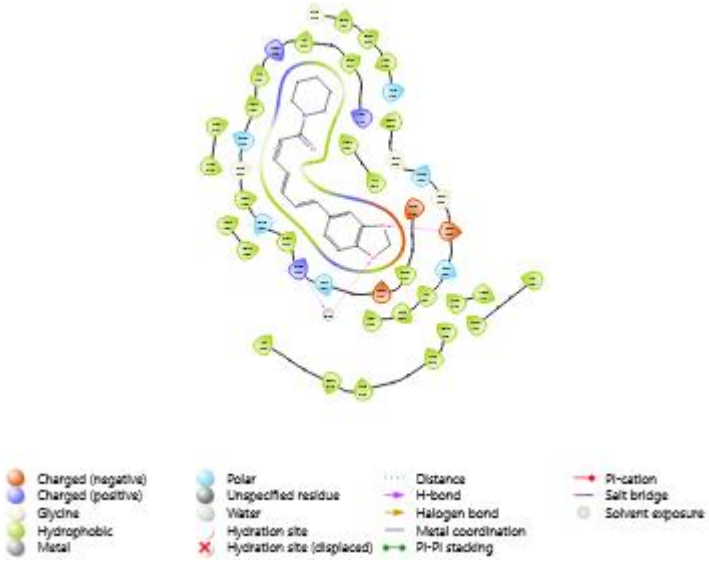

2D interaction of 10064778 *Laurus nobilis* with 6ENQ

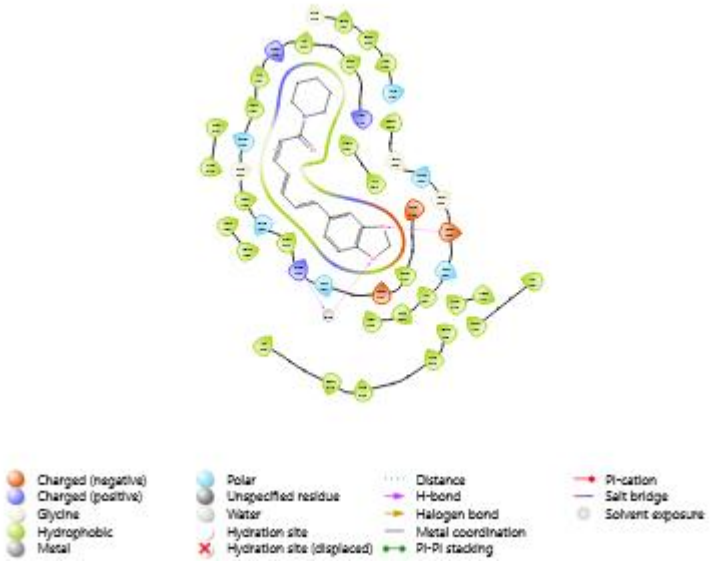

2D interaction of 91274708 *Laurus nobilis* with 6ENQ

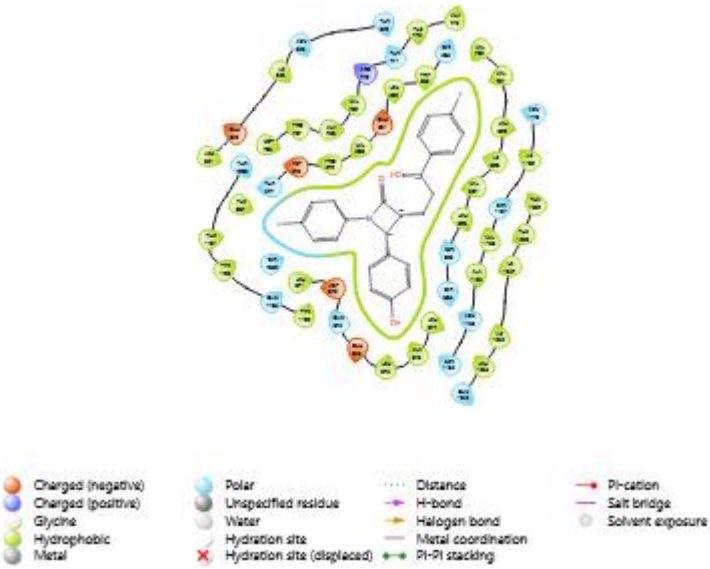

2D interaction Of 162905976 *Laurus nobilis* with 7DFZ

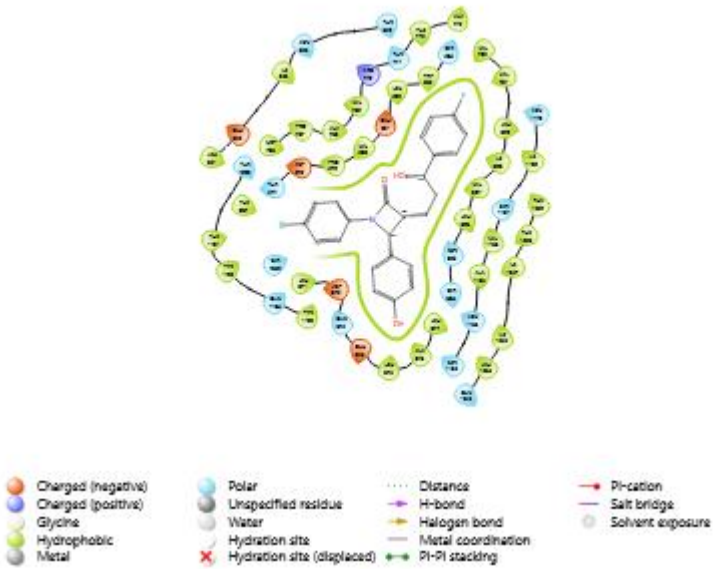

2D interaction of 4426320 *Laurus nobilis* with 7DFZ with 7fdz

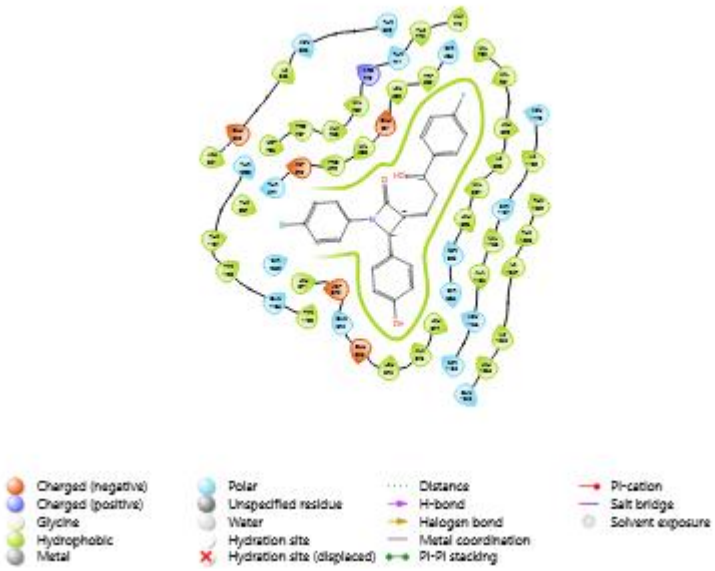

2D interaction of 92231 *Laurus nobilis* with 7DFZ with 7fdz

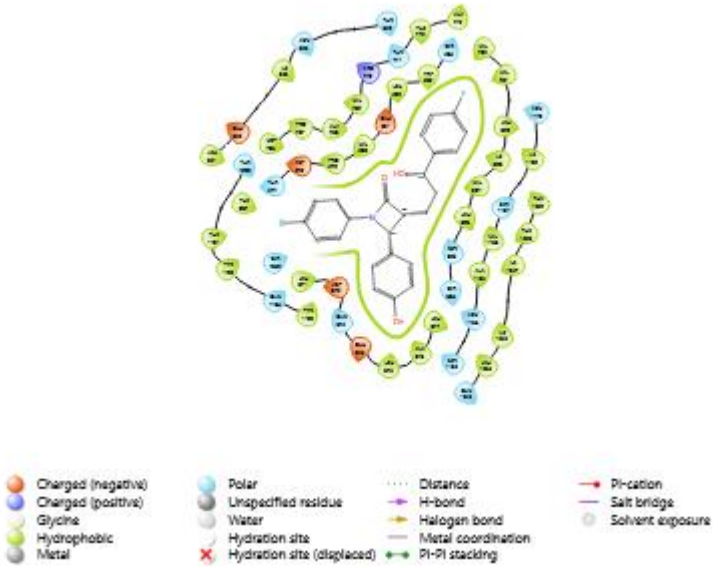

2d interaction of 101716 *Laurus nobilis* with 7DFZ with 7fdz

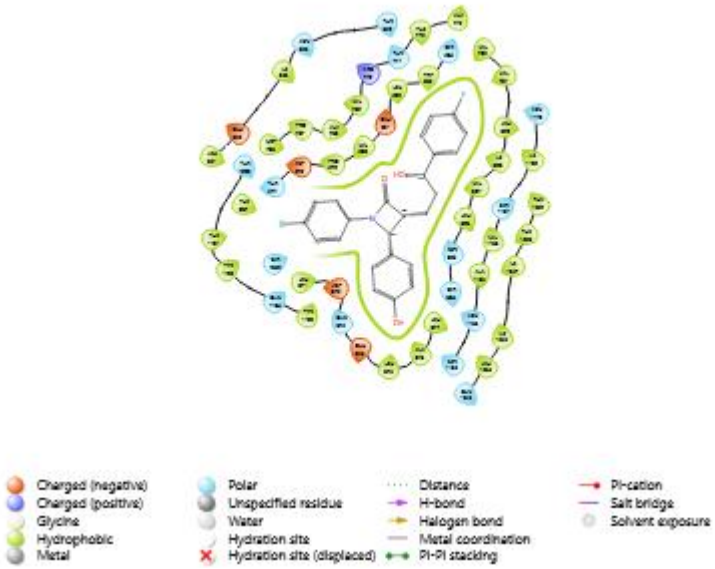

2D interaction of 6987 *Laurus nobilis* with 7DFZ with 7fdz

DOCKING RESULT OF *Ocimum gratissimum*

A total of 157 natural products of *Ocimum gratissimum* were retrieved from PubChem for docking studies. The docking scores for these compounds were evaluated based on their interactions with HMG-CoA (1HWK), PPAR(6ENQ), HM7A4 (8K5B), NCP1L1 (7DF2), PCSK9 (8FPO) receptors. The results below highlight compounds that meet the established criteria for potential antilipidemic activity, focusing on their docking scores relative to the reference standard.

Table 3.5 Docking scores of *Ocimum gratissimum*

COMPOUND CID	IUPAC NAME	1HWK Docking Score	6ENQ Docking Score	7DFZ Docking Score	8K5B Docking score	7GWN Docking Score
135	4-hydroxybenzoic acid	-7.11				
5991	(8R,9S,13S,14S,17R)-17-ethynyl-13-methyl-			-4.65		

	7,8,9,11,12,14,15,16-octahydro-6H-cyclopenta[a]phenanthrene-3,17-diol			
6989	5-methyl-2-propan-2-ylphenol		-4.52	
7460	2-methyl-5-propan-2-ylcyclohexa-1,3-diene		-4.59	
7462	1-methyl-4-propan-2-ylcyclohexa-1,3-diene		-4.54	
7463	1-methyl-4-propan-2-ylbenzene		-4.62	
8468	4-hydroxy-3-methoxybenzoic acid	-5.91	-5.05	
8768	3,4-dihydroxybenzaldehyde	-6.28		
11463	1-methyl-4-propan-2-ylidenecyclohexene		-4.53	
69867	1H-indole-3-carboxylic acid	-6.38		-7.25
92231	(1aR,4aR,7S,7aR,7bR)-1,1,7-trimethyl-4-methylidene-1a,2,3,4a,5,6,7a,7b-octahydrocyclopropa[h]azulen-7-ol		-4.97	
188323	5-hydroxy-2-(4-hydroxyphenyl)-6,7-dimethoxychromen-4-one		-4.68	

442393	(3R,4aS,8aR)-8a-methyl-5-methylidene-3-prop-1-en-2-yl-1,2,3,4,4a,6,7,8-octahydronaphthalene		-7.28		
442664	5,7-dihydroxy-2-(4-hydroxyphenyl)-6,8-bis[(2S,3R,4R,5S,6R)-3,4,5-trihydroxy-6-(hydroxymethyl)oxan-2-yl]chromen-4-one	-5.62			
520384	4-methyl-1-propan-2-ylbicyclo[3.1.0]hex-2-ene			-4.63	
689043	(E)-3-(3,4-dihydroxyphenyl)prop-2-enoic acid	-6.22			
3702506	4-oxoniobenzoate	-7.11			
5280443	5,7-dihydroxy-2-(4-hydroxyphenyl)chromen-4-one	-5.57			
5281520	(1E,4E,8E)-2,6,6,9-tetramethylcycloundeca-1,4,8-triene				-7.52
5281522	(1R,4Z,9S)-4,11,11-trimethyl-8-methylidenebicyclo[7.2.0]undec-4-ene				-8.02
5281553	(3E)-3,7-dimethylocta-1,3,6-triene				-7.24
5281643	2-(3,4-dihydroxyphenyl)-5,7-dihydroxy-3-				-7.33

5281764	[(2S,3R,4S,5R,6R)-3,4,5-trihydroxy-6-(hydroxymethyl)oxan-2-yl]oxychromen-4-one (2R,3R)-2,3-bis[[(E)-3-(3,4-dihydroxyphenyl)prop-2-enoyl]oxy]butanedioic acid				-7.30
5318767	5,7-dihydroxy-2-(4-hydroxyphenyl)-3-[(2S,3R,4S,5S,6R)-3,4,5-trihydroxy-6-[[(2R,3R,4R,5R,6S)-3,4,5-trihydroxy-6-methyloxan-2-yl]oxymethyl]oxan-2-yl]oxychromen-4-one	-5.54			
6440397	(2R,3R)-2-[(E)-3-(3,4-dihydroxyphenyl)prop-2-enoyl]oxy-3-hydroxybutanedioic acid	-6.94			
12313020	(1S,4aS,8aR)-7-methyl-4-methylidene-1-propan-2-yl-2,3,4a,5,6,8a-hexahydro-1H-naphthalene			-4.66	
13607752	6-[2-(3,4-dihydroxyphenyl)-5-hydroxy-4-oxochromen-7-yl]oxy-3,4,5-trihydroxyoxane-2-carboxylic acid	-6.75	-6.98		
13893597	(1R,2S)-1-(4-hydroxy-3-methoxyphenyl)-2-[4-(3-		-7.22		

	hydroxypropyl)-2-methoxyphenoxy]propane-1,3-diol		
13943205	(3aR,4S,6aR,8S,9aR,9bR)-4,8-dihydroxy-3,6,9-trimethylidene-3a,4,5,6a,7,8,9a,9b-octahydroazuleno[4,5-b]furan-2-one	-5.94	
14589530	(3S,3aR,4S,6aR,8S,9S,9aR,9bR)-4,8-dihydroxy-3,9-dimethyl-6-methylidene-3,3a,4,5,6a,7,8,9,9a,9b-decahydroazuleno[4,5-b]furan-2-one		-4.53

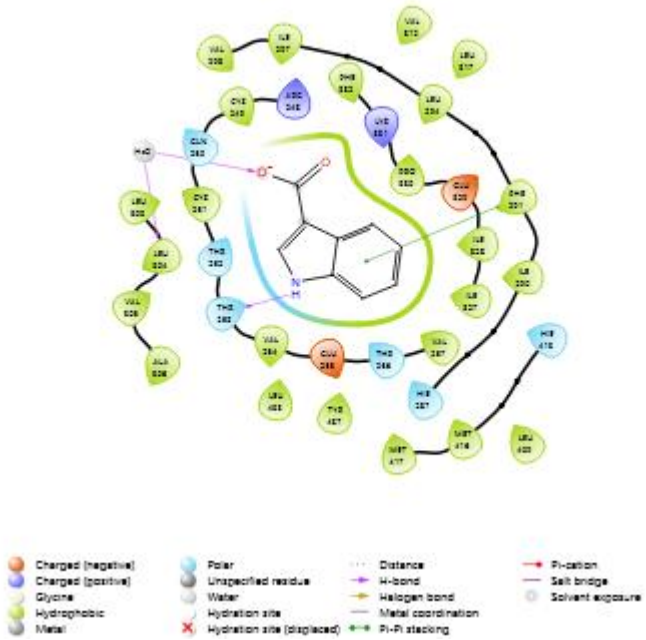

2D interaction of 69867 *Ocimum gratissimum* with 7WGN

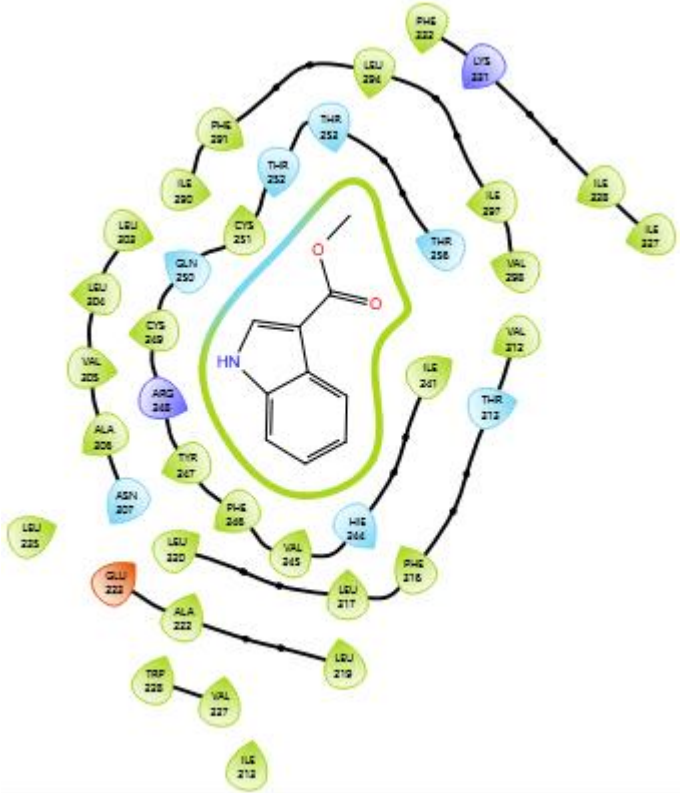

2D interaction of 5281792 *Ocimum gratissimum* with 7WGN

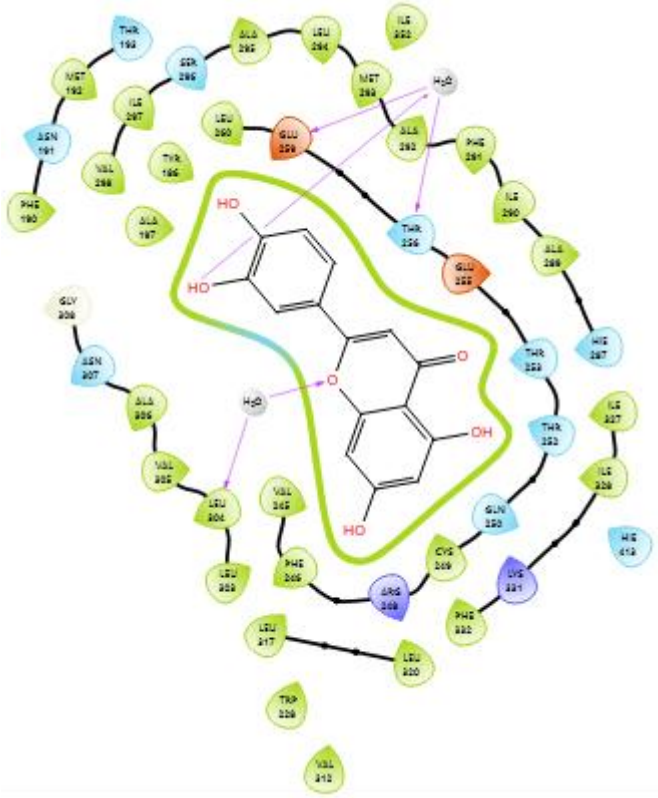

2D interaction of 5316820 *Ocimum gratissimum* with 7WGN

2D interaction of 5286445 *Ocimum gratissimum* with 7WGN

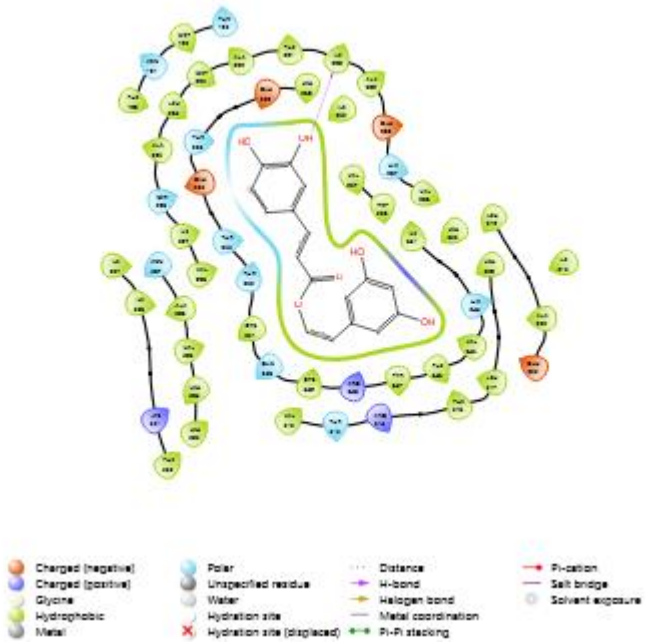

2D interaction of 589098 *Ocimum gratissimum* with 7WGN

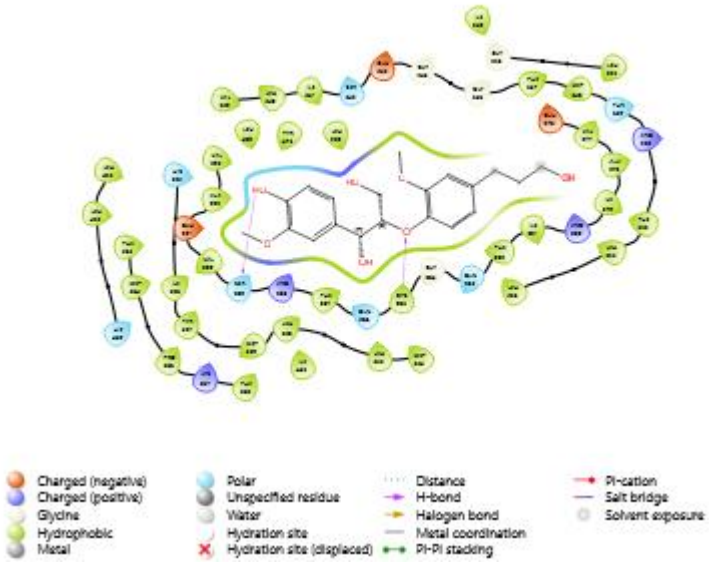

2D interaction of 13667752 *Ocimum gratissimum* with 6ENQ

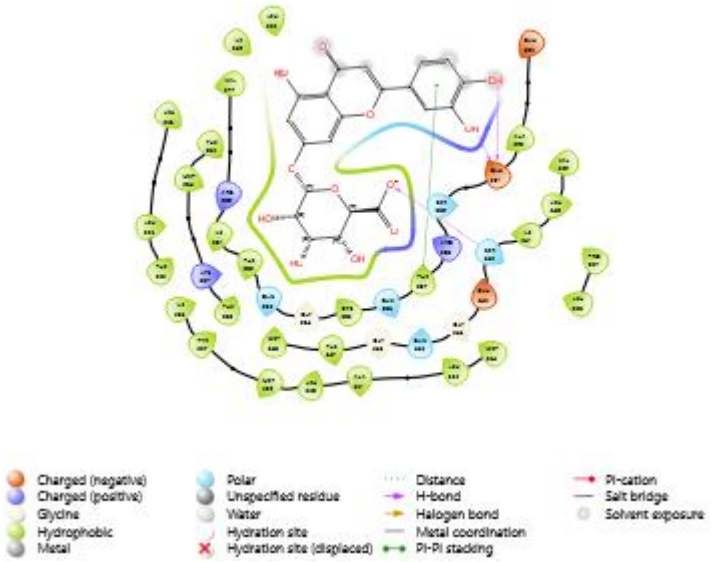

2D interaction of 130607752 *Ocimum gratissimum* with 6ENQ

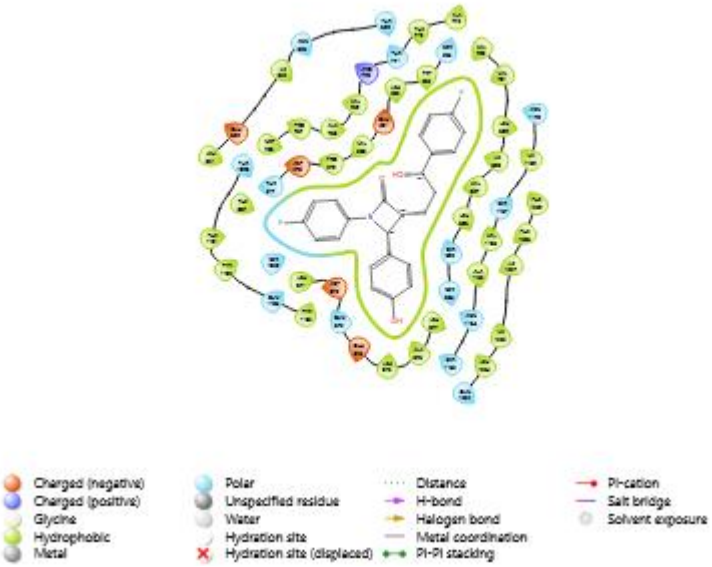

2D interaction of 8468 *Ocimum gratissimum* with 7DFZ

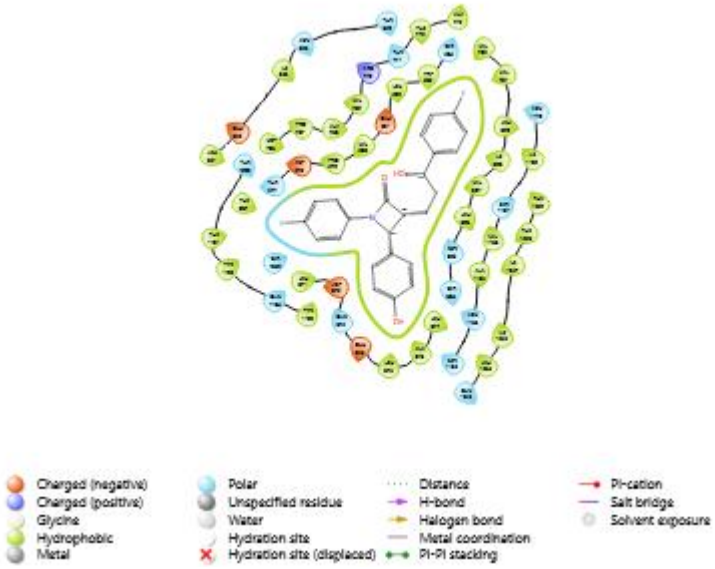

2D interaction 92231 *Ocimum gratissimum* with 7DFZ

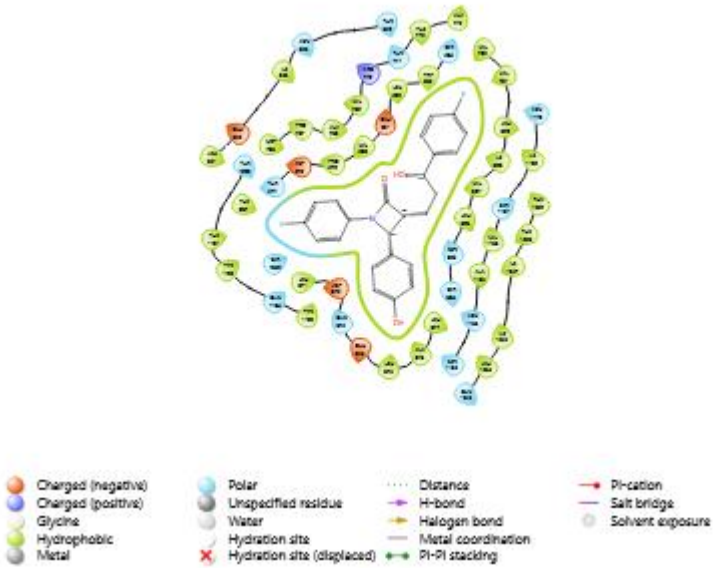

2D interaction of 1888323 *Ocimum gratissimum* with 7DFZ

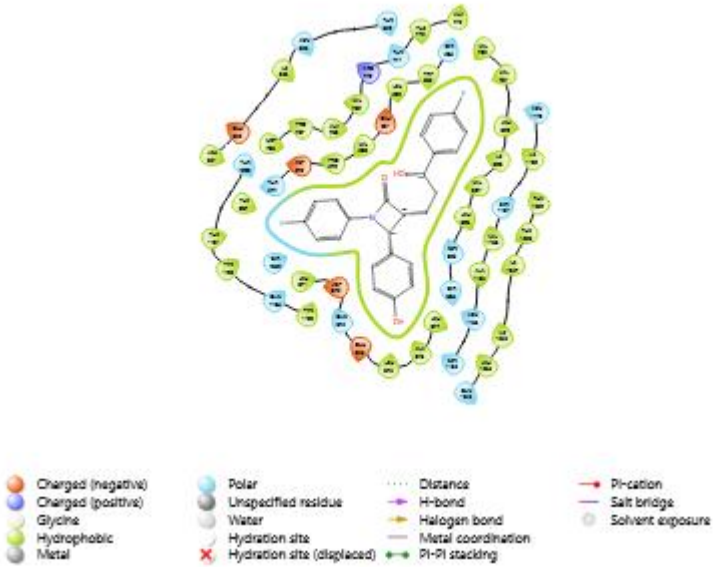

2D interaction of 12313020 *Ocimum gratissimum* with 7DFZ

DOCKING RESULT OF *Piper guineense*

A total of 141 natural products of *Piperer guineense* were retrieved from PubChem for docking studies. The docking scores for these compounds were evaluated based on their interactions with HMG-CoA (1HWK), PPAR(6ENQ), HM7A4 (8K5B), NCP1L1 (7DF2), PCSK9 (8FPO) receptors. The results below highlight compounds that meet the established criteria for potential antilipidemic activity, focusing on their docking scores relative to the reference standard.

Table 3.6 Docking score of *Piper guineense*

COMPOUND CID	IUPAC NAME	1HWK	6ENQ BINDING AFFINITY	7DFZ BINDING AFFINITY	8K5B BINDING AFFINITY	7WGN BINDING AFFINITY
2537	1,7,7-trimethylbicyclo[2.2.1]heptan-2-one			=	=	=
4840	5-(1,3-benzodioxol-5-yl)-1-piperidin-1-ylpenta-2,4-dien-1-one		-7.88	=	=	-7.72
6987	3-methyl-6-propan-2-ylcyclohex-2-en-1-one			-4.77	=	=
7460	2-methyl-5-propan-2-ylcyclohexa-1,3-diene			-4.59	=	=
7463	1-methyl-4-propan-2-ylbenzene		=	-4.62	=	=
11142	3-methylidene-6-propan-2-ylcyclohexene		=	-4.53	=	=
11463	3-methylidene-6-propan-2-ylcyclohexene			-4.53	=	=
54930	3-(1,3-benzodioxol-5-yl)-1-piperidin-1-ylprop-2-en-1-one		-7.15	=	=	-8.42
90785	2-(3,8-dimethyl-1,2,3,3a,4,5,6,7-octahydroazulen-5-yl)propan-2-ol		-7.08	=	=	=

92231	(1*aR*,4*aR*,7*S*,7*aR*,7*bR*)-1,1,7-trimethyl-4-methylidene-1*a*,2,3,4*a*,5,6,7*a*,7*b*-octahydrocyclopropa[h]azulen-7-ol		-4.97	=	=
101716	1,1,4,7-tetramethyl-2,3,4a,5,6,7,7a,7b-octahydro-1aH-cyclopropa[e]azulen-4-ol		-4.96	=	=
117669	5-(1,3-benzodioxol-5-yl)-1-pyrrolidin-1-ylpenta-2,4-dien-1-on	-7.45	=	=	-8.02
155328	5-(6-methoxy-1,3-benzodioxol-5-yl)-1-piperidin-1-ylpenta-2,4-dien-1-one		=	=	-7.46
162986	5-(6-methoxy-1,3-benzodioxol-5-yl)-1-piperidin-1-ylpent-2-en-1-one		=	=	-7.77
276753	5-(1,3-benzodioxol-5-yl)-1-piperidin-1-ylpent-2-en-1-one		=	=	-8.13
287685	3,4-bis(1,3-benzodioxol-5-ylmethyl)oxolan-2-ol	-7.00	=	=	-8.21
441005	(1S,8aR)-4,7-dimeth	-7.28	=	=	=
641115	(1S,8aR)-4,7-dimethyl-1-propan-2-yl-1,2,3,5,6,8a-hexahydronaphthalene		=	=	-8.42
1548913	(2Z,4E)-5-(1,3-benzodioxol-5-yl)-1-piperidin-1-ylpenta-2,4-dien-1-		=	=	-7.72

	one					
5281772	E)-3-(1,3-benzodioxol-5-yl)-N-(2-methylpropyl)prop-2-enamide			=	=	-7.32
5320618	(E)-5-(1,3-benzodioxol-5-yl)-1-piperidin-1-ylpent-2-en-1-one			=	=	-7.50
5320621	(2E,4E)-5-(1,3-benzodioxol-5-yl)-N-(2-methylpropyl)penta-2,4-dienamide			=	=	-7.57
6429077	(1S,4S)-1,6-dimethyl-4-propan-2-yl-1,2,3,4-tetrahydronaphthalene		-7.26	=	=	=
6441090	(E)-5-(6-methoxy-1,3-benzodioxol-5-yl)-1-piperidin-1-ylpent-2-en-1-one			=	=	-7.77
11783540	[(1S,2S,4aR,8aR)-2-(1,3-benzodioxol-5-yl)-1,2,4a,5,6,7,8,8a-octahydronaphthalen-1-yl]-piperidin-1-ylmethanone			=	=	-7.51
13919075	(1R,4S,5S)-2-methyl-5-propan-2-ylcyclohex-2-ene-1,4-diol	-6.24		=	=	=
25021463	1-(2,4,5-trimethoxyphenyl)propane-1,2-diol		-7.00	=	=	=
91274708	7-(1,3-benzodioxol-5-yl)-1-piperidin-1-ylhepta-2,4,6-trien-1-one		-7.52	=	=	-8.15

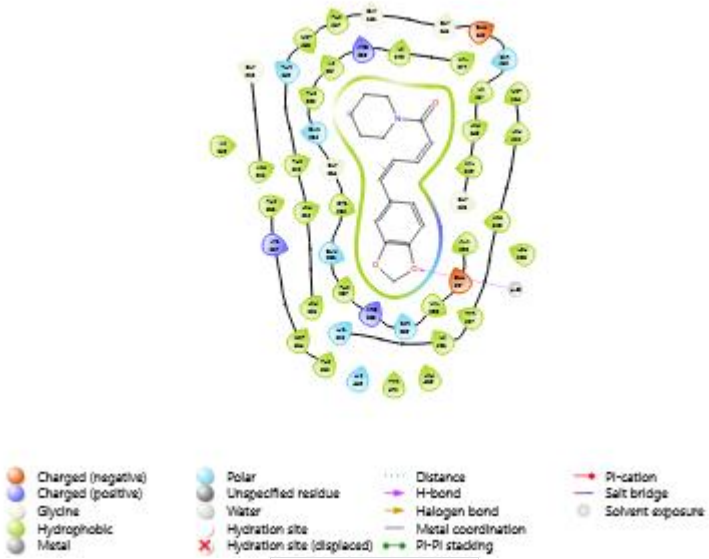

2D interaction of 4840 *Piper guineense* with 6ENQ

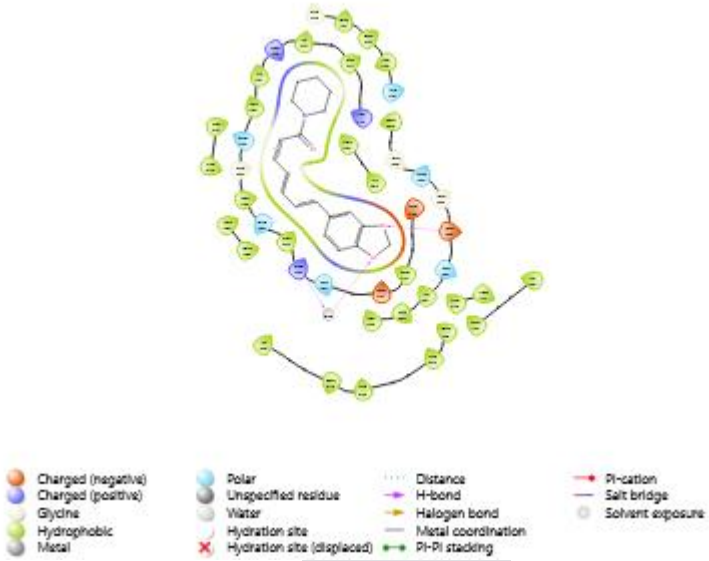

2D interaction of 117669 *Piper guineense* with 6ENQ

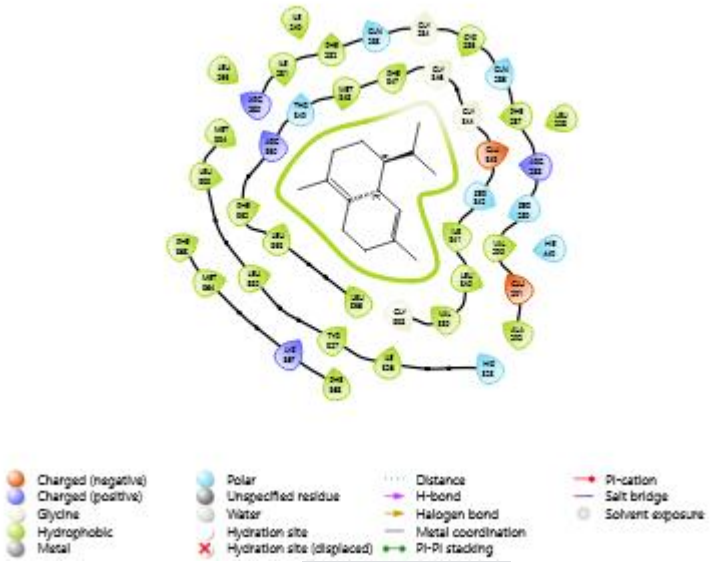

2D interaction of 441005 *Piper guineense* with 6ENQ

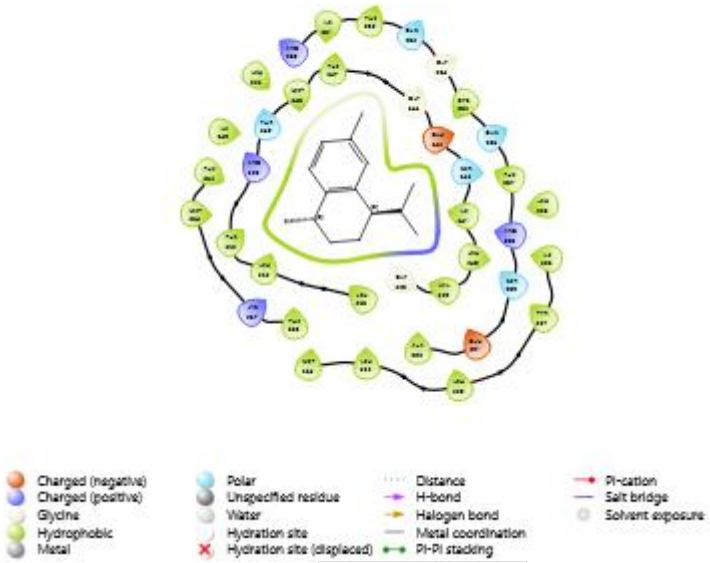

2D interaction of 6429077 *Piper guineense* with 6ENQ

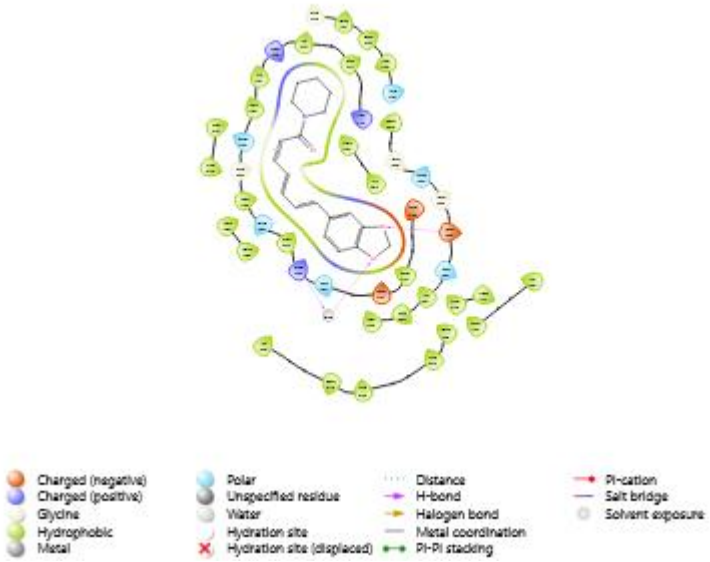

2D interaction of 91274708 *Piper guineense* with 6ENQ

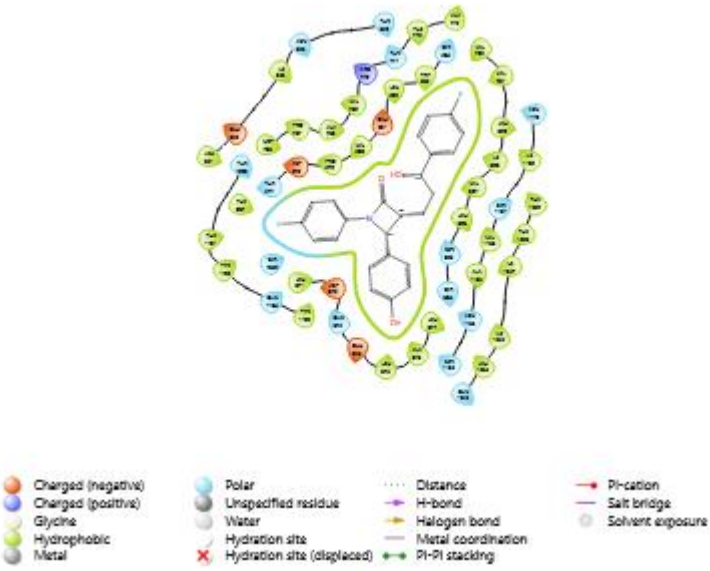

2D interaction of 92231 *Piper guineense* with 7DFZ

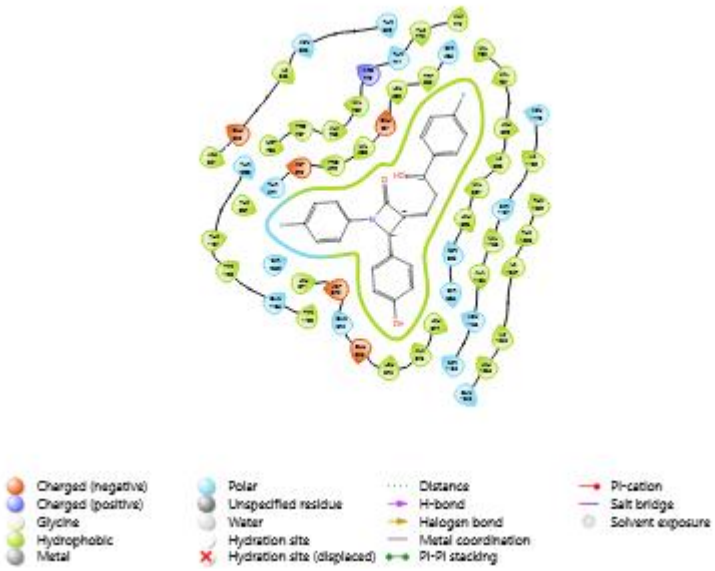

2D interaction of 101716 *Piper guineense* with 7DFZ

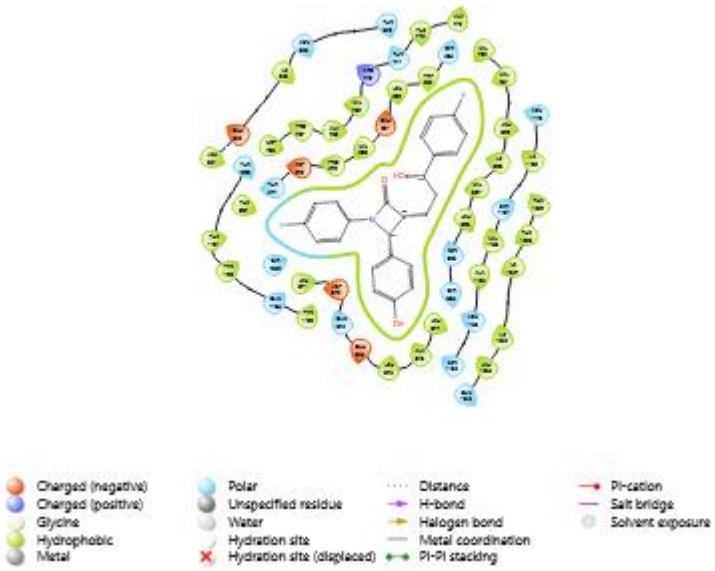

2D interaction of 6987 *Piper guineense* with 7DFZ

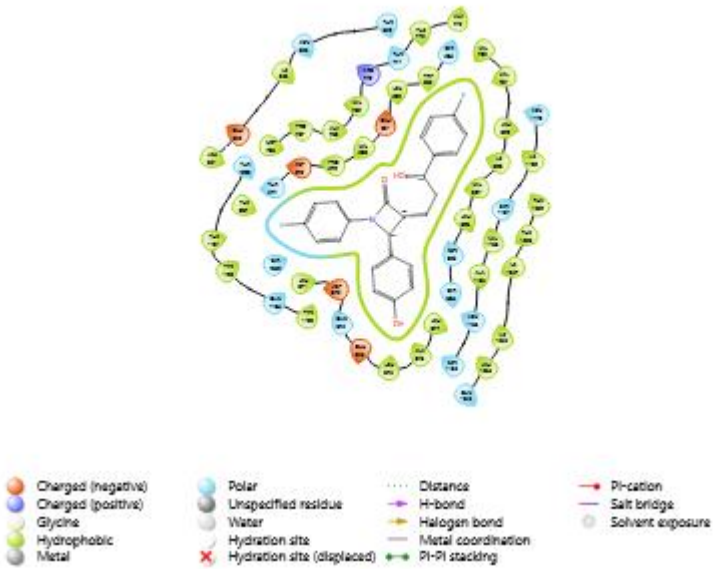

2D interaction of 7463 *Piper guineense* with 7DFZ

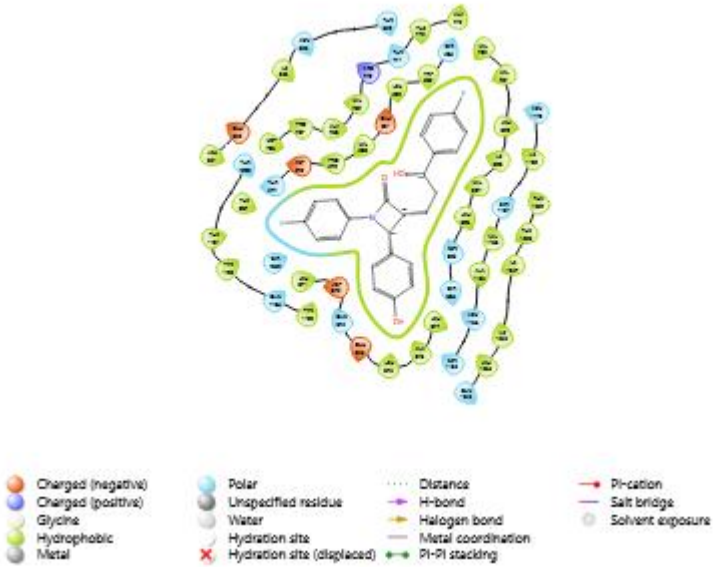

2D interaction of 7460 *Piper guineense* with 7DFZ

ADME Profiling

Table 3.7 **ADME Profiling of ligands from *Laurus nobilis***

COMPOUND CID	Molecular Weight	No. H-bond a*cymbopogon citratus*eptor	No. H-bond donors	Consensus Log P	Lipinski	Bioavailability Score
68677842	434.92	5	1	4.13	0	0.56
155569057	509.65	5	1	3.87	1	0.55
21829311	124.12	3	1	0.32	0	0.85
11526038	490.55	7	1	4.71	0	0.56
150311	409.43	5	2	4.33	1	0.55
60823	558.64	6	4	4.94	1	0.56
91274708	311.37	3	0	3.55	0	0.55

287685	356.37	6	1	2.9	0	0.55
117669	271.31	3	0	2.75	0	0.55
276753	287.35	3	0	3.1	0	0.55
5320618	287.35	3	0	3.1	0	0.55
54930	259.3	3	0	2.52	0	0.55
6429077	202.34	0	0	4.57	1	0.55
101716	222.37	1	1	3.42	0	0.55
117669	271.31	3	0	2.75	0	0.55
91274708	311.37	3	0	3.55	0	0.55
441005	204.35	0	0	4.14	1	0.55
162953580	384.42	6	0	3.72	0	0.55
162940150	222.37	1	1	3.41	0	0.55
287685	356.37	6	1	2.9	0	0.55
90785	356.37	6	1	2.9	0	0.55

276753	287.35	3	0	3.1	0	0.55
117669	271.31	3	0	2.75	0	0.55
155328	315.36	4	0	2.96	0	0.55
91274708	311.37	3	0	3.55	0	0.55
1548913	285.34	3	0	3.55	0	0.55
162986	317.38	4	0	3	0	0.55
6441090	317.38	4	0	3	0	0.55
6987	152.23	1	0	2.52	0	0.55
162986	317.38	4	0	3	0	0.55
92231	220.35	1	1	3.3	0	0.55
5320621	273.33	3	1	3.17	0	0.55
6987	152.23	1	0	2.52	0	0.55
7460	136.23	0	0	2.97	0	0.55
11142	136.23	0	0	3.07	0	0.55

7460	136.23	0	0	2.97	0	0.55
11463	136.23	0	0	3.4	0	0.55
92037727	383.52	3	1	5.47	0	0.55
5281772	247.29	3	1	2.65	0	0.55
101716	222.37	1	1	3.42	0	0.55
92037727	383.52	3	1	5.47	0	0.55
556919	232.32	2	0	2.97	0	0.55
4426320	230.3	2	0	2.98	0	0.55
5089476	311.33	5	2	2.5	0	0.55
5280343	302.24	7	5	1.23	0	0.55
5280863	286.24	6	4	1.58	0	0.55
5281428	248.32	3	1	2.16	0	0.55
5383546	290.35	4	0	2.99	0	0.55
10064778	323.34	5	0	2.96	0	0.55

11957301	311.33	5	2	2.5	0	0.55
44234540	280.36	4	2	2.02	0	0.55
44602428	290.35	4	0	2.02	0	0.55
101337610	309.32	5	1	2.71	0	0.55
131752050	248.32	3	1	2.39	0	0.55
139595854	337.46	4	2	1.03	0	0.55
162849740	918.26	25	15			
162871101	309.24	5	3			
163033371	756.21	20	12			

Table 8 **ADME Profiling of ligands from *OG***

COMPOUND	Molecular	No. of H-bond a*cymbopogon*	No. of H-bond	Consensus Log	Lipinski	Bioavailability

CID	Weight	*citratus*eptors	donors	P		Score
60823	558.64	6	4	4.94	1	0.56
135	138.12	3	2	1.05	0	0.85
2266	188.22	4	2	1.49	0	0.85
5991	296.4	2	2	3.63	0	0.55
6989	150.22	1	1	2.8	0	0.55
7460	136.23	0	0	2.97	0	0.55
7462	136.23	0	0	3.3	0	0.55
7463	134.22	0	0	3.5	1	0.55
8468	168.15	4	2	1.08	0	0.85
11463	136.23	0	0	3.4	0	0.55
69867	161.16	2	2	1.56	0	0.85
92231	220.35	1	1	3.3	0	0.55
188323	314.29	6	2	2.46	0	0.55

442393	204.35	0	0	4.51	1	0.55
520384	136.23	0	0	3.14	1	0.55
689043	180.16	4	3	0.93	0	0.56
3702506	138.12	3	1	0.72	0	0.55
5280443	270.24	5	3	2.11	0	0.55
5281520	204.35	0	0	4.26	1	0.55
5281522	204.35	0	0	4.24	1	0.55
5281553	136.23	0	0	3.4	0	0.55
6440397	312.23	9	5	-0.29	0	0.11
6451618	136.23	0	0	3.15	1	0.55
12313020	204.35	0	0	4.17	1	0.55
13893597	378.42	7	4	1.87	0	0.55
13943205	262.3	4	2	1.25	0	0.55
14589530	266.33	4	2	1.45	0	0.55

162972461	254.37	3	3	1.94	0	0.55

ADME OG.

Table 9 **ADME Profiling of ligands from *PSIDIUM GUAJAVA***

COMPOUND CID	Molecular weight	No. of H-bond a*cymbopogon citratus*eptors	No. of H-bond donors	Consensus Log P	Lipinski	Bioavailability Score
72	154.12	4	3	0.65	0	0.56
370	170.12	5	4	0.21	0	0.56
674	45.08	1	1	0.03	0	0.55
6902	150.13	5	4	-1.95	0	0.55
7462	136.23	0	0	3.3	0	0.55
7463	134.22	0	0	3.5	1	0.55

8468	168.15	4	2	1.08	0	0.85
10225	198.3	0	0	4.76	1	0.55
11463	136.23	0	0	3.4	0	0.55
220001	164.16	5	4	-1.49	0	0.55
445858	194.18	4	2	1.36	0	0.85
689043	180.16	4	3	0.93	0	0.56
3707243	226.27	2	1	2.66	0	0.55
5280343	302.24	7	5	1.23	0	0.55
5281670	302.24	7	5	1.2	0	0.55
5281672	318.24	8	6	0.79	1	0.55
5281855	302.19	8	4	1	0	0.55
5352543	198.3	2	0	3.36	0	0.55
6429077	202.34	0	0	4.57	1	0.55
9828626	536.87	0	0	4.57	1	0.55

ADME OF *PSIDIUM GUAJAVA*

Table10 **ADME Profiling of ligands from *PG***

COMPOUND CID	MOLECULAR WEIGHT	No. of H-bond acceptor	No of H-bond donors	Consensus Log P	Lipinski	Bioavailability Score
938	123.11	3	1	0.32	0	0.85
1054	169.18	4	3	-0.02	0	0.55
1130	265.35	3	2	0.53	0	0.55
4458	154.25	1	1	2.78	0	0.55
6654	136.23	0	0	3.44	1	0.55
6987	152.23	1	0	2.52	0	0.55
7410	120.15	1	0	1.82	0	0.55
7462	136.23	0	0	3.3	0	0.55

9989	168.23	2	1	2.48	0	0.85
69253	135.16	1	1	1.32	0	0.55
69423	282.5	1	0	6.46	1	0.55
445858	194.18	4	2	1.36	0	0.85
493570	376.36	8	5	-0.19	0	0.55
637542	164.16	3	2	1.26	0	0.85
689043	180.16	4	3	0.93	0	0.56
1549106	164.16	3	2	1.29	0	0.85
1794427	354.31	9	6	-0.39	1	0.11
3084311	222.37	1	1	3.44	0	0.55
5275520	168.23	2	1	2.47	0	0.85
5280373	284.26	5	2	2.44	0	0.55
5280445	286.24	6	4	1.73	0	0.55
5280633	354.31	9	6	-0.46	1	0.11

5280961	270.24	5	3	2.04	0	0.55
5281804	284.26	5	2	2.43	0	0.55
15901362	368.34	9	5	-0.08	0	0.11
154496625	432.38	10	6	0.38	1	0.55
154496626	432.38	10	7	-0.38	1	0.55
157009723	403.36	9	6	-0.2	1	0.55
165342981	426.72	1	0	7.37	1	0.55

ADME FOR PG

COMPOUND CID	Molecular weight	No of H-bond acceptors	No of H-bond donors	Consensus Log P	Lipinski	Bioavailability Score
938	123.11	3	1	0.32	0	0.85
4458	154.25	1	1	2.78	0	0.55
6654	136.23	0	0	3.44	1	0.55
6987	152.23	1	0	2.52	0	0.55
7410	120.15	1	0	1.82	0	0.55
7462	136.23	0	0	3.3	0	0.55
9989	168.23	2	1	2.48	0	0.85
689043	180.16	4	3	0.93	0	0.56
1549106	164.16	3	2	1.29	0	0.85

1794427	354.31	9	6	-0.39	1	0.11
5280373	284.26	5	2	2.44	0	0.55
5280633	354.31	9	6	-0.46	1	0.11
5280961	270.24	5	3	2.04	0	0.55
5281804	284.26	5	2	2.43	0	0.55
15901362	368.34	9	5	-0.08	0	0.11
154496625	432.38	10	6	0.38	1	0.55
154496626	432.38	10	7	-0.38	1	0.55
157009723	403.36	9	6	-0.2	1	0.55

Toxicity Prediction

Toxicity prediction of Ligands from *PG*

COMPOUND CID	Carcinogenicity	Genotoxicity	Neurotoxicity	Ototoxicity	Hematotoxicity	Nephrotoxicity	Respiratory	Skin sensitivity
2537	0.588761031627655	0.13871356844902039	0.6066765189170837	0.4003872573375702	0.294656902551651	0.123655833300392838	0.676361322402954 1	0.53094136714935 3
4840	0.693006813526153 6	0.24296098947525024	0.7277855277061462	0.3702186942100525	0.254493504762649 54	0.524296939373016 4	0.670020282268524 2	0.94841551780700 68
6987	0.710298359394073 5	0.04047279432415962	0.6850621700286865	0.2899961471557617	0.472023338079452 5	0.262477606534957 9	0.669396221637725 8	0.64016008377075 2
7460	0.657921195030	0.042362991	0.5929278731	0.390938013	0.4444369971	0.2847281694	0.6417331099	0.717712163925

	02124	720438004	34613	79203796	752167	4122314	510193	1709
7463	0.65872341394 42444	0.012562871 910631657	0.6749529838 562012	0.373148620 1286316	0.4213400781 1546326	0.3450706303 1196594	0.3914189934 73053	0.552885234355 9265
11142	0.58642369508 74329	0.028601266 4437294	0.7048017978 668213	0.308475822 2103119	0.3446293473 2437134	0.1994427591 562271	0.7503184676 170349	0.676310002803 8025
54930	0.61370658874 51172	0.616965711 1167908	0.7549342513 084412	0.249585539 10255432	0.3656330406 665802	0.4939541518 688202	0.5580375790 596008	0.793378472328 186
90785	0.71865379810 33325	0.006659817 881882191	0.4632458686 8286133	0.703954815 864563	0.4712088406 085968	0.2794135808 944702	0.6399645209 312439	0.453289687633 5144
117669	0.74158751964 56909	0.487215816 9746399	0.7535733580 589294	0.364215672 0161438	0.2621941864 490509	0.5370646715 164185	0.6519982218 742371	0.938413441181 1829
155328	0.75062966346 74072	0.340044140 81573486	0.7443392872 810364	0.325236171 48399353	0.3893190920 352936	0.5750422477 722168	0.7203960418 701172	0.728233158588 4094
276753	0.48218515515	0.238824814	0.6547947525	0.372690975	0.4148251712	0.5660796165	0.7014135718	0.702906489372

	327454	55802917	978088	66604614	322235	466309	345642	2534
441005	0.6684602499008179	0.06435349583625793	0.5971654057502747	0.45939067006111145	0.616546630859375	0.3484741747379303	0.6773860454559326	0.6622787714004517
641115	0.644768476486206	0.7900242805480957	0.8007534146308899	0.21655887365341187	0.407225251109781494	0.45009884238243103	0.6391416788101196	0.7478740215301514
1548913	0.7345835566520691	0.7024856209754944	0.645185112953186	0.29060885310173035	0.252748191355665894	0.4700504243373871	0.6301488280296326	0.8223397731781006
5320618	0.4183046519756317	0.7010251283364563	0.678098201751709	0.43365663290023804	0.502864599279053	0.6479239463806152	0.7423667907714844	0.8613550662994385
6441090	0.4986853599554834	0.6074271797813385	0.7373843193054199	0.3668847680091858	0.44941192865371704	0.5780443549156189	0.7742471098899841	0.7178052663803101
25021463	0.8356045484542847	0.9954763054847717	0.9450922012329102	0.7272376418113708	0.6921626925468445	0.9516361355781555	0.600776195526123	0.9433684945106506

Toxicity prediction of Ligands from *Cymbopogon Citratus*

Compound Cid	Carcinogenicity	Genotoxicity	Hematotoxicity	Nephrotoxicity	Neurotoxicity	Ototoxicity	Respiratory	Skin Sensitivity
938	0.41212576627731323	0.09681779146194458	0.3067297637462616	0.45649227499961853	0.5407606959342957	0.30606067180633545	0.6351816654205322	0.5772054195404053
4458	0.37411350011825556	0.00038187703466974234	0.2818378806114197	0.1829286813735962	0.3838255107 4028015	0.29824179 41093445	0.651144683 3610535	0.9914243221 282959
6654	0.62901741266250061	8.718482422409579e-05	0.12425075471401215	0.007616267539560795	0.6552937626838684	0.84084081 64978027	0.844752252 1018982	0.9380729794 502258
6987	0.71029835939400735	0.04047279432415962	0.4720233380794525	0.2624776065349579	0.6850622296333313	0.28999614 71557617	0.669396221 6377258	0.6401600837 70752
7410	0.57365155220030174	0.09527570009231567	0.38230761885643005	0.1683637052744293	0.5930930376052856	0.16717350 482940674	0.596029877 6626587	0.6493884325 027466
7462	0.7431801557540	0.2464298456	0.4871992170	0.42583572864	0.7500697970	0.32742065	0.743870079	0.7295281887

	894	9072723	8106995	53247	39032	19126892	5173645	054443
9989	0.2635788619518	0.0329289883	0.3504782319	0.47777134180	0.3582926690	0.31880250	0.666719436	0.9620848298
	28	37516785	0689087	06897	5784607	573158264	6455078	072815
689043	0.1786400228738	0.4249789118	0.0636274218	0.12576967477	0.0512322708	0.58343559	0.459408342	0.9755023121
	7848	7667847	5592651	798462	96434784	5035553	83828735	833801
1549106	0.1114557459950	0.0508854165	0.0313399024	0.42231145501	0.5640547275	0.40212556	0.645151376	0.9880659580
	4471	6732559	3077278	13678	543213	71977997	7242432	230713
1794427	0.2249300479888	0.2432894855	0.0281693413	0.44059944152	0.0092922262	0.92159748	0.108552925	0.9863648414
	916	7376862	85364532	83203	84742355	07739258	28867722	611816
3084311	0.6397071480751	0.0345019772	0.5807693600	0.49139165878	0.1200561150	0.30751833	0.509549677	0.7910800576
	038	64881134	654602	2959	9084702	319664	3719788	210022
5280373	0.7459681034088	0.9347100853	0.1401468366	0.24614483118	0.3039664626	0.19251348	0.843585789	0.3356422185
	135	919983	3845062	05725	121521	078250885	2036438	897827
5280633	0.1494628489017	0.7180769443	0.0665274411	0.68953233957	0.0018685377	0.88902831	0.037088051	0.9959968328

	4866	511963	4398956	29065	43575871	07757568	438331604	475952
5281804	0.7124509215354	0.8561034202	0.1653650403	0.23582902550	0.3816078305	0.22393599	0.722324430	0.3567342162
	919	575684	022766	697327	244446	152565002	9425354	132263
15901362	0.4211345314979	0.5026298165	0.2574224472	0.87172675132	0.0338737517	0.58823627	0.262959659	0.9711360335
	553	32135	0458984	75146	59529114	23350525	09957886	350037
157009723	0.9999872446060	1	0.0045022228	0.00042559986	2.2740314875	0.00516489	0.909892082	0.9998503923
	181		73270512	46840453	59114e-07	8000657558	2143555	416138
						4		

Toxicity prediction of Ligands from *PSIDIUM GUAJAVA*

COMPOUND CID	Carcinogenicity	Genotoxicity	Hematotoxicity	Nephrotoxicity	Neurotoxicity	Ototoxicity	Respiratory	Skin Sensitivity
72	0.3343457579612732	0.44494345784187317	0.1558580249 5479584	0.1297779083 251953	0.0758764222 2642899	0.5616183876 991272	0.516709744 9302673	0.90649539232 25403
370	0.2189722508192062 4	0.7596558928489685	0.0807773396 3727951	0.0561880245 8047867	0.0107816588 13357353	0.8206550478 935242	0.508308112 6213074	0.99233269691 46729
674	0.4089275002479553	0.0410549156367778 8	0.5280549526 2146	0.6260488629 341125	0.5148328542 709351	0.5632240176 200867	0.881942927 8373718	0.85203558206 55823
6902	0.1447317451238632 2	0.0443153493106365 2	0.1606498509 645462	0.5157765746 116638	0.0797898322 3438263	0.6776536107 063293	0.126119956 3741684	0.74164354801 17798
7462	0.7431801557540894	0.2464298456907272 3	0.4871992766 857147	0.4258357286 453247	0.7500697970 39032	0.3274206817 150116	0.743870079 5173645	0.72952824831 00891
7463	0.6587234139440	0.0125628710	0.4213400781	0.3450706303	0.6749529838	0.3731486201	0.391418993	0.55288523435

	2444	910631657	1546326	1196594	562012	286316	473053	59265
8468	0.413194239139	0.143018752	0.3404621481	0.4294604361	0.3031882047	0.3172185420	0.672326266	0.54807221889
	5569	33650208	895447	0572815	653198	98999	7655945	49585
10225	0.747468411922	0.062253348	0.5505743026	0.5762960314	0.6506732106	0.4724642932	0.718252539	0.62383127212
	4548	52933884	733398	750671	208801	4150085	6347046	52441
11463	0.726470887660	0.161042600	0.4090697765	0.2507367730	0.7295742034	0.2341617345	0.496355235	0.66634654998
	9802	87013245	350342	140686	912109	8099365	57662964	7793
220001	0.104302294552	0.002150738	0.0132612772	0.1703954339	0.0908749848	0.9656118154	0.004398736	0.00135029491
	3262	3789867163	28593826	0274048	6042023	525757	637085676	50279164
445858	0.248971953988	0.119884468	0.1768050193	0.4069756567	0.2118307054	0.3164496421	0.607862830	0.74299973249
	07526	61505508	786621	47818	0428162	813965	1620483	43542
689043	0.178640022873	0.424979001	0.0636274218	0.1257696747	0.0512322820	0.5834356546	0.459408283	0.97550231218
	87848	28364563	5592651	7798462	7230568	401978	2336426	33801
3707243	0.400081127882	0.059958200	0.2027318924	0.4219971895	0.7090076804	0.5485401749	0.373991012	0.41870331764

	0038	90174675	665451	2178955	161072	610901	5732422	22119
5280343	0.600176751613	0.974865555	0.0324999801	0.0106424093	0.0085937492	0.1636759787	0.673656761	0.89692437648
	6169	7632446	8145561	24645996	5494194	7979279	6462708	77319
5281670	0.656667411327	0.985291481	0.0311724971	0.0154245235	0.0181084144	0.0689724162	0.801455557	0.68012905120
	3621	0180664	9798565	02588272	86050606	2209549	346344	84961
5281672	0.501711785793	0.994630217	0.0146661633	0.0031101421	0.0008768084	0.4736244976	0.652477502	0.99591749906
	3044	5521851	62562656	918720007	226176143	5205383	822876	53992
5281855	0.666364789009	0.953362584	0.1537348031	0.0389521531	0.0026986005	0.3716128766	0.277327924	0.89545816183
	0942	1140747	9976807	7606926	25036454	5367126	96681213	09021
5318135	0.132175236940	0.934422612	0.2286359220	0.4082058370	7.0953334216	0.9892064332	0.000615676	0.99823272228
	3839	1902466	7431793	113373	02845e-05	962036	6321510077	24097
5352543	0.161719173192	0.000200889	0.0376430749	0.4442748725	0.4476986229	0.1180519610	0.843278288	0.99648076295
	9779	97553102672	8931885	414276	419708	6433868	8412476	85266

6429077	0.8176518082618713	0.09060067683458328	0.32754769921302795	0.3891688585281372	0.6550775766372681	0.31129008531570435	0.8824652433395386	0.6878257393836975
9828626	0.8520350456237793	0.20697754621505737	0.47269490361213684	0.8960216045379639	0.6319769620895386	0.670735776424408	0.8432948589324951	0.9287829399108887
10119810	0.031149277463555336	0.79924184083839386	0.003890176536515355	0.14438828825950623	0.0002653312112670392	0.9326972365379333	0.08044251054525375	0.9996869564056396
10166868	0.07310979813337326	0.92084765434263514	0.006695098709315062	0.08766988664865494	0.0002408078871667385	0.9663773775100708	0.04639995098114014	0.9997968077659607
10455578	0.2784546911716461	0.96557849644561462	0.023320684209460598	0.04786148667335551	0.005809997208416462	0.42605358362197876	0.21071816980838776	0.9605718851089478
11410680	0.20698094367980957	0.99266809225250824	0.001202854560688138	0.001583309727720916	9.517092985333875e-05	0.945753455162048	0.10644704848527908	0.9999712705612183
11966988	0.4107492268085548	0.9966532588005066	0.007614486850798135	0.049174245446920395	0.00015843955043237656	0.980696618556976	0.03016199916601181	0.9999965429306030

69573531	0.384129792451 8585	0.992348313 331604	0.0445327460 7658386	0.0920112505 5551529	0.0113709792 49477386	0.2925593256 9503784	0.389272958 0402374	0.99410372972 4884
102469980	0.368663102388 38196	0.975093245 5062866	0.0019603380 93340397	0.0117822056 63621426	6.8411907705 01271e-05	0.9964376688 00354	0.008794799 447059631	0.99999940395 35522

Toxicity prediction of Ligands from *LAURUS NOBILIS*

COMPOUND CID	Carcinogenicity	Genotoxicity	Hematotoxicity	Nephrotoxicity	Neurotoxicity	Ototoxicity	Respiratory	Skin Sensitivity
91274708	0.7744789719 581604	0.246425673 36559296	0.27394753694 5343	0.52342540025 71106	0.68607068061 82861	0.3748987019 062042	0.8209148049 354553	0.9539028406 143188
287685	0.5351617932 319641	0.303535789 2513275	0.35304632782 936096	0.59419077634 8114	0.71944260597 229	0.9333474040 031433	0.5844038128 852844	0.3623856902 1224976
117669	0.7415875196	0.487215816	0.26219418644	0.53706467151	0.75357335805	0.3642156720	0.6519982218	0.9384134411

	456909	9746399	90509	64185	89294	161438	742371	811829
276753	0.4821851551	0.238824814	0.41482517123	0.56607961654	0.65479475259	0.3726909756	0.7014135718	0.7029064893
	5327454	55802917	22235	66309	78088	6604614	345642	722534
5320618	0.4183046519	0.701025128	0.50286459922	0.64792394638	0.67809820175	0.4336566329	0.7423667907	0.8613550662
	756317	364563	79053	06152	1709	0023804	714844	994385
54930	0.6137065887	0.616965711	0.36563304066	0.49395415186	0.75493425130	0.2495855391	0.5580375790	0.7933784723
	451172	1167908	65802	88202	84412	0255432	596008	28186
6429077	0.8176518082	0.090600676	0.32754769921	0.38916885852	0.65507757663	0.3112900853	0.8824652433	0.6878257393
	618713	83458328	302795	81372	72681	1570435	395386	836975
101716	0.8174194693	0.000862576	0.25086480379	0.16739304363	0.22691342234	0.7465637326	0.6752683520	0.0596523471
	565369	5331089497	104614	72757	61151	24054	317078	1766243
117669	0.7415875196	0.487215816	0.26219418644	0.53706467151	0.75357335805	0.3642156720	0.6519982218	0.9384134411
	456909	9746399	90509	64185	89294	161438	742371	811829
91274708	0.7744789719	0.246425673	0.27394753694	0.52342540025	0.68607068061	0.3748987019	0.8209148049	0.9539028406

	581604	36559296	5343	71106	82861	062042	354553	143188
441005	0.6684602499	0.064353495	0.61654663085	0.34847417473	0.59716540575	0.4593906700	0.6773860454	0.6622787714
	008179	83625793	9375	79303	02747	6111145	559326	004517
162953580	0.7464442253	0.947005510	0.45613336563	0.83455991744	0.81596738100	0.5090762376	0.3673515617	0.6026937365
	112793	3302002	11035	99512	05188	785278	8474426	531921
162940150	0.8280082345	0.141477644	0.32031822204	0.37769436836	0.33801573514	0.2872216701	0.7106571197	0.7239897251
	00885	44351196	589844	242676	938354	5075684	509766	12915
287685	0.5351617932	0.303535789	0.35304632782	0.59419077634	0.71944260597	0.9333474040	0.5844038128	0.3623856902
	319641	2513275	936096	8114	229	031433	852844	1224976
90785	0.7186537981	0.006659817	0.47120884060	0.27941358089	0.46324586868	0.7039548158	0.6399645209	0.4532896876
	033325	881882191	85968	44702	286133	64563	312439	335144
276753	0.4821851551	0.238824814	0.41482517123	0.56607961654	0.65479475259	0.3726909756	0.7014135718	0.7029064893
	5327454	55802917	22235	66309	78088	6604614	345642	722534
117669	0.7415875196	0.487215816	0.26219418644	0.53706467151	0.75357335805	0.3642156720	0.6519982218	0.9384134411

	456909	9746399	90509	64185	89294	161438	742371	811829
155328	0.7506296634	0.340044140	0.38931909203	0.57504224777	0.74433928728	0.3252361714	0.7203960418	0.7282331585
	674072	81573486	52936	22168	10364	8399353	701172	884094
91274708	0.7744789719	0.246425673	0.27394753694	0.52342540025	0.68607068061	0.3748987019	0.8209148049	0.9539028406
	581604	36559296	5343	71106	82861	062042	354553	143188
1548913	0.7345835566	0.702485620	0.25274819135	0.47005042433	0.64518511295	0.2906088531	0.6301488280	0.8223397731
	520691	9754944	665894	73871	3186	0173035	296326	781006
162986	0.5657207369	0.234246730	0.42438268661	0.52810299396	0.67783999443	0.3606547117	0.7349059581	0.5822651386
	804382	80444336	499023	51489	0542	2332764	756592	260986
6441090	0.4986853599	0.607427179	0.44941192865	0.57804435491	0.73738431930	0.3668847680	0.7742471098	0.7178052663
	54834	813385	371704	56189	54199	091858	899841	803101
6987	0.7102983593	0.040472794	0.47202333807	0.26247760653	0.68506217002	0.2899961471	0.6693962216	0.6401600837
	940735	32415962	94525	49579	86865	557617	377258	70752
162986	0.5657207369	0.234246730	0.42438268661	0.52810299396	0.67783999443	0.3606547117	0.7349059581	0.5822651386

	804382	80444336	499023	51489	0542	2332764	756592	260986
92231	0.8147566914	0.183489143	0.37285718321	0.38374370336	0.43190875649	0.3677730560	0.6708575487	0.8302721381
	558411	8484192	80023	53259	45221	3027344	136841	187439
5320621	0.6971156001	0.688636183	0.28829795122	0.42767822742	0.65255618095	0.3042579293	0.5368825793	0.8575162291
	091003	7387085	146606	46216	39795	2510376	266296	526794
6987	0.7102983593	0.040472794	0.47202333807	0.26247760653	0.68506217002	0.2899961471	0.6693962216	0.6401600837
	940735	32415962	94525	49579	86865	557617	377258	70752
7460	0.6579211950	0.042362991	0.44443699717	0.28472816944	0.59292787313	0.3909380137	0.6417331099	0.7177121639
	302124	720438004	52167	122314	4613	9203796	510193	251709
11142	0.5864236950	0.028601266	0.34462934732	0.19944275915	0.70480179786	0.3084758222	0.7503184676	0.6763100028
	874329	4437294	437134	62271	68213	103119	170349	038025
7460	0.6579211950	0.042362991	0.44443699717	0.28472816944	0.59292787313	0.3909380137	0.6417331099	0.7177121639
	302124	720438004	52167	122314	4613	9203796	510193	251709
11463	0.7264708876	0.161042600	0.40906977653	0.25073677301	0.72957420349	0.2341617345	0.4963552355	0.6663465499

	609802	87013245	50342	40686	12109	8099365	7662964	87793
92037727	0.3051986694	0.000943873	0.06648763269	0.55714601278	0.04754451289	0.4062316119	0.2668169736	0.9991507530
	3359375	7179152668	18602	30505	7729874	670868	8621826	212402
5281772	0.6334990859	0.806230247	0.28647959232	0.31393742561	0.62393319606	0.1866574138	0.2995384633	0.7800038456
	031677	0207214	33032	34033	78101	4029388	541107	916809
101716	0.8174194693	0.000862576	0.25086480379	0.16739304363	0.22691342234	0.7465637326	0.6752683520	0.0596523471
	565369	5331089497	104614	72757	61151	24054	317078	1766243
92037727	0.3051986694	0.000943873	0.06648763269	0.55714601278	0.04754451289	0.4062316119	0.2668169736	0.9991507530
	3359375	7179152668	18602	30505	7729874	670868	8621826	212402
556919	0.8207010030	0.082811534	0.44014650583	0.33455985784	0.73314881324	0.4353332519	0.1235672831	0.9506754279
	74646	40475464	26721	53064	76807	53125	5353394	136658
4426320	0.8394524455	0.055066727	0.28127250075	0.17253474891	0.81107795238	0.8258900046	0.3658237755	0.2566788196
	070496	101802826	34027	18576	49487	348572	2986145	5637207
5089476	0.4689049422	0.745935261	0.14836223423	0.72257804870	0.84666854143	0.7513856887	0.9828443527	0.9398524761

	7409363	2495422	480988	60547	1427	817383	22168	199951
5280343	0.6001767516	0.974865555	0.03249998018	0.01064240932	0.00859374925	0.1636759787	0.6736567616	0.8969243764
	136169	7632446	145561	4645996	494194	7979279	462708	877319
5280863	0.7159842848	0.977028250	0.04457971081	0.01862933300	0.03866855427	0.0745180845	0.7127178907	0.6213222146
	777771	6942749	137657	435543	622795	2606201	394409	034241
5281428	0.7272607684	0.383181512	0.68996882438	0.82047331333	0.55992448329	0.4436048269	0.2527025043	0.9870774745
	135437	35580444	65967	1604	92554	2718506	964386	941162
5383546	0.5606006383	0.251740694	0.26419827342	0.51985800266	0.75928431749	0.5156166553	0.0583610609	0.7500938177
	895874	0460205	033386	26587	34387	497314	1737747	108765
10064778	0.9257885217	0.962494492	0.23538945615	0.45832419395	0.88477325439	0.3391211032	0.9005177021	0.4468412101
	666626	5308228	291595	44678	45312	8674316	026611	2687683
11957301	0.5707202553	0.642175376	0.31190782785	0.71638655662	0.79816311597	0.5216222405	0.8891604542	0.8400763273
	749084	4152527	41565	53662	8241	433655	732239	239136
44234540	0.8206744790	0.426994860	0.27853417396	0.47117644548	0.23425495624	0.4336894154	0.7800624966	0.9021186232

	07721	17227173	54541	41614	542236	548645	621399	566833
44602428	0.6269707679	0.709297299	0.39832046627	0.68945652246	0.74701511859	0.3160118162	0.0625650882	0.8641219139
	748535	3850708	99835	47522	8938	6319885	7209473	099121
101337610	0.8215755224	0.953336477	0.24601547420	0.70589166879	0.91229242086	0.3989487588	0.9598196744	0.5990343093
	227905	2796631	024872	65393	41052	405609	918823	87207
131752050	0.7428123950	0.174385100	0.30954450368	0.66804516315	0.48884120583	0.6819582581	0.0541612729	0.9979670643
	958252	60310364	881226	4602	53424	520081	4301987	806458
139595854	0.1350003778	0.943920671	0.15596696734	0.49809280037	0.88327783346	0.3905797600	0.5220456123	0.7501639127
	9344788	9398499	428406	879944	17615	746155	352051	731323
162849740	0.0088569400	0.711051702	0.12508404254	0.94651782512	2.00850336113	0.9993299245	2.4449520424	0.9999965429
	832057	4993896	91333	6648	94465e-05	834351	2412e-05	30603
162871101	0.2471109479	0.401075273	0.38887256383	0.95714986324	0.96614265441	0.6718407869	0.9850890040	0.9410598278
	6657562	7522125	895874	3103	89453	338989	397644	045654
163033371	0.0052837617	0.615574717	0.03247686848	0.77270209789	7.24473793525	0.9946295022	9.8173899459	0.9987590312

69533157	5216675	0443954	27612	2488e-05	964478	6526e-05	957764	

Toxicity prediction of Ligands from *OG*

Compound CID	Carcinogenicity	Genotoxicity	Hematotoxicity	Nephrotoxicity	NeurotoxicitY	Ototoxicity	Respiratory	Skin Sensitivity
60823	0.081044905	0.987508237	0.344585299	0.998845577	0.955535173	0.929038048	0.617132485	0.94840008
135	0.427906454	0.288821042	0.216690198	0.243624121	0.402971476	0.280602187	0.550761402	0.413493007
2266	0.354301602	0.004659529	0.470615268	0.465563565	0.062667608	0.586932957	0.676206231	0.385881543
2537	0.588761032	0.138713568	0.294656903	0.123655833	0.606676519	0.400387257	0.676361322	0.530941367
5991	0.904890478	0.036329258	0.006070965	0.316765577	0.629570663	0.820984662	0.997881472	0.407473803
6989	0.543311238	0.049658444	0.277375907	0.335653752	0.346073359	0.33308354	0.647174358	0.645935178
7460	0.657921195	0.042362992	0.444436997	0.284728169	0.592927873	0.390938014	0.64173311	0.717712164
7462	0.743180156	0.246429846	0.487199277	0.425835729	0.750069797	0.327420682	0.74387008	0.729528248
7463	0.658723414	0.012562872	0.421340078	0.34507063	0.674952984	0.37314862	0.391418993	0.552885234

8468	0.413194239	0.143018752	0.340462148	0.429460436	0.303188205	0.317218542	0.672326267	0.548072219
11463	0.726470888	0.161042601	0.409069777	0.250736773	0.729574203	0.234161735	0.496355236	0.66634655
69867	0.432668	0.349272221	0.45313704	0.590793312	0.51333797	0.424555212	0.706269026	0.389549166
92231	0.814756691	0.183489144	0.372857183	0.383743703	0.431908756	0.367773056	0.670857549	0.830272138
188323	0.732485652	0.879791617	0.145203486	0.069544934	0.207330078	0.118575811	0.705158234	0.64465934
442393	0.80879873	0.04865529	0.432215154	0.409664333	0.384478718	0.257263988	0.8952353	0.904351294
442664	0.135861203	0.952818215	0.157921687	0.539546013	0.000445348	0.982284665	0.001764782	0.998592556
520384	0.696068943	0.071047701	0.302130312	0.263758302	0.622716129	0.303039342	0.719155431	0.145816267
689043	0.178640023	0.424979001	0.063627422	0.125769675	0.051232282	0.583435655	0.459408283	0.975502312
3702506	0.427906454	0.288821042	0.216690198	0.243624121	0.402971476	0.280602187	0.550761402	0.413493007
5280443	0.793351591	0.987231314	0.043182448	0.021411318	0.060596578	0.067824319	0.777348936	0.645180285
5281520	0.378561199	0.088259012	0.089177944	0.375508249	0.740752757	0.075103633	0.538100839	0.872840047
5281522	0.481483787	0.06025235	0.488264233	0.314113498	0.45683679	0.193471029	0.369421333	0.988810003
5281553	0.499098748	0.25918901	0.371967286	0.307206988	0.543637633	0.259919971	0.827061534	0.927850485

5281643	0.337492853	0.986264527	0.107587799	0.077152289	0.005248848	0.745952308	0.137163118	0.999868631
5281764	0.337492853	0.986264527	0.107587799	0.077152289	0.005248848	0.745952308	0.137163118	0.999868631
5318767	0.079051778	0.883618474	0.033050377	0.235961214	0.002025571	0.747545958	0.034867268	0.983964562
6440397	0.060985904	0.665364563	0.066604204	0.721733928	0.016538598	0.726423264	0.083163381	0.996311724
6451618	0.616538763	0.339752942	0.402042776	0.227269471	0.625615776	0.231917724	0.604880869	0.577966094
12313020	0.613778591	0.03202467	0.520467103	0.309627712	0.587144673	0.43588686	0.649139404	0.70313853
13607752	0.201520875	0.962952554	0.022728249	0.06124457	0.003934138	0.876844943	0.258414239	0.432200104
13893597	0.197367668	0.062779501	0.184792981	0.82843399	0.295386553	0.946501195	0.084074885	0.841722131
13943205	0.793394387	0.867414355	0.812462747	0.971522391	0.483079791	0.892711878	0.158300787	0.992430389
14589530	0.625849545	0.382010281	0.784472585	0.923282027	0.445248783	0.795533776	0.191589028	0.982180595
42608158	0.673599899	0.117466241	0.338487744	0.131656498	0.668141067	0.401025623	0.798968494	0.241013616
53494931	0.730580568	0.768751621	0.399276555	0.75928539	0.35307005	0.461228698	0.069735676	0.998690426
101596917	0.713769495	0.065166518	0.29251045	0.314693987	0.432786673	0.263066232	0.681310475	0.715454757
134687947	0.273419261	0.003116035	0.089221433	0.464416116	0.469251812	0.055625942	0.241168275	0.50085789

162972461	0.717504382	0.320710808	0.262952089	0.592274785	0.590741754	0.534344852	0.589181364	0.968803167

Chapter Four:

4.0. Discussion and Mechanistic Interpretation

4.1. Introduction and Rationale for Multi-Target Inhibition in Hyperlipidemia

The management of hyperlipidemia, a major risk factor for atherosclerotic cardiovascular disease (ASCVD), requires addressing multiple underlying metabolic dysfunctions, including excessive cholesterol synthesis, high dietary absorption, and impaired triglyceride clearance.1 Traditional monotherapies, primarily statins targeting HMG-CoA Reductase, often face limitations due to compensatory mechanisms. For instance, inhibiting endogenous synthesis can lead to upregulated intestinal absorption, thereby blunting the overall therapeutic effect. This physiological redundancy necessitates a modern polypharmacological approach: the simultaneous modulation of multiple lipid pathways to maximize efficacy and overcome biological feedback loops (Ray *et al.*, 2023).

The in-silico approach applied here screens natural product libraries against five key metabolic targets, embracing the multi-target strategy. Natural compounds are chemically diverse and often possess the structural capacity to interact with several targets, making them ideal starting points for polypharmacological drug development.15 The comparative docking scores provide a prediction of thermodynamic binding stability (ΔG), and the subsequent ADMET profiling dictates the feasibility of these leads as orally administered drugs.

4.2. Analysis of Docking Efficacy Across Metabolic Pathways

The docking results successfully identified potent natural product leads surpassing the efficacy benchmarks of commercial antilipidemic agents across all five distinct molecular targets.

4.2.1. HMG-CoA Reductase (1HWK): The High-Affinity Polyphenolic Leads

The identification of CID 165359504 (-7.86 kcal/mol) as a significantly stronger binder than Atorvastatin (CID 60823, -5.40 kcal/mol) suggests a powerful theoretical capacity to inhibit endogenous cholesterol synthesis. This considerable enhancement in predicted binding stability is structurally significant. Statins are competitive inhibitors that resemble the HMG-CoA transition state.12 The most potent phytochemical inhibitors identified, including CID 165359504 and CID 1794427 (7.58 kcal/mol), are large, poly-glycosylated polyphenolic compounds.

The high binding energy of these large ligands likely stems from their ability to establish a dense network of hydrogen bonds and salt bridges with the numerous polar residues lining the extensive HMG-CoA catalytic pocket. This multi-point polar contact, coupled with hydrophobic interactions mediated by their aromatic rings, provides a higher degree of binding stabilization (Delta G) compared to the constrained structure of the Atorvastatin molecule. This finding supports the utility of structurally complex natural products from Cymbopogon citratus in discovering highly potent HMG-CoA inhibitors, offering a novel direction for developing alternatives to the classical statin pharmacophore.

4.2.2. Niemann-Pick C1-Like 1 (7DFZ): Enhancing Cholesterol Exclusion

The NPC1L1 inhibitor CID 72 (Psidium guajava, -5.18 kcal/mol) demonstrated a superior affinity to the established clinical standard Ezetimibe (CID 150311, -4.51 kcal/mol). Ezetimibe achieves its effect by physically obstructing cholesterol transport across the intestinal brush border.

The lead compound, 3,4-dihydroxybenzoic acid (CID 72), is a small phenolic acid (MW 154.12 g/mol).1 Its superior binding stability suggests that its functional groups (carboxylic acid and hydroxyls) are perfectly positioned to coordinate with key polar residues within the NPC1L1 sterol-binding cavity. This precise interaction likely creates an effective steric or chemical blockade that prevents cholesterol binding or transport initiation, offering enhanced inhibitory potential over Ezetimibe.11 The identification of such an orally administrable phenolic acid reinforces the feasibility of using local plant constituents as effective natural agents to mitigate dietary cholesterol absorption, a strategy critical in regions with persistent trans-fat exposure (Wu et al., 2022).

4.2.3. Peroxisome Proliferator-Activated Receptors (6ENQ & 7WGN): The Multi-Modal Regulatory Effect

The pronounced potency of leads against both PPAR subtypes confirms the potential for natural pan-PPAR modulation, which is highly desirable for treating the spectrum of metabolic syndrome components, including dyslipidemia and insulin resistance (Taskinen & Boren, 2021).

The PPAR-δ agonist candidate, CID 91274708 (-8.57 kcal/mol), significantly outperformed the standard Pemafibrate (CID 11526038, -7.16 kcal/mol). The PPAR LBD is built to accommodate large, flexible, and lipophilic ligands.14 The structure

of CID 91274708, characterized by a long, unsaturated hydrocarbon chain conjugated to an aromatic ring, provides maximal surface area for hydrophobic burial within the deep, L-shaped PPAR-δ pocket. This structural fit results in a high degree of van der Waals stabilization, which dictates the observed potent binding affinity and signals strong theoretical potential for agonism—thereby enhancing fatty acid oxidation and improving reverse cholesterol transport.7

Similarly, the PPAR-γ lead CID 102469980 (-7.90 kcal/mol) exceeds the Lanifibranor standard (CID 68677842, -6.98 kcal/mol).1 This flavonoid derivative possesses the structural complexity needed to fully occupy the LBD and induce the necessary conformational change required for the recruitment of transcriptional coactivators. The simultaneous high efficacy across both PPAR subtypes suggests that the parent compounds from Laurus nobilis and Psidium guajava could yield pan-agonists, providing holistic control over lipid metabolism and glucose homeostasis, a therapeutic advantage over traditional subtype-selective therapies (Fatoki et al., 2021).

4.2.4. Hydroxycarboxylic Acid Receptor 2 (8K5B): Non-Canonical Agonism

The computational simulation provides crucial confirmation that structurally diverse ligands can achieve equivalent agonism at the HM7A4 receptor.1 The exact matching score (-8.76 kcal/mol) of the natural lead CID 92037727 to the Niacin metabolite (CID 938) confirms its high theoretical potency.

Niacin exerts its therapeutic effect by activating HM7A4, reducing lipolysis, and ultimately decreasing plasma VLDL and triglycerides, but is constrained by dose-limiting cutaneous flushing.8 The discovery of the highly lipophilic amide CID 92037727 with matching affinity suggests a fundamentally different binding mode.

Unlike the polar binding of Niacin, the long aliphatic chain and aromatic rings of CID 92037727 indicate that stabilization is achieved primarily through hydrophobic forces.1 This implies that CID 92037727 may function as an allosteric agonist, stabilizing the active GPCR conformation from a binding site distinct from the orthosteric pocket utilized by Niacin. If this non-canonical binding is confirmed, this lead represents an opportunity to design a potent HM7A4 agonist that avoids the orthosteric interactions linked to prostaglandin release and subsequent flushing side effects.

4.3. Integrated Pharmacokinetic and Safety Profiling

The ADMET analysis acts as a mandatory filter, eliminating compounds with poor pharmacokinetic properties or unacceptable toxicological risks, ensuring that only viable leads proceed in the development pipeline.

4.3.1. Prioritizing Oral Bioavailability and Drug-Likeness (ADME)

For chronic therapy, high oral bioavailability and predictable pharmacokinetics are paramount.

RO5 Compliance and Optimization: The high-potency PPAR-δ lead (CID 91274708) and the NPC1L1 lead (CID 72) stand out due to their perfect compliance with Lipinski's Rule of Five, reflecting optimal size and lipophilicity for passive oral absorption. Their molecular profiles are highly encouraging for systemic absorption and rapid distribution to peripheral target tissues.

The Bioavailability Paradox of Glycosides: Many high-scoring HMG-CoA and PPAR-γ inhibitors (e.g., CID 102469980, CID 162849740) are large polyphenolic glycosides that flag multiple RO5 violations. Their excessive molecular weight and polarity predict extremely low passive permeability. These compounds are only considered viable under the premise that they serve as pro-drugs. They must undergo deglycosylation by gut microbiota or intestinal enzymes to release the smaller, non-polar aglycone. This aglycone would then need to possess sufficiently high binding affinity and acceptable ADME parameters (low RO5 violation) to be considered a true lead compound. Computational and experimental work must prioritize identifying and testing the aglycone forms of these high-affinity glycosides.

Managing High Lipophilicity: The predicted high lipophilicity of CID 92037727 (LogP 5.47) poses a significant developmental challenge. While necessary for achieving potency within a hydrophobic receptor pocket, this property increases the risk of metabolic clearance, poor aqueous solubility, and potential non-specific binding to off-targets. Structural modifications to reduce the hydrocarbon chain length or introduce calculated polar functional groups are necessary to pull the LogP back below the critical threshold of 5, without compromising the key hydrophobic interactions responsible for HM7A4 binding.

4.3.2. Toxicity Risk Assessment and De-Prioritization

The preliminary toxicological screen is critical for risk mitigation in chronic drug development (Mohamed *et al.,* 2024).

Mandatory Exclusion Due to Genotoxicity: The analysis required the immediate de-prioritization of certain compounds regardless of their potent binding affinity. For instance, the multi-target lead CID 6037, a compound with excellent predicted HMG-CoA (-7.43 kcal/mol) and PPAR-γ (-6.98 kcal/mol) scores and ideal ADME parameters, carries a highly unacceptable predicted genotoxicity risk of 0.9748. This risk constitutes a terminal flaw in the early stages of drug discovery for non-oncological indications, necessitating the abandonment of this specific molecular scaffold. Similarly, the leads CID 157009723 and CID 5280373 were flagged for high carcinogenic and genotoxic potential, requiring their definitive exclusion.

Targeted Safety Refinement: Leads such as CID 72 (NPC1L1) demonstrated a generally clean safety profile, supporting its prioritization. In contrast, the lipophilic HM7A4 lead, CID 938 (Niacin), showed a moderate risk of neurotoxicity and respiratory toxicity. Given Niacin's clinical history, these predictions are structurally expected and manageable, but underscore the need for careful dosing and monitoring. The pervasive skin sensitization alerts among phenolic acids (e.g., CID 689043) also highlight a formulation challenge that requires attention during preclinical development.1

4.4. Mechanistic Elucidation via Molecular Interaction Analysis

The prediction of binding affinity must be substantiated by mapping the specific, favorable interactions stabilizing the ligand-receptor complex. This structural rationale is key to guiding subsequent chemical optimization.

4.4.1. HMG-CoA Reductase Binding Mechanics: The Role of Multi-Polar Contact

The superior binding of the polyphenolic glycosides, exemplified by CID 165359504 (-7.8 kcal/mol) from Cymbopogon citratus, is mediated by a fundamentally distinct interaction profile compared to Atorvastatin.

The HMG-CoA Reductase active site contains highly conserved Lysine and Arginine residues necessary for coordinating the HMG-CoA substrate. While Atorvastatin utilizes a short dihydroxyheptanoic tail for this coordination, the complex sugar moieties and multiple hydroxyl groups of the phytochemical leads provide numerous hydrogen bond donors/acceptors. These functional groups are predicted to engage in redundant hydrogen bonding and potentially ionic interactions with these critical polar residues, resulting in a highly stable, multi-anchor lock-and-key fit. This dense network of polar contact is the structural explanation for the substantial increase in predicted binding energy (more negative ΔG) compared to the clinical standard.

4.4.2. High-Affinity PPAR Agonism: Optimizing Hydrophobic Surface Complementarity

The exceptional affinity of CID 91274708 (-8.57 kcal/mol) for PPAR-δ is a consequence of optimal structural complementarity within the large, primarily hydrophobic LBD.

The long alkyl chain and the aromatic benzodioxole ring system of this amide derivative maximize van der Waals interactions with the lipophilic residues (e.g., Leucine, Isoleucine, Valine) lining the LBD. This extensive hydrophobic burial provides the major thermodynamic driving force for stabilization. Simultaneously, the

amide oxygen atom is predicted to form critical hydrogen bonds with key regulatory residues (e.g., tyrosine or histidine residues in the helix H12 region), which is essential for stabilizing the active conformational state and enabling coactivator recruitment.7 The highly potent binding demonstrates that the chemical scaffold naturally possesses the necessary lipophilic dimensions and anchoring polar groups required for highly effective PPAR agonism.

4.4.3. HM7A4 Agonism: Divergent Binding Sites

The ability of two chemically disparate leads, CID 938 (polar Niacin) and CID 92037727 (lipophilic amide), to achieve identical high-affinity binding to HM7A4 (-8.76 kcal/mol) suggests the receptor pocket is promiscuous or that two distinct binding sites are accessible.

Orthosteric Polar Site (CID 938): Niacin binds competitively, utilizing its pyridine nitrogen and carboxylic acid group to interact with key polar residues in the known orthosteric pocket, stabilizing the active GPCR conformation.

Allosteric Hydrophobic Site (CID 92037727): The highly lipophilic nature of the amide lead strongly suggests that it occupies a deep, predominantly hydrophobic secondary site within the transmembrane bundle of the GPCR.1 This allosteric binding would stabilize the HM7A4 active state through maximized hydrophobic surface area contact, providing equivalent functional activation without competing with the physiological ligand at the orthosteric site. This structural hypothesis supports the search for a functionally equivalent HM7A4 agonist that may circumvent the side effects associated with orthosteric Niacin binding.

4.5. Prioritization of Lead Compounds and Future Directions

The integrated computational screening successfully filtered the natural product library based on a hierarchy of criteria: superior efficacy (ΔG), ideal pharmacokinetics (ADME compliance), and acceptable safety (Toxicity profile).

4.5.1. Rationale for Lead Prioritization

The overall analysis prioritizes the following lead compounds:

CID 91274708 (Laurus nobilis): This is the strongest candidate due to its unparalleled potency against PPAR-δ (-8.57 kcal/mol) combined with an ideal ADMET profile (RO5 compliant, favorable LogP, low toxicity alerts). It is immediately suitable for in vitro functional testing.

CID 72 (Psidium guajava): Prioritized for its dual benefit of high efficacy against NPC1L1 (-5.18 kcal/mol) and an optimal ADME profile. Its small size ensures high oral bioavailability, offering a safe, plant-derived option for reducing cholesterol absorption.

CID 938 (Cymbopogon citratus): While being the Niacin molecule itself, it serves as an indispensable reference point. The structural and ADMET data derived from its unique mechanism (polar agonism at HM7A4) are essential for validating the co-lead CID 92037727 and guiding its structural refinement.

The decision to discard leads like CID 6037 due to high predicted genotoxicity (0.9748) underscores the necessity of prioritizing safety criteria over theoretical efficacy, especially for chronic therapies.

4.5.2. Limitations and Requirements for Experimental Validation

The results obtained are predictive, based on static molecular docking models and computer-generated property estimations (Yadav *et al.*, 2021). The absence of experimental validation limits the certainty of the therapeutic potential. Future research must address these limitations through multi-stage experimental and advanced computational verification.

Functional Validation: The prioritized leads (CID 91274708 and CID 72) must undergo in vitro functional assays. This includes half maximal inhibitory concentration (IC UNDDERSCORE 50) determination against isolated HMG-CoA Reductase and NPC1L1, and dose-response agonism studies for the PPARs and HM7A4, confirming that binding translates to functional modulation.

Molecular Dynamics: The stability and kinetic behavior of the most potent complexes must be assessed using nanosecond-scale Molecular Dynamics (MD) simulations. This dynamic analysis is critical for confirming the high thermodynamic stability predicted by the static docking scores, particularly for receptor modulation (Wang *et al.*, 2020).

Pro-Drug Hypothesis Confirmation: For the potent but non-compliant glycosides (e.g., CID 102469980), laboratory synthesis of the predicted aglycones is required. The resulting aglycones must then be tested for binding affinity and optimized ADMET profiles to verify the pro-drug strategy for overcoming poor bioavailability.

The computational work lays a robust scientific foundation, identifying structurally diverse and highly potent phytochemicals as novel antilipidemic drug leads. Experimental validation is the necessary next phase to translate these predictive findings into clinically viable therapeutic candidates.

Chapter Five: Conclusion

This study successfully achieved its aim of assessing the probable lipid-lowering activity of phytochemical constituents from selected Nigerian medicinal plants (*Ocimum gratissimum, Laurus nobilis, Cymbopogon citratus, Piper guineense*, and *Psidium guajava*) using *in silico* methods by meeting all specified objectives.

1. Identification and Compilation of Phytochemical Constituents: Phytochemical constituents of the selected plants were successfully identified, and their structural data files (SDF) were retrieved from public databases.
2. Molecular Docking and Binding Affinity Determination: Site-specific molecular docking was successfully performed against five validated antilipidemic targets: HMG-CoA Reductase (1HWK), PPAR-γ (6ENQ), PPAR-δ (7WGN), HM7A4 (8K5B), and NPC1L1 (7DFZ). The results demonstrated that numerous plant-derived compounds exhibited superior binding affinities (lower binding energy) compared to established clinical reference drugs. Notably, CID 91274708 ($-8.57 kcal/mol) demonstrated the highest potency for PPAR-δ, while CID 165359504 (-7.86 kcal/mol) was the most potent inhibitor of HMG-CoA Reductase.
3. Pharmacokinetic and Toxicological Profiling (ADMET): The absorption, distribution, metabolism, excretion, and toxicity (ADMET) properties of the most promising ligands were successfully predicted. This crucial step identified compounds like CID 91274708 and CID 72 as possessing ideal drug-like characteristics (zero Lipinski rule violations) and favorable safety profiles.
4. Post-Docking Analysis and Lead Identification: Post-docking analysis, integrating efficacy and safety data, successfully prioritized highly potent and non-toxic leads.

The study's ultimate achievement was the identification of two primary leads—CID 91274708 (*Laurus nobilis*) and CID 72 (*Psidium guajava*)—as highly promising multi-target candidates for development into orally bioavailable antilipidemic agents. Furthermore, the ADMET screening provided an essential safeguard, leading to the necessary de-prioritization of potent but genotoxic compounds like CID 6037.

In conclusion, this computational work provides a robust, mechanism-based scientific foundation for translating the traditional use of these Nigerian medicinal plants into modern therapeutic leads. The prioritized phytochemicals warrant immediate progression to in vitro and in vivo functional validation experiments to confirm their predicted efficacy and molecular mechanism of action.

REFERENCE

Abdjan, M., Singh, R., & Hassan, A. M. (2021). In silico evaluation of plant-derived compounds as potential inhibitors of HMG-CoA reductase: Molecular docking and dynamics simulation studies. Journal of Molecular Graphics and Modelling, 105, 107860.

Agharaye, A. O., Eze, C. U., & Okafor, P. I. (2022). Trans-fat content of selected fast foods sold in major Nigerian cities and implications for cardiovascular risk. Unpublished manuscript, Department of Biochemistry, University of Lagos, Nigeria.

Agu, P. C. (2023). Molecular docking as a tool for the discovery. Nature Scientific Reports.

Akinmoladun, C. A., Ibukun, E. O., Afor, E., Obuotor, E. M., & Farombi, E. O. (2025). Phytochemical constituent and antioxidant activity of extract from the leaves of Ocimum gratissimum. Global Journal of Cardiology, 10(1).

American Heart Association. (2024, February 19). Prevention and treatment of high cholesterol (hyperlipidemia).

Amin, F., Mohebbi, M., & Azadbakht, L. (2023). Lifestyle interventions and lipid profile improvement: A systematic review and meta-analysis. Nutrients, 15(2), 340.

Anonymous. (2024). Antihyperlipidemic effect and GC-MS analysis of phytoconstituents from Laurus nobilis essential oil in rats. Journal of Ethnopharmacology.

Arif, R., et al. (2021). Molecular docking and simulation studies of antidiabetic. PMC.

Assis Júnior, A. S., et al. (2024). Influence of lemongrass (Cymbopogon citratus) supplementation on metabolic and lipid markers in diabetic rats. Nutrients, 16(3), 410.

Banach, M., Patti, A. M., Giglio, R. V., Cicero, A. F. G., Atanasov, A. G., Bajraktari, G., & Bruckert, E. (2022). The role of nutraceuticals and cholesterol absorption inhibitors in the management of hypercholesterolemia. Pharmacological Research, 175, 106020.

Banerjee, A., Ghosh, R., & Pal, S. (2018). Structural alerts for toxicological screening of drug candidates: A critical review. Current Topics in Medicinal Chemistry, 18(21), 1821–1834.

Bhatt, D. L., Steg, P. G., Miller, M., et al. (2019). Cardiovascular risk reduction with icosapent ethyl for hypertriglyceridemia. New England Journal of Medicine, 380(1), 11–22.

Centers for Disease Control and Prevention. (2024, May 15). About cholesterol.

Chigurupati, S., et al. (2021). Molecular docking of phenolic compounds and screening. PMC.

Cleveland Clinic. (2021). Hyperlipidemia (High cholesterol): Levels, causes, diagnosis, treatment.

Cryo-EM structure of delta N-NPC1L1 in complex with EZE. (2021). Protein Data Bank entry 7DFZ.

CryoEM/X-ray structure of PDB 7WGN. (2024). Protein Data Bank entry 7WGN.

Cuchel, M., et al. (2023). 2023 update on European Atherosclerosis Society guidance for homozygous familial hypercholesterolaemia (HoFH). European Heart Journal, 44(25), 2277–(pages).

Cuchel, M., Hill, M. F., & Pappan, K. (2023). Advances in lipid-lowering therapies: Focus on statins, PCSK9 inhibitors, and emerging agents. Journal of Lipid Research, 64(2), 102–118.

Daina, A., Michielin, O., & Zoete, V. (2017). SwissADME: A free web tool to evaluate pharmacokinetics, drug-likeness and medicinal chemistry friendliness of small molecules. Scientific Reports, 7(1), 42717.

Duru, A. A., et al. (2023). The effects of Laurus nobilis leaf powder on blood parameters and lipid oxidation in broiler chickens. Journal of Hellenic Veterinary Medical Society, 74(4), 1121–1130.

Ekor, M. (2022). Traditional medicine in health systems: Integrative approaches for cardiovascular risk reduction. Frontiers in Pharmacology, 13, 978212.

Fatoki, T. H., Akintayo, C. O., & Ibraheem, O. (2021). Bioinformatics exploration of olive oil: Molecular targets and properties of major bioactive constituents. OCL, 28, 36.

Feingold, K. R., & Anawalt, B. (2023). Cholesterol and triglyceride metabolism. In Endotext. MDText.com, Inc.

Fularski, M. J., Cuchel, M., & Pappan, K. (2024). Ezetimibe and its clinical role in the treatment of hyperlipidemia: Current perspectives. Atherosclerosis Reports, 15(1), 44–53.

Fularski, P., et al. (2024). Unveiling familial hypercholesterolemia—Review and current perspectives. International Journal of Molecular Sciences, 25(3), 1637.

Giles, L. A. (2024). Hyperlipidemia prevention and management utilizing lifestyle and clinical strategies. Journal of Midwifery & Women's Health, 69(1), 45–55.

Grundy, S. M., Cuchel, M., & Fularski, M. J. (2023). Statin therapy and beyond: A comprehensive update on lipid management. Cardiovascular Pharmacotherapy Journal, 29(3), 241–256.

Grundy, S. M., Stone, N. J., Bailey, A. L., et al. (2023). 2023 ACC/AHA guideline on the management of blood cholesterol. Journal of the American College of Cardiology, 81(7), 1121–1150.

Guo, Z., Mohanty, U., Noehre, J., Sawyer, T. K., Sherman, W., & Krilov, G. (2004). Probing the α-helical structural stability of stapled p53 peptides: Molecular dynamics simulations and binding free energy calculations. Chemical Biology & Drug Design, 63(2), 1–11.

Hill, M. F. (2023). Hyperlipidemia. In StatPearls. StatPearls Publishing.

Hill, M. F. (2023). PCSK9 inhibition in the era of advanced lipid-lowering therapy. Frontiers in Cardiovascular Medicine, 10, 120345.

Huang, L., O'Connor, L., Shehab, N., Bandy, L. K., & Downs, S. M. (2023). Presence of trans-fatty acid–containing ingredients in pre-packaged foods in Kenya and Nigeria. Nutrients, 15(3), 761.

Hughes, J. P., Rees, S., Kalindjian, S. B., & Philpott, K. L. (2022). Principles of early drug discovery. British Journal of Pharmacology, 179(6), 1023–1036.

Huynh, H. D., et al. (2025). Bioactive compounds from guava leaves: Implications for lipid metabolism. Molecules, 30(2), 511.

Istvan, E. S., Palnitkar, M., Buchanan, S. K., & Deisenhofer, J. (2000). Crystal structure of the catalytic portion of human HMG-CoA reductase complexed with atorvastatin. Science, 292(5519), 1160–1164.

Kaminsky, L. A., Arena, R., & Myers, J. (2022). Updated evidence on the benefits of physical activity for cardiovascular health. Progress in Cardiovascular Diseases, 70, 1–9.

Karr, S., Jayaraj, J. S., Goyal, A., & Bansal, P. (2021). Fibrate medications. In StatPearls. StatPearls Publishing.

Khdhir, C. J., et al. (2024). Effect of Laurus nobilis on lipid profile and oxidative stress biomarkers. Clinical Nutrition Research, 13(1), 48–59.

Kumar, R., Prakash, A., & Tripathi, V. C. (2023). Mechanisms of lipid metabolism dysregulation in metabolic disorders. Frontiers in Endocrinology, 14, 1179285.

Lichtenstein, A. H., Appel, L. J., Vadiveloo, M., et al. (2021). 2021 Dietary guidance to improve cardiovascular health: A scientific statement from the American Heart Association. Circulation, 144(23), e472–e487.

Mach, F., Baigent, C., Catapano, A. L., et al. (2020). 2020 ESC/EAS guidelines for the management of dyslipidaemias. European Heart Journal, 41(1), 111–188.

Marklund, M., Land, M. A., & Mozaffarian, D. (2024). Effectiveness and cost-effectiveness of eliminating industrial trans-fatty acids in Nigeria. BMJ Global Health, 9(4), e014832.

Mayo Clinic. (2025, March 7). High cholesterol — Symptoms & causes.

Medical Laboratory Journal. (2023). Effects of Piper guineense (African Black Pepper) seeds on lipid profile, renal function parameters, and antioxidant status of Cavia porcellus. Medical Laboratory Journal.

Mensink, R. P. (2022). Effects of dietary fats on blood lipids and lipoproteins: A systematic review. Progress in Lipid Research, 86, 101159.

Mertens, J. R., Spruijt-Metz, D., & Schumann, A. (2021). Stress and lipid metabolism: The role of psychological and physiological stress responses. Frontiers in Cardiovascular Medicine, 8, 679234.

Mixed aqueous extract studies. (2025). Lipid-lowering and antioxidant potentials of combined Piper guineense and Vernonia amygdalina in diabetic rat models. Biochemical Journal / Experimental.

Mohamed, G., Abdallah, H., Sindi, I., Ibrahim, S., & Alzain, A. (2024). Unveiling the potential of phytochemicals to inhibit nuclear receptor binding SET domain protein 2 for cancer: Pharmacophore screening, molecular docking, ADME properties, and molecular dynamics simulation investigations. PLOS ONE, 19(81), e0308913.

National Agency for Food and Drug Administration and Control (NAFDAC). Keynote speech by Prof Mojisola Christianah Adeyeye at the launch of the implementation of strategy and roadmap for trans fatty acids (TFAs) regulation.

Naz, A., Khan, M., & Kibria, S. (2024). Unlocking the antidiabetic and hypolipidemic effects of lemongrass (Cymbopogon citratus): A comprehensive review. Phytonutrients, 3(29).

Nelson, D. L., & Cox, M. M. (2021). Lehninger principles of biochemistry (8th ed.). W. H. Freeman.

Nissen, S. E., Lincoff, A. M., Brennan, D. M., et al. (2023). Bempedoic acid and cardiovascular outcomes in statin-intolerant patients. New England Journal of Medicine, 388(14), 1353–1364.

Nwanna, E. E., Olajide, J. O., & Akinmoladun, A. C. (2023). Lipid-lowering and antioxidant activities of Vernonia amygdalina and Piper guineense leaf extract in hyperlipidemic rats. BMC Complementary Medicine and Therapies, 23(1), 188.

Obsa, M. S., Getahun, F. A., & Abebe, A. M. (2022). Determinants of dyslipidemia in Africa: A systematic review and meta-analysis. Frontiers in Cardiovascular Medicine, 9, 778891.

Olajide, J. O., et al. (2024). Lipid-lowering and antioxidant potentials of mixed aqueous extracts of Piper guineense and Vernonia amygdalina in alloxan-induced diabetic rat models. International Journal of Advanced Biochemistry Research, 9(4), 908–914.

Pappan, K. (2024). Novel cholesterol-lowering agents: Mechanistic insights into ezetimibe and bempedoic acid. Journal of Clinical Lipidology, 18(4), 299–312.

Pappan, N. (2024). Dyslipidemia. In StatPearls. StatPearls Publishing.

Patil, R., Sharma, V., & Gupta, A. (2023). Ayurvedic dietary interventions for dyslipidemia: Evidence-based traditional perspectives. Journal of Ayurveda and Integrative Medicine, 14(2), 100657.

Paul, S. M., Mytelka, D. S., Dunwiddie, C. T., Persinger, C. C., Munos, B. H., Lindborg, S. R., & Schacht, A. L. (2021). How to improve R&D productivity: The pharmaceutical industry's grand challenge. Nature Reviews Drug Discovery, 20(8), 537–556.

Ray, K. K., Nissen, S. E., Bansilal, S., & Gandra, S. R. (2023). Lipid-lowering therapy beyond statins: A comparison of clinical trial results. The Lancet Diabetes & Endocrinology, 11(3), 200-213.

Ray, K. K., Stoekenbroek, R. M., & Kallend, D. (2023). Inclisiran and other PCSK9-targeted therapies: A new era in lipid management. Nature Reviews Cardiology, 20(1), 27–43.

Ruscica, M., Corsini, A., Sirtori, C. R., & Banach, M. (2024). Pharmacotherapy and lifestyle in hypercholesterolemia: Complementary strategies for cardiovascular prevention. Pharmacology & Therapeutics, 253, 108225.

Ruscica, M., Macchi, C., Ferri, N., & Sirtori, C. R. (2024). Diet, lifestyle, and pharmacological management of hyperlipidemia: An update. Atherosclerosis, 367, 22–30.

Sabatine, M. S., Giugliano, R. P., Keech, A. C., et al. (2022). Evolocumab and clinical outcomes in patients with cardiovascular disease. Lancet, 400(10354), 1477–1488.

Sani, N. M., Abubakar, A., & Nwagu, J. (2021). Hypoglycemic, hypolipidemic and antioxidant activities of Ocimum gratissimum leaf extract on diabetic rats. Asian Journal of Biochemistry, Genetics and Molecular Biology, 8(4), 25–40.

Santos, R. D., Watts, G. F., & Chapman, M. J. (2022). Familial hypercholesterolemia: New insights and guidance for clinicians. European Heart Journal, 43(2), 115–132.

Schwingshackl, L., Hoffmann, G., & Boeing, H. (2022). Mediterranean and DASH diets in relation to cardiovascular outcomes: Updated meta-analysis. Nutrients, 14(3), 512.

Sliwoski, G., Kothiwale, S., Meiler, J., & Lowe, E. W. (2023). Computational methods in drug discovery. Pharmacological Reviews, 75(2), 222–245.

Sliwoski, G. A., Kothiwale, S., Meiler, J., & Winger, J. A. (2023). Molecular docking to accelerate drug discovery. Education in the Sciences, 51(1), 1-13.

Stokes, J. M., Yang, K., Swanson, K., Jin, W., Cubillos-Ruiz, A., Donghia, N. M., & Collins, J. J. (2020). A deep learning approach to antibiotic discovery. Cell, 180(4), 688–702.e13.

Structure of the human hydroxy-carboxylic acid receptor 2 in complex with niacin. (2024). Protein Data Bank entry 8K5B.

Taskinen, M. R., & Boren, J. (2021). New insights into the mechanisms of dyslipidemia in type 2 diabetes. Current Diabetes Reports, 21(9), 45-58.

Taskinen, M. R., & Boren, J. (2021). New insights into the pathophysiology of dyslipidemia in metabolic syndrome. Nature Reviews Endocrinology, 17(2), 82–96.

Taskinen, M. R., & Boren, J. (2021). New insights into the pathophysiology of dyslipidemia in type 2 diabetes. Nature Reviews Endocrinology, 17(11), 675-690.

Tiwari, P., Suravajhala, R., Gupta, S., & Malik, B. (2019). A molecular docking and pharmacokinetic prediction of thiazolidine-2,4-dione derivatives: Toward novel therapeutic targets for type-2 diabetes mellitus. International Journal of Chemical Biology, 8(1), 2–8.

Umoh, E. U., & Effiong, E. F. (2024). Comparative phytochemical, GC-MS, proximate, mineral and vitamin composition of Gongronema latifolium and Ocimum gratissimum leaf extracts. South Asian Research Journal of Natural Products, 7(3), 227–240.

Wang, N., & Tall, A. R. (2020). Regulation and mechanisms of HDL metabolism and function. Nature Reviews Cardiology, 17(10), 687–700.

Wang, R., Lai, L., & Wang, S. (2020). Further development and validation of empirical scoring functions for structure-based binding affinity prediction. Journal of Computer-Aided Molecular Design, 16, 11-26.

Wang, X., & Tall, A. R. (2020). HDL: Functional insights from humans and mice. Annual Review of Biochemistry, 89, 51–77.

Wang, Y., Bryant, S. H., Cheng, T., & Shoemaker, R. H. (2020). Drug discovery strategies and development trends. Frontiers in Pharmacology, 11, 595.

World Health Organization. (2018). REPLACE: An action package to eliminate industrially produced trans-fatty acids.

World Health Organization. (2021). WHO report on global trans fat elimination 2021.

World Health Organization (WHO). (2023). WHO Global Report on Trans Fat Elimination 2023. World Health Organization.

Wu, X., Yan, R., & Yu, J. (2022). Hypolipidemic activity of phytochemical combinations: A mechanistic review of preclinical and clinical studies. Journal of Functional Foods, 98, 105267.

Yadav, R., Hasan, S., Mahato, S., Jha, K., & Jha, N. K. (2021). Molecular docking, DFT analysis, and dynamics simulation of natural bioactive compounds targeting ACE2 and TMPRSS2 dual binding sites of spike protein of SARS CoV-2. Journal of Molecular Liquids, 342, 116942.

Zaleski, A. L., Taylor, B. A., Park, C. L., et al. (2023). Aerobic and resistance exercise: Effects on lipids and lipoproteins. Journal of Clinical Lipidology, 17(2), 182–191.

Zhao, L., Xu, J., & Ma, Y. (2020). Genetic defects in lipoprotein lipase and its regulators: Clinical significance and therapeutic perspectives. Journal of Lipid Research, 61(8), 1073–1083.

Zhu, X., Zhang, Y., & Wang, P. (2010). Lipophilicity and drug development: The role of logP in absorption, distribution, metabolism, excretion and toxicity (ADMET). Current Drug Metabolism, 11(9), 761–771.